SANDIA REPORT

SAND98–1715
Unlimited Release
Printed August 1998

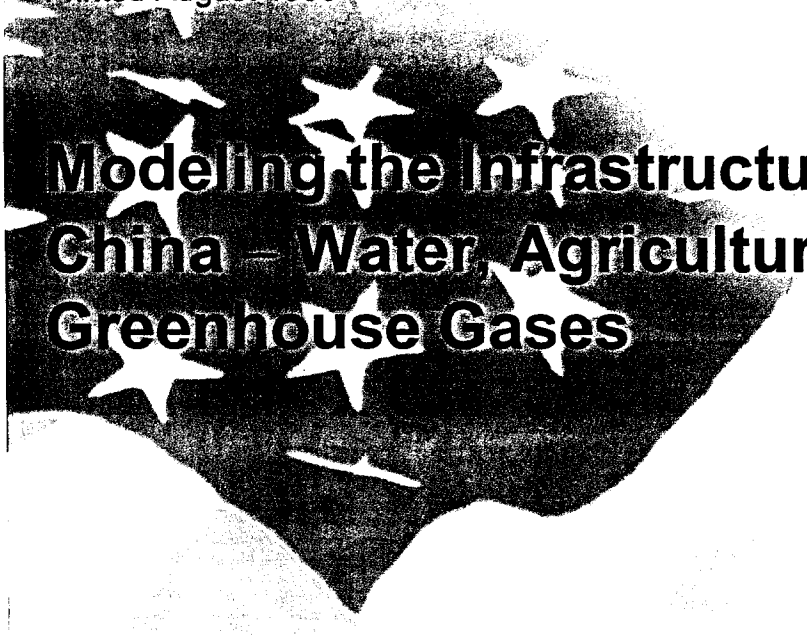

Modeling the Infrastructure Dynamics of China – Water, Agriculture, Energy, and Greenhouse Gases

Stephen H. Conrad, Thomas E. Drennen, Dennis Engi, David L. Harris, David M. Jeppesen, Richard P. Thomas

Prepared by
Sandia National Laboratories
Albuquerque, New Mexico 87185 and Livermore, California 94550

Sandia is a multiprogram laboratory operated by Sandia Corporation, a Lockheed Martin Company, for the United States Department of Energy under Contract DE-AC04-94AL85000.

Sandia National Laboratories

Issued by Sandia National Laboratories, operated for the United States Department of Energy by Sandia Corporation.

Available to DOE and DOE contractors from
Office of Scientific and Technical Information
P.O. Box 62
Oak Ridge, TN 37831

Prices available from (615) 576-8401, FTS 626-8401

Available to the public from
National Technical Information Service
U.S. Department of Commerce
5285 Port Royal Rd
Springfield, VA 22161

NTIS price codes
Printed copy: A08
Microfiche copy: A01

SAND98-1715
Unlimited Release
Printed August 1998

Modeling the Infrastructure Dynamics of China – Water, Agriculture, Energy, and Greenhouse Gases

Stephen H. Conrad
Environmental Risk and Decision Analysis Department

Thomas E. Drennen
Energy and Critical Infrastructure Policy and Planning Department

Dennis Engi
Strategic Initiatives Department

David L. Harris
Infrastructure Systems Engineering Department

David M. Jeppesen
Infrastructure Systems Engineering Department

Richard P. Thomas
Environmental Restoration for Tech Areas and Miscellaneous Sites

Sandia National Laboratories
P.O. Box 5800
Albuquerque, NM 87185-1345

ABSTRACT

A comprehensive critical infrastructure analysis of the People's Republic of China was performed to address questions about China's ability to meet its long-term grain requirements and energy needs and to estimate greenhouse gas emissions in China likely to result from increased agricultural production and energy use. Four dynamic computer simulation models of China's infrastructures—water, agriculture, energy, and greenhouse gas—were developed to simulate, respectively, the hydrologic budgetary processes, grain production and consumption, energy demand, and greenhouse gas emissions in China through 2025. The four models were

integrated into a state-of-the-art comprehensive critical infrastructure model for all of China. This integrated model simulates diverse flows of commodities, such as water and greenhouse gas, between the separate models to capture the overall dynamics of the integrated system. The model was used to generate projections of China's available water resources and expected water use for 10 river drainage regions representing 100% of China's mean annual runoff and comprising 37 major river basins. These projections were used to develop estimates of the water surpluses and/or deficits in the three end-use sectors—urban, industrial, and agricultural—through the year 2025. Projections of the all-China demand for the three major grains (corn, wheat, and rice), meat, and "other" (other grains and fruits and vegetables) were also generated. Each region's share of the all-China grain demand (allocated on the basis of each region's share of historic grain production) was calculated in order to assess the land and water resources in each region required to meet that demand. The land required to meet each region's share of the grain demand was compared with an initial estimate of arable land in each region. Growth in energy use in six historically significant sectors and growth in greenhouse gas loading were projected for all of China. The greenhouse gases modeled were carbon dioxide (CO_2) and methane (CH_4) emissions from the production, consumption, and distribution of energy and CH_4 emitted directly from animals and their waste products and from flooded rice paddies. The results of the modeling and analysis indicate that, based on 100 Monte Carlo replications of the model, water deficits occur in the study period in 8 of the 10 regions at a frequency of never or almost never. In two regions, however, the Haihe and Huanghe, located in northeastern China, significant and/or ongoing deficits in the agricultural sector are experienced throughout the study period. In these regions, water use requirements exceed the sustainable yield and it is assumed that deficits are met by mining groundwater. This assumption is confirmed by reports that groundwater mining is already under way in the most intensively cultivated and populated areas of northeastern China, particularly around the Beijing area. Comparisons of initial estimates of arable land in the Haihe and Huanghe with the amount of land needed to meet each region's share of the grain demand indicate that the amount of arable land is more than sufficient to meet the need. The availability of water appears to be the limiting factor in meeting these regions' share of the total grain demand. The results further indicate that the total all-China energy demand will increase by a factor of 4.7 (or 370%) from 1995 to 2025, and that coal will remain the dominant fuel source in China, growing by a factor of 3.5 (or 250%) by the year 2025. China could also import as much as 8.1 million barrels of oil per day by 2015 and 15 million barrels per day by 2025. Finally, the analysis indicates that from 1995 to 2025, CO_2 emissions in China will increase by a factor of 4.5 (or 350%), CH_4 emissions from the energy sector will increase by a factor of 4.1 (or 307%), and CH_4 emissions from the agricultural sector will increase from approximately 26.4 million metric tons of CH_4 ($MmtCH_4$) to 37.3 $MmtCH_4$ (over 40%). These results indicate that it may be difficult to effectively limit future worldwide greenhouse gas emissions without Chinese cooperation.

ACKNOWLEDGMENTS

The analysis of China's critical infrastructures was a team effort that required the dedicated commitment of many people. We would first like to thank Eric Webb who was largely responsible for the design of the first version of the China water model, and James E. Nickum, who traveled to China during August and September 1996 to collect, translate, and summarize data from Chinese government agency publications and maps.

We would also like to thank Chui Fan Chen Cheng of Sandia National Laboratories, who provided assistance with the initial province-to-water-basin data transformation and Doug Rizor of Science Applications International Corporation, who assisted with geographic information service (GIS) mapping of the Chinese provinces. Christopher Chiesa of the Environmental Research Institute of Michigan (ERIM) Geographic Information Systems and Applications Department, Earth Sciences Group, provided data from ERIM's *GIS Database of China Land Use*. The estimated water use coefficient ranges for each of the grains were provided by Joe Ritchie, Professor of Agronomy at Michigan State University, and the return flow percentages were provided by Professor John W. Hernandez of the Department of Civil, Agricultural, and Geological Engineering at New Mexico State University. Frederick W. Crook and W. Hunter Colby of the U.S. Department of Agriculture/Economic Research Service provided China grain production and consumption data, the Country Projection and Policy Analysis (CPPA) Model, and CPPA Model reports. Arnold Baker of Sandia National Laboratories assisted in conceptualizing the energy and greenhouse gas models, and Professor Jon D. Erickson and Peter Kobos of the Department of Economics at Rensselaer Polytechnic Institute provided assistance with the development of those models.

Thanks are also due to Belinda Garcia of Sandia National Laboratories, who wrote the Java code that enabled World Wide Web access to the integrated model, and to Nancy Hetrick at Tech Reps, Inc., who provided invaluable technical writing and documentation support. Finally, we would like to thank Chuck Meyers of the Lab-Directed Research and Development Program at Sandia National Laboratories, who was instrumental in continuing the essential financial support.

Intentionally Left Blank

EXECUTIVE SUMMARY

This report presents the results of a comprehensive critical infrastructure analysis of the People's Republic of China. The analysis is part of an ongoing effort at Sandia National Laboratories to study infrastructures throughout the world in order to promote economic and political stability in regions important to the U.S. China's increasing population, rapid industrialization, and rising affluence have raised questions about whether it can meet its long-term food needs and about the impact of a potential grain deficit on the world economy. Questions have also been raised about the amounts and the impact of greenhouse gases likely to be emitted in China as a result of increased energy use and agricultural production. The purpose of this analysis was to use these questions about China's ability to meet its grain requirements and energy needs and about greenhouse gas emissions as a vehicle to demonstrate a valuable approach to modeling and analyzing critical infrastructures.

Four dynamic computer simulation models of China's critical infrastructures—water, agriculture, energy, and greenhouse gas—were developed to simulate, respectively, the hydrologic budgetary processes, grain production and consumption, energy demand, and greenhouse gas emissions in China through the year 2025. The four models were integrated into a state-of-the-art comprehensive critical infrastructure model for all of China to allow for the exchange of information between the separate models and to capture the overall dynamics of the integrated system. This integration involved coupling the flows for the commodities water, methane (CH_4), and carbon dioxide (CO_2) between the separate models. The integrated model was designed to operate on a platform that generates results quickly (within minutes rather than hours or weeks), presents the results visually, demonstrates the relationships between the key variables, and allows the user to make adjustments for various "what if" scenarios and policy options concerning available water and water use, water-constrained grain production, caloric consumption, population growth, grain yield, sectoral gross domestic product (GDP) growth, sectoral energy intensities, fuel shares, energy requirements, and greenhouse gas emissions.

The analysis presented in this report involved generating projections of China's available water resources, expected water use, and grain consumption and production for 10 river drainage regions representing 100% of China's mean annual runoff and comprising 37 major river basins. Growth in energy use in six historically significant sectors and in greenhouse gas loading were projected for all of China. Greenhouse gases analyzed in the modeling effort were CO_2 and CH_4 emissions from the energy sector and CH_4 emissions from the agricultural sector. The study period extended from 1980 to 2025.

The analysis specifically included projecting the total available water in each river drainage region through the year 2025 and comparing these results with projections of total water use in each region in the three end-use sectors—urban, industrial, and agricultural—to determine the expected frequency of each region experiencing a water deficit through the study period. The model estimates violations of the sustainable yield constraint, as follows: the constraint is violated when groundwater withdrawals exceed an amount equal to the average recharge plus agricultural return flows; if the available water does not meet the water use requirements, a deficit results. The model also assumes a water use priority scheme in which the impact of a deficit is felt first by the agricultural sector, second by the industrial sector, and lastly by the

urban sector. Projections of the all-China demand for the three major grains (corn, wheat, and rice), meat, and "other" (other grains and fruits and vegetables) were also generated through 2025. Each region's share of the all-China grain demand (allocated on the basis of each region's share of historic grain production) were generated to produce projections of the land and water required in each region to meet this allocated demand. Agricultural land requirements were compared with an initial approximation of arable land estimated using a geographic information system (GIS) analysis that identified all land having a slope less than 1%. The projected water requirements were provided to the water model for comparison with projections of available water.

Growth in energy use for coal, oil, natural gas, hydroelectric power, and nuclear power was projected in each of six historically significant sectors—agriculture, industry, construction, transportation, commerce, and residential (and other)—on the basis of GDP and decreasing sectoral energy intensities. Energy demand and fuel consumption were projected for China through 2025 for the case where nuclear and hydropower capture increasing shares (corresponding to official plans of the Chinese government) and for an alternative scenario with accelerated use of nuclear and hydropower. CO_2 and CH_4 emissions resulting from the production (extraction), distribution (primarily natural gas pipelines), and consumption (burning) of coal, oil and natural gas were projected through 2025 and compared with U.S. and world-wide emissions for 1995. Projections of CO_2 emissions for the scenario of accelerated use of nuclear and hydropower were also generated. Agricultural emissions of CH_4 directly from animals and their waste products and from flooded rice paddies were also projected.

The results of the analysis indicate that, on the basis of regional data, 5 of the 10 regions show a surplus of water in China throughout the study period. Based on 100 Monte Carlo replications of the model, these regions—Chang Jiang, Southeast Coastal, Pearl River, Southwest China, and the Region of Inland Rivers—all located in southern and northwestern China, are expected to experience no deficits through 2025. In the five regions located in northeastern China, however, water use requirements exceed the sustainable yield and deficits occur to varying degrees. Three of these regions, the Heilongjiang, Liaohe, and Huaihe, are likely to experience deficits late in the study period in the agricultural sector. Based on 100 Monte Carlo replications of the model, the expected frequency of experiencing a water deficit through the year 2025 in both these regions is "almost never." Two of the regions in northeastern China, the Haihe and Huanghe, however, experience significant and/or ongoing deficits in the agricultural sector throughout the study period. In the Huanghe, a deficit also appears in the industrial sector in the second half of the period. Based on 100 replications of the water model, the expected frequencies of experiencing a water deficit through the year 2025 for the Haihe and the Huanghe are "always" and "almost always," respectively. The deficit in Haihe's agricultural sector is likely to reach between 22 and 30 billion cubic meters by the year 2025. Although the Huanghe region begins the study period with a much smaller water deficit than that in the Haihe region, by 2025 the deficit for the Huanghe region is likely to reach between 18 and 38 billion cubic meters. Because the Haihe receives interbasin transfers from the Huanghe region, deficits in these regions are likely to play a significant role in water scarcity issues in both regions in the coming years. Moreover, because water use requirements exceed the sustainable yield in these regions, it is assumed that the water deficit must be met by mining groundwater. This assumption is confirmed by reports that groundwater mining has been under way in the most intensively

cultivated and populated areas of northeastern China for several years, particularly around the Beijing area.

Comparisons of initial estimates of arable land in the Haihe and Huanghe regions with the amount of land needed to meet each region's projected share of the all-China grain demand generated in the China agronomic model indicate that the amount of arable land is more than sufficient to meet land needs in both regions. The availability of water for agriculture in these regions appears to be the limiting factor in meeting grain demand.

The results also indicate that total energy demand in China will increase by a factor of 4.7 (or 370%) from 1995 to 2025. Although the demand for coal will decrease slightly relative to oil, natural gas, and nuclear energy, coal will remain the dominant fuel source in China, growing by a factor of 3.5 (or 250%) by the year 2025. As a result of this increased energy use, total CO_2 emissions in China will increase by a factor of 4.5 (or 350%) from 1995 to 2025, indicating that it may be difficult to effectively limit future worldwide emissions without Chinese cooperation. CH_4 emissions from the energy sector will increase from 11.3 to 46.0 million metric tons of CH_4 ($MmtCH_4$) (a factor of 4.1, or 307%), and CH_4 emissions from the agricultural sector will increase from approximately 26.4 $MmtCH_4$ in 1995 to 37.3 $MmtCH_4$ in 2025 (over 40%). Although the agricultural sector is currently the primary source of CH_4 in China, the energy sector will overtake the agricultural sector as the primary source by the year 2025.

Assuming that China is to remain on its current course of rapid economic growth and expanding population, the results of this modeling and analysis have several implications. In particular:

1) The future availability of water in the northeastern provinces may depend on additional transfers of water from southern China and the Chang Jiang (Yangtze River) (economic, technical, and political feasibility will play a role);

2) Agricultural production may need to move from northeastern China to the water-plentiful provinces in southern China (assuming that there is land available for agriculture);

3) China may need to concentrate on growing fruits and vegetables while relying on imports to satisfy increasing grain requirements;

4) China's energy demand will continue increasing at an annual rate of approximately 5.3%, even with improvements in overall energy intensities. This is likely to result in increased oil imports and translates into a 350% increase in CO_2 emissions and a 300% increase in CH_4 emissions by the year 2025.

5) Chinese greenhouse gas emissions will continue growing at a rapid rate, even if the country is able to meet is ambitious plans for increasing reliance on both hydro and nuclear power.

Intentionally Left Blank

ACRONYMS AND ABBREVIATIONS

C	carbon
CH_4	methane
CO_2	carbon dioxide
CPPA	Country Projections and Policy Analysis Model
DSSAT	Decision Support System for Agrotechnology Transfer
EIA	Energy Information Administration
ERIM	Environmental Research Institute of Michigan
GDP	gross domestic product
GIS	geographic information system
HFCs	hydrofluorocarbons
IPCC	Intergovernmental Panel on Climate Change
m^3	cubic meters
Mha	millions of hectares
mtce	metric tons of coal equivalent
mtC	metric tons of carbon
Mmt	million metric tons
Mmtce	million metric tons of coal equivalent
MmtC	million metric tons of carbon
$MmtCH_4$	million metric tons of CH_4
N_2O	nitrous oxide
PFCs	perfluorocarbons
SF_6	sulfur hexafluoride
SNL	Sandia National Laboratories
USDA/ERS	U.S. Department of Agriculture/Economic Research Service
WRI	World Resources Institute

Intentionally Left Blank

CONTENTS

EXECUTIVE SUMMARY v
ACRONYMS AND ABBREVIATIONS ix
INTRODUCTION 1
BACKGROUND 5
APPROACH 7
Model Integration 7
Coupling of Water and Agronomic Models 8
Coupling of Agronomic and Greenhouse Gas Models 9
Coupling of Energy and Greenhouse Gas Models 9
Fully Integrated China Infrastructure Model 9
Drainage Regions 10
The Water Model 12
The Agronomic Model 13
The Energy Model 15
The Greenhouse Gas Model 15
Collaborative Environment 16
RESULTS 17
Water Resources 17
Haihe 18
Huanghe 21
Agriculture 24
Energy 27
Base Case Simulation 27
High-Nuclear-and-Hydropower Investment Scenario 28
Constant Energy Intensities 28
Low- (Base Case) Versus High-Infrastructure Investment 30
Greenhouse Gas Emissions 31
CO_2 Emissions From Energy Production, Distribution, and Consumption – Base Case 31

CONTENTS (cont.)

CO_2 Emissions – High-Nuclear-and-Hydropower Investment Scenario 33
CO_2 Emissions – Constant Energy Intensities 33
CH_4 from the Agricultural and Energy Sectors – Base Case 34
VALIDITY 35
Water Model 35
Water Model Assumptions 35
Water Model Data 36
Agronomic Model 37
Assumptions for the Agronomic Model 37
Data for the Agronomic Model 38
Energy and Greenhouse Gas Models 38
Comparison with Other Studies 39
COMMENTARY 41
Summary and Conclusions 41
Recommendations 42
Model Integration 43
Water Model 43
Agronomic Model 44
Energy and Greenhouse Gas Models 45
Expanding the Models 46
REFERENCES 47
APPENDIX A – THE CHINA WATER MODEL A-1
APPENDIX B – THE CHINA AGRONOMIC MODEL B-1
APPENDIX C – THE CHINA ENERGY MODEL C-1
APPENDIX D – THE CHINA GREENHOUSE GAS MODEL D-1
APPENDIX E – ADDITIONAL CHINA INFRASTRUCTURE MODEL RESULTS E-1

FIGURES

Figure 1. Model logic diagram. 3

Figure 2. Coupled flows of commodities between the infrastructure models in the integrated China model. 8

Figure 3. The 10 river drainage regions of China. 11

Figure 4. Distribution of land area, runoff, and cultivated land between the northeastern, southern, and northwestern river drainage regions of China. 12

Figure 5. All-China population growth, 1980–2025. 14

Figure 6. Comparison of the results of a single run of stochastic modeling of available water and surface and groundwater use with two projections of total water requirements in the Haihe region. 19

Figure 7. Comparison of the results of a single run of stochastic modeling of total available water and water use in the urban, industrial, and agricultural sectors with projected total water requirements in the Haihe region. 20

Figure 8. Predicted water deficit for the Haihe region through the year 2025 generated in 100 replications of the simulation model. 21

Figure 9. Comparison of the results of a single run of stochastic modeling of available water and surface and groundwater use with two projections of total water requirements in the Huanghe region. 22

Figure 10. Comparison of the results of a single run of stochastic modeling of total available water and water use in the urban, industrial, and agricultural sectors with projected total water requirements in the Huanghe region 23

Figure 11. Predicted water balance for the Huanghe region through the year 2025 generated in100 replications of the simulation model. 24

Figure 12. All-China grain, meat, and “other” demand, 1980–2025. 25

Figure 13. Grain and “other” demand for each water drainage region, 1980–2025. 25

Figure 14. Grain demand and land and water needs and availability for the Haihe region, 1980–2025. 26

Figure 15. Grain demand and land and water needs and availability for the Huanghe region, 1980–2025. 27

Figure 16. Projected energy demand and per capita GDP for China through 2025. 29

Figure 17. Fuel consumption for China through 2025. 29

Figure 18. Nuclear and hydropower shares for the base case and for the high-nuclear-and-hydropower scenario through 2025. 30

Figure 19. Comparison of excess demand for coal, oil, and natural gas for the low- (base case) and high-production infrastructure investment scenarios. 31

FIGURES (cont.)

Figure 20. Projected total Chinese CO_2 emissions for 2005, 2015, and 2025 compared with Chinese, U.S., and total world CO_2 emissions for 1995. 32

Figure 21. Projected CO_2 emissions for the base case and for the high-nuclear-and-hydropower investment scenario. 33

Figure 22. Estimated methane from energy and agriculture, 1995–2025..... 34

Figure 23. Enhanced integration of commodity exchange between critical infrastructures..... 43

TABLES

Table 1. Expected Frequency of Each Region Experiencing a Water Deficit through the Year 2025 and the End-Use Sector Affected 18

Table 2. Projected Energy Demand and Fuel Consumption for China through 2025..... 28

Table 3. Results of the Constant-Energy-Intensities Scenario 30

Table 4. China's Projected Oil Import Requirements 31

Table 5. Chinese Greenhouse Gas Emissions (CO_2) from Energy Production, Distribution, and Consumption through 2025 32

Table 6. Results of Constant Energy Intensities Scenario for CO_2 Emissions..... 33

Table 7. CH_4 Emissions from Energy Production, Distribution, and Consumption and from Agriculture in China through 2025 ($MmtCH_4$) 34

Table 8. Comparisons of the 1995 Projected Grain and Meat Demand Values Generated by the Agronomic Model with 1994–96 Consumption Data from the USDA/ERS 39

Table 9. Comparison of Base Case Energy and Greenhouse Gas Results to Other Studies 40

INTRODUCTION

Infrastructure systems, such as those supplying water, agricultural goods, and energy, constitute the foundation of economic, social, and political systems. Understanding the global dynamics of these complex systems, including the environmental impacts, is becoming crucial for making intelligent policy decisions as we prepare for the twenty-first Century and the emerging integrated world economy. China's increasing population, rapid industrialization, and rising affluence have raised questions about China's capacity for meeting its long-term food needs and about the impact of a potential Chinese grain deficit on the world economy. Questions have also been raised about the impact of greenhouse gas emissions that are likely to be generated as a result of increased energy use and agricultural production. As indicated in the following statements, these issues are of no small concern.

"For the first time in history, the environmental collision between expanding human demand for food and some of the earth's natural limits will have an economic effect that will be felt around the world." —Lester R. Brown, *Who Will Feed China?*, W.W. Norton & Company, New York & London, 1995.

"We have reached a fundamentally new stage in the development of human civilization, in which it is necessary to take responsibility for a recent but profound alteration in the relationship between our species and our planet. Because of our technological power and our growing numbers, we now must pay careful attention to the consequences of what we are doing to the Earth—especially to the atmosphere." —Al Gore, Vice President of the United States, Third Conference of the Parties to the United Nations Framework Convention on Climate Change, Kyoto, Japan, December 8, 1997.

The purpose of this report is to present the results of a comprehensive analysis of the critical infrastructures[1] of the People's Republic of China. This analysis is part of Global Approaches to Infrastructure Analysis (GAIA), an ongoing effort at Sandia National Laboratories (SNL) to study infrastructures throughout the world in order to promote economic and political stability in regions that are important to the U.S. GAIA is a unique and effective approach to analyzing critical infrastructures. It was designed to provide assistance to international decision makers who deal with complex issues involving the management of critical infrastructures by providing them with timely worldwide access to relevant information, expertise, and technology. Additional information on GAIA can be found at http://www.igaia.sandia.gov.

The integrated China infrastructure model presented in this report is a comprehensive state-of-the-art model that successfully combines four dynamic infrastructure models—water, agronomic, energy, and greenhouse gas—to simulate, respectively, hydrologic budgetary processes, grain production and consumption, energy demand, and greenhouse gas emissions in China through the year 2025. The purpose of the analysis is to obtain a better understanding of China's ability to meet its increasing grain requirements and energy needs and the greenhouse

[1] For the purposes of this report, an infrastructure is defined as "critical" if its management is of vital importance of the interests of the United States.

gas emissions that are likely to be generated as a result of increased energy use and agricultural production through the year 2025. The integrated model simulates diverse flow networks of commodities, such as water and greenhouse gas, between the separate models to capture the overall dynamics of the system and more accurately project the outcomes of changes in the commodity flows. It operates on a platform that generates results quickly (within minutes rather than hours or weeks), presents the results visually, demonstrates the relationships between the key variables, and allows the user to make adjustments for various "what if" scenarios and policy options concerning available water use, water-constrained grain production, caloric consumption, population growth, grain yield, sectoral gross domestic product (GDP) growth, sectoral energy intensities, fuel shares, energy requirements, and greenhouse gas emissions.

As shown in Figure 1, the integrated model couples commodity flows for water, methane (CH_4), and carbon dioxide (CO_2) (solid arrows) between the separate infrastructure models. Additional commodity flows that have been proposed for future modeling are also presented in the figure (dotted arrows). The figure also identifies the six greenhouse gases addressed in the Kyoto Protocol.[2] Only two of these, CH_4 and CO_2, were modeled for the analysis presented in this report.

The integrated China infrastructure model was used to generate projections of China's available water resources, expected water use, and grain consumption and production for 10 river drainage regions representing 100% of China's mean annual runoff and comprising 37 major river basins. Projections of growth in energy use for all of China in each of six historically significant sectors—agriculture, industry, construction, transportation, commerce, and residential (and other) are also generated, as are projections of greenhouse gas emissions for all of China from energy production, consumption, and distribution and from animals and their waste products as well as flooded rice paddies.

The approach section immediately following this introduction describes the logic that was used in the analysis and the model integration, summarizes the four infrastructure models, and describes the analyses that were performed. The section following the approach presents the results. This is followed by a section that discusses the validity of the models and the data. The report closes with a commentary section, which provides a summary and recommendations.

[2] The Kyoto Protocol was adopted at the Third Conference of the Parties (COP-3) to the United National Framework Convention on Climate Change (FCCC) on December 11, 1997. The signing parties agreed to commitments to reduce their overall emissions of six greenhouse gases—CO_2, nitrous oxide (N_2O), CH_4, hydrofluorocarbons (HFCs), perfluorocarbons (PFCs) and sulphur hexafluoride (SF_6)—between 2008 and 2012 to at least 5% below 1990 levels.

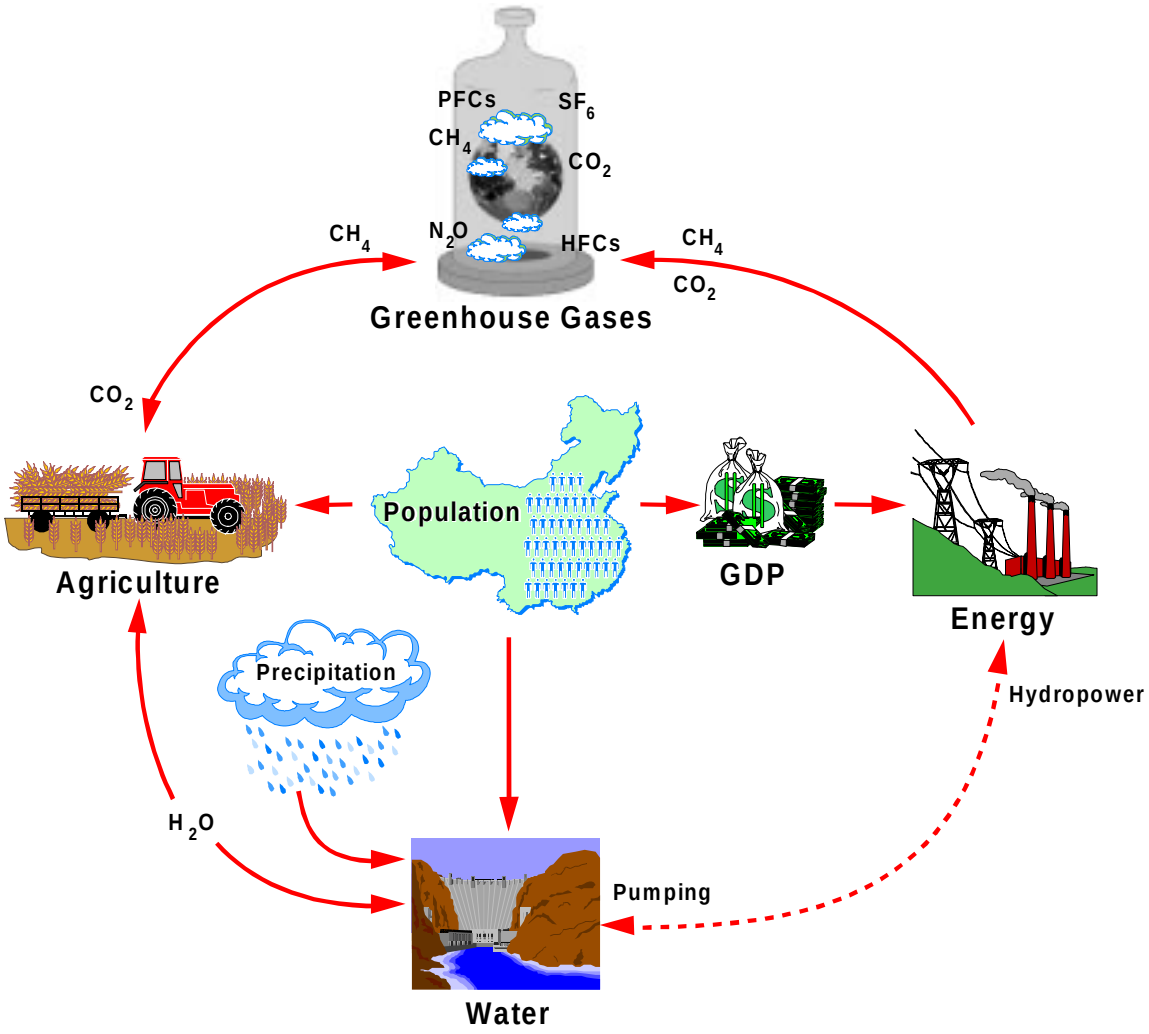

Figure 1. Model logic diagram.

Intentionally Left Blank

BACKGROUND

In January 1996, a project was initiated by the Medea group of scientists at the request of the National Intelligence Council (NIC) to improve the understanding of future grain production and consumption in the People's Republic of China and to make a preliminary assessment of the impact of potential grain shortfalls in China on the world grain market. This effort, the NIC-Medea China Project, was undertaken to address the question raised by Lester R. Brown in his book *Who Will Feed China?:* Will China's economic and population growth, coupled with a declining amount of arable land, drive major increases in the demand for grain imports and result in dramatically increased world food prices in the near future?[3] The complete effort involved input from the U.S. Department of Agriculture (USDA), the U.S. Geological Survey (USGS), the Environmental Research Institute of Michigan (ERIM), the National Photographic Interpretation Center (NPIC), the Central Intelligence Agency (CIA), SNL, and the Defense Intelligence Agency (DIA). Sandia's contribution to the project included an analysis of China's water resources.[4]

Sandia's analysis of China's water resources for the NIC-Medea China Project involved developing a dynamic water model that would simulate the hydrologic budgetary processes in five river basins in northeastern, central, and southern China: the Chang Jiang (Yangtze River), Huanghe (Yellow River), Haihe, Huaihe, and Liaohe. The model was designed to assess the effects of changes in water use in the three end-use sectors—urban, industrial, and agricultural—on the availability of water in each basin and to develop estimates of the water surpluses and/or deficits in each basin through the year 2025. A dynamic agronomic model was also developed to generate projections of the water required to service China's agricultural sector and to compare China's projected grain production with projected grain consumption requirements to estimate any grain surplus and/or deficit. The results of the NIC-Medea analysis, published in *Understanding the Dynamics of Water Availability and Use in China* (Thomas et al., 1997), were considered preliminary.

In the year following the NIC-Medea Project, SNL embarked on an effort to expand and refine the China water and agronomic models. This effort became Phase II of the China infrastructure analysis. In the initial effort, these two models were designed to interface bidirectionally in order to provide for the exchange of information on projected water use requirements and available water. The interface, however, had not yet been completed at the time that the NIC-Medea preliminary results were generated, and for that project it was necessary to enter output on water available for agriculture generated by the water model into the agronomic model manually. One of the first refinements in the year following the NIC-Medea Project was the completion of this interface. The geographic area analyzed in the models was also expanded from five river basins to all of China, and the data on interbasin water transfers in the water model was updated to include three interbasin transfers that have been planned for the future by the Chinese government. In addition, the Decision Support System for Agrotechnology

---

[3] See Brown (1995). The issues raised in Brown's book were originally published as an article by Worldwatch Institute in 1994 under the same title.

[4] The DIA and Ogden Energy and Environmental Services also contributed to the effort.

Transfer (DSSAT) crop model was engaged to obtain statistical yield coefficients and both nominal average and stochastic water consumption rates for the three major grains under investigation.

Additional efforts during Phase II of the modeling effort involved the development of two additional dynamic models—energy and greenhouse gas—to simulate energy demand and greenhouse gas emissions in China through the year 2025. The energy model was developed to project the growth in energy use in all of China in six historically significant end-use sectors. The greenhouse gas model was designed to generate projections of greenhouse gas emissions from the production, consumption, and distribution of energy and from animals and their waste products as well as flooded rice paddies. The four models—water, agronomic, energy, and greenhouse gas—were then integrated into a comprehensive critical infrastructure model for all of China that would allow for the exchange of information between the separate models and capture the overall dynamics of the integrated system. As described in the report, this involved coupling the commodity flows for water, CH_4, and CO_2 between the separate infrastructure models.

APPROACH

Dynamic models of four critical infrastructures—water, agriculture, energy, and greenhouse gas—were developed to simulate, respectively, the hydrologic budgetary processes, grain production and consumption, energy demand, and greenhouse gas emissions in China for the period 1980–2025. Each model was developed using the POWERSIM Constructor 2.5 modeling system.[5] The four models were integrated into a comprehensive critical infrastructure model for all of China. Each model was required to meet the following three general design constraints:

1) While simulating the flows of various commodities through its respective infrastructure, each model must be capable of being integrated into a single dynamic system model in a straightforward fashion to allow for the simulation of the flows of commodities between the models;
2) Each model must be executable on a World Wide Web-based server engine; and
3) Each model must be robust in that it can be applied to a variety of geographic regions by simply changing the input database.

The integration of the four infrastructure models is described below. This is followed by a description of the water drainage regions used in the water and agronomic models, summaries of each of the four models, and a description of the collaborative environment that was created by installing the fully integrated executable model on the World Wide Web.

Model Integration

Infrastructures such as energy, agriculture, transportation, and water constitute the foundation of economic, social, and political systems. They are complex and dynamic systems that can be thought of as diverse flow networks of commodities. Changes in the flows of commodities in one infrastructure often affect the flows of commodities in other infrastructures—positively and/or negatively, creating interdependencies. Although modeling the separate infrastructures as discrete systems may provide useful information, integrating the models allows for the exchange of information between the separate models, captures the overall dynamics of the integrated system or set of systems, and can more accurately project the outcomes of changes in the commodity flows. When the fully integrated model is executed, the resulting projections provide information about changes that occur in the flows over time resulting from changes in the system's basic drivers (such as available water, population growth, GDP, and arable land) as well as about the interactions between commodities.

Each of the four models was developed to provide information regarding its respective infrastructure. To summarize, the water model was designed to assess the effects of changes in water use requirements in the urban, industrial, and agricultural end-use sectors on the availability of water and to develop estimates of China's water surplus and/or deficit. The

[5] POWERSIM is a dynamic simulation tool that allows the user to track the flow or movement of a commodity, such as water or greenhouse gas, over time. POWERSIM provides feedback mechanisms so that both the internal and external dynamics of the system being modeled can be simulated.

agronomic model was developed to compare China's projected grain consumption requirements based on population growth with projected grain production to estimate any grain surplus and/or deficit. The agronomic model was also designed to generate projections of the cultivated land area and the amount of water required to service China's agricultural sector. The energy model was developed to project the growth in use of coal, oil, natural gas, hydroelectric power, and nuclear power in each of six sectors (agriculture, industry, construction, transportation, commerce, and residential (and other)) based on alternative scenarios of future growth in China's GDP and sector energy intensities. The greenhouse gas model was designed to project the greenhouse gas loading (CH_4 and CO_2) for all of China and to compare these projections with world totals.

The integration of the four China infrastructure models consisted of the coupling of commodity flows for water, CH_4, and CO_2 between 1) the water model and the agronomic model, 2) the agronomic model and the greenhouse gas model, and 3) the energy model and the greenhouse gas model. Figure 2 illustrates the flows of commodities between the models.

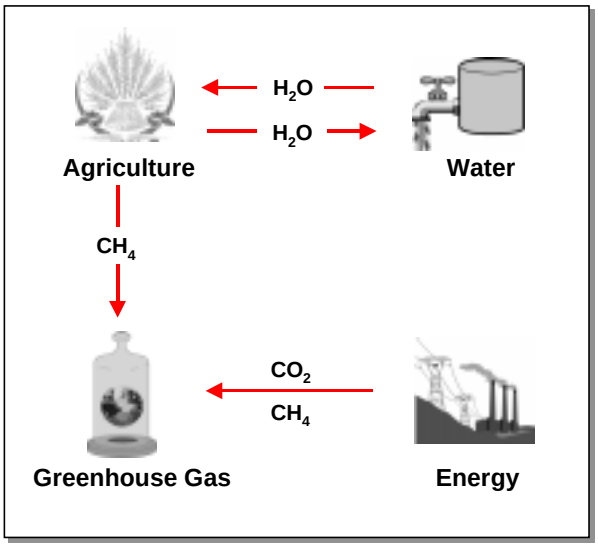

Figure 2. Coupled flows of commodities between the infrastructure models in the integrated China model.

Coupling of Water and Agronomic Models

The water and agronomic models were coupled to exchange information on projected water use requirements and available water. The allocation of the available water is a dynamic process that is dependent on changes in water use requirements. The water available for the agricultural sector is projected by the water model as a function of 1) the total extractable water and 2) water management policies for allocating water between the urban, industrial, and agricultural end-use sectors. The projected water available for agriculture is input directly into the agronomic model as a constraint on the ability of the agricultural sector to produce grain. Using this input, the agronomic model then projects the water-constrained grain production.

The agronomic model also determines the amount of water needed by the agricultural sector on the basis of population-driven grain demand.[6] The resulting projected agricultural water use requirement is linked to the water model where it is used to calculate the water surplus and/or deficit.

Coupling of Agronomic and Greenhouse Gas Models

The agronomic model provides information to the greenhouse gas model on methane (CH_4) emissions resulting from the biomass decay in rice paddies and from enteric and anaerobic fermentation in farm animals. The total area in millions of hectares (Mha) that is cultivated in rice to meet each region's projected share of the all-China grain demand (allocated on the basis of each region's share of historic grain production in order to project the land and water required in each region to meet that demand) is projected in the agronomic model, and the results are linked directly with the greenhouse gas model where the agricultural contribution to the greenhouse gas loading level is calculated. Animal population projections are used to calculate farm animal contributions to greenhouse gas emissions.[7]

Coupling of Energy and Greenhouse Gas Models

The energy model was integrated with the greenhouse gas model to calculate projected changes in the greenhouse gas loading resulting from changes in energy production, distribution, and consumption.[8] The energy model projects the demand for coal, oil, natural gas, hydropower, and nuclear energy. This energy demand is used to determined the CO_2 and CH_4 loading from the energy sector.

Fully Integrated China Infrastructure Model

Precipitation and, more specifically, runoff is the primary driver in the analysis for quantifying the amount of available water over time (both surface water and groundwater). Water use projections through 2025 are generated using population growth as a basis for the industrial and urban end-use sectors and using historical grain production[9] as the basis for the agricultural sector. The analysis accounts for return flow (recycled water) from each of the three sectors back to the water supply. Note that the water model imposes sustainable yield constraints. These are violated when groundwater withdrawals exceed an amount equal to the average recharge plus agricultural return flows; if the available water does not meet the water use

---

[6] In the model, the amount of water needed by the agricultural sector in each region is further allocated on the basis of regional grain production.

[7] For purposes of the China model, historical data on herd populations were used to calculate the animal greenhouse gas emissions.

[8] For the analysis presented in this report, the greenhouse gas model calculated CH_4 and carbon dioxide (CO_2) emissions.

[9] The grain production data was provided by the U.S. Department of Agriculture/Economic Research Service (USDA/ERS) Country Projection and Policy Analysis (CPPA) Model (*Medea Project (2/10/97): LOTUS Spreadsheet)).*

requirements, a deficit results.[10] The projected total water requirements are compared with projections of available water to estimate any water surplus and/or deficit and to determine the expected frequency of water deficits. Population-driven all-China grain consumption requirements can also be computed and compared with projected domestic grain production to estimate any grain surplus and/or deficit.

The primary drivers for quantifying energy demand are GDP and the energy intensities for the six historically significant sectors—agriculture, industry, construction, transportation, commerce, and residential (and other). The energy demand is translated into production and consumption by fuel type—coal, oil, natural gas, hydroelectric, and nuclear energy. These translations are used to determine the CO_2 and CH_4 loading from the energy sector. CO_2 and CH_4 emissions resulting from biomass decay in rice paddies and from enteric and anaerobic fermentation in farm animals are also computed.

Drainage Regions

The projections of China's available water resources, expected water use, and grain consumption and production were made in the water and agronomic models for 10 river drainage regions representing 100% of China's mean annual runoff and comprising 37 major river basins.[11] The locations of the 10 regions are shown in Figure 3. Two of the regions, the Chang Jiang (Yangtze River) and the Huanghe (Yellow River), consist of single large river basins; the other eight, the Heilongjiang, Liaohe, Haihe, Huaihe, Southeast Coastal, Pearl River, Southwest China, and Inland Rivers are aggregations of two or more smaller river basins. Table A-1 in Appendix A identifies the river basins in each region.

The ten drainage regions can be grouped into three major geographic areas that are nearly equal in area but that have unequal amounts of cultivated land and water resources—northeastern, northwestern, and southern China. The regions in northeastern China are more intensively cultivated and populated than those in southern and northwestern China. They also receive less rainfall. Three of the four cities with the greatest populations are located in northeastern China, in the Haihe (Beijing and Tianjin) and in the Liaohe (Shenyang) (the fourth is Shanghai, which is located in the Chang Jiang region on the eastern seaboard).

The most abundant water is in the less populated and less cultivated area of southern China. The four regions located in southern China, Chang Jiang, Southeast Coastal, Pearl River, and Southwest China, represent 84% of the runoff[12] but only 36% of the cultivated land,[13] while the five regions in northeastern China, Heilongjiang, Liaohe, Haihe, Huaihe, and Huanghe, represent 12% of the runoff and 60% of the cultivated land (see Figure 4). Data from China's Ministry of Water Resources indicate that the average annual surface water runoff in the Chang Jiang region alone consists of more than a third of China's total runoff. Another 22% of China's runoff flows from the region of Southwest China into South Asia (Department of Hydrology, Ministry of

---

[10] The sustainable yield constraint was imposed because estimates for groundwater reserves were not available (see Appendix A for further discussion on the sustainable yield constraint).

[11] Energy use and greenhouse gas loading were projected for all of China only.

[12] *Water Resources Assessment for China* (Department of Hydrology, Ministry of Water Resources, 1992).

[13] Calculated from data from the ERIM *GIS Database of China Land Use* (ERIM Earth Sciences Group, 1997).

Figure 3. The 10 river drainage regions of China.

Water Resources, 1992). Northwestern China, which consists of only one drainage region, the Region of Inland Rivers, represents only 4% of both total cultivated land and runoff.

The most abundant water is in the less populated and less cultivated area of southern China. The four regions located in southern China, Chang Jiang, Southeast Coastal, Pearl River, and Southwest China, represent 84% of the runoff[14] but only 36% of the cultivated land,[15] while the five regions in northeastern China, Heilongjiang, Liaohe, Haihe, Huaihe, and Huanghe, represent 12% of the runoff and 60% of the cultivated land (see Figure 4). Data from China's Ministry of Water Resources indicate that the average annual surface water runoff in the Chang Jiang region alone consists of more than a third of China's total runoff. Another 22% of China's runoff flows from the region of Southwest China into South Asia (Department of Hydrology, Ministry of Water Resources, 1992). Northwestern China, which consists of only one drainage region, the Region of Inland Rivers, represents only 4% of both total cultivated land and runoff.

[14] *Water Resources Assessment for China* (Department of Hydrology, Ministry of Water Resources, 1992).

[15] Calculated from data from the ERIM *GIS Database of China Land Use* (ERIM Earth Sciences Group, 1997).

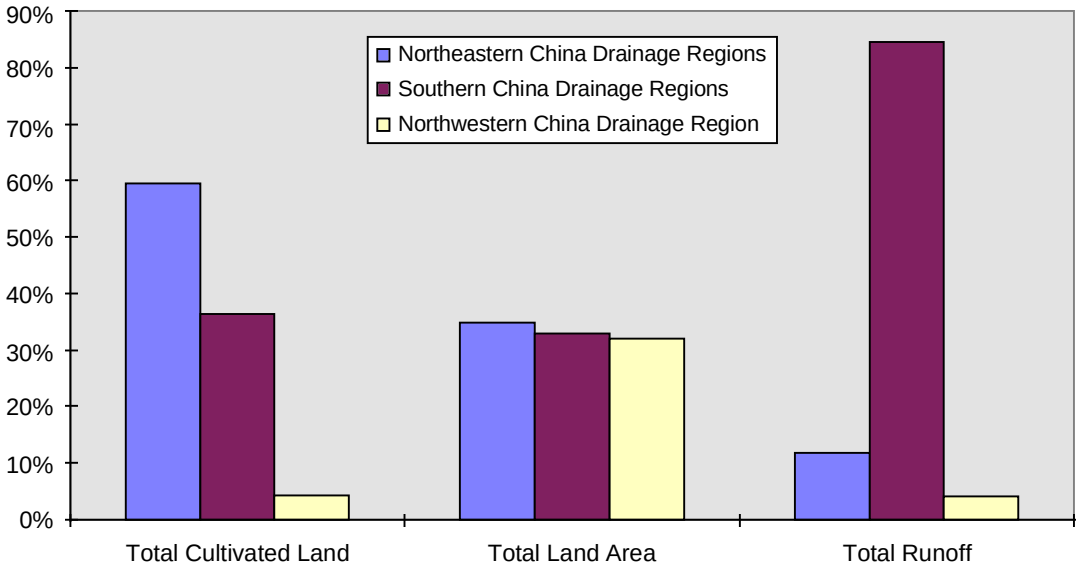

Figure 4. Distribution of land area, runoff, and cultivated land between the northeastern, southern, and northwestern river drainage regions of China.

The Water Model

The water model has two main simulation components: 1) a model of the hydrologic system that quantifies the amount of extractable water available within each of the 10 water drainage regions and 2) a model of the water use requirements. The hydrologic component simulates the main elements of the hydrologic cycle—precipitation, surface water, and groundwater—in each region and the movement of water to and from these components via runoff, groundwater recharge, groundwater discharge, evapotranspiration, and discharge to the ocean, as well as the transfer of water from one region to another by canal (interbasin transfer). The water use component projects the extraction of water from both surface water and groundwater and its allocation between the urban, industrial, and agricultural sectors. A water use priority scheme is imposed as follows: urban sector requirements are met first, industrial requirements are met second, and agricultural requirements receive the lowest priority. Agricultural water requirements can either be 1) computed within the water model using data obtained from the Chinese government or 2) imported from the agronomic model, which computes water use on the basis of historical grain production.

The water model allows for both deterministic and stochastic modeling of precipitation and runoff. In the deterministic setting, average annual precipitation and average annual runoff are used in each time step. In the stochastic setting, a series of correlated random values is generated for annual rainfall and runoff using a normal distribution, mean, and standard deviation for each of these parameters. Projections of total available water and total water use requirements as well as water use requirements for each end-use sector in each region can be compared to estimate any water surplus or deficit and determine the expected frequency of each region experiencing a water deficit.

For purposes of the results presented in this report, the analysis included 1) stochastic modeling of the total available water in each region through the year 2025 using an array of data representing the 10 drainage regions[16] and 2) comparison of these results with projections of total water use in each region for the period from 1980 to 2025 to determine the expected frequency of each region experiencing a water deficit through the year 2025. Agricultural water use requirements for each region were computed in the China agronomic model and channeled directly into the water model. Water use requirements for the industrial and urban sectors were based on a linear function using values for 1980 water use and for expected water use in the year 2000 obtained from the China Ministry of Water Resources.[17] The water deficit was estimated for each region by generating 100 replications of the simulation model and computing the mean and standard deviation of the water deficit for each year through 2025. The available water and total water use were also modeled for all of China and for the northeastern and southern geographic areas using the regional data to obtain an overview of China's water balance. Appendix A contains a detailed description of the China water model and the data elements that were used in the analysis.

The Agronomic Model

The China agronomic model was designed to:

- Generate population-driven projections of China's grain and meat demand;
- Generate projections of regional and all-country land and water resources required to meet the grain demand;
- Generate projections of each region's contribution to China's total grain production;
- Compare China's projected grain demand with projected grain production to estimate grain surpluses and deficits;
- Provide projections of agricultural water requirements to the water model; and
- Provide projections of the total land area cultivated in rice and estimates of livestock population to the greenhouse gas model.

The agronomic model is composed of two segments, a *demand projection segment* and a *production transformation segment*. The demand projection segment computes population-driven all-China projected grain and meat demand. It also allocates the all-China grain demand among the 10 water drainage regions so that each region's projected share of the all-China grain demand is proportional to its share of the historical grain production. This allows the user to generate projections of the land and water required in each region to meet this allocated demand and then, by comparing these projections with projections of available land and water in each region, determine whether each region has sufficient water and land resources to continue to produce its share of the grain needed to meet the all-China demand. The segment also provides

[16] The data were compiled from several sources, including Chinese government agency publications and maps. See Appendix A for a full listing of the sources and for detailed information on the data that were used.

[17] These data appear in Tables A-7 and A-8 of Appendix A.

computed values for agricultural water requirements to the water model for use in the water balance computations and receives in return computed values for available water for use in projecting water-constrained agricultural production levels. The demand projection segment also provides projections of the total land area cultivated in rice and estimates of livestock population to the greenhouse gas model for modeling China's greenhouse gas emissions balance.

The production transformation segment of the model is used to convert the Chinese grain production agricultural-region data obtained from the U.S. Department of Agriculture/Economic Research Service (USDA/ERS) Country Projections and Policy Analysis (CPPA) Model (Medea Project, 1997) to grain production data for the water drainage regions by mapping the USDA/ERS agricultural regional data onto the water drainage regions. This region-to-region transformation is necessary because the China water model simulates hydrologic budgetary processes on the basis of river drainage regions rather than agricultural regions or political provinces, and converting the data makes it possible for the agronomic model to compute the production-based agricultural water requirements and the water-constrained grain production by water drainage region.

Figure 5 presents the all-China population growth, the driver for the agronomic model. This curve is based upon annual-percentage-increase data from *The Future of China's Grain Market* (Crook and Colby, 1996) through the year 2005, and from the United Nations' *World Population Prospects* (United Nations Department of International Economic and Social Affairs, 1993) thereafter.

See Appendix B for a detailed description of the China agronomic model and the data elements that were used in the analysis.

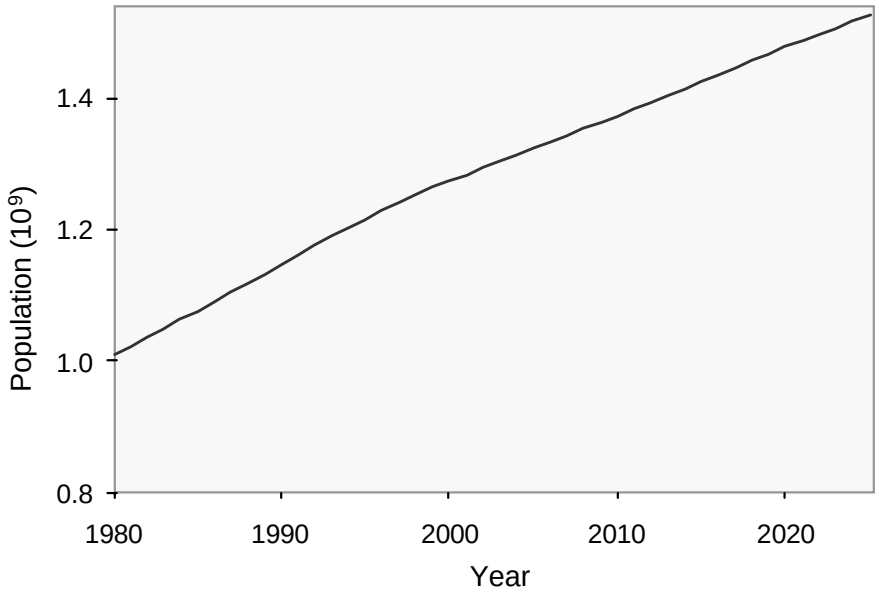

Figure 5. All-China population growth, 1980–2025.

The Energy Model

The China energy model projects the growth in energy use in all of China in six historically significant sectors—agriculture, industry, construction, transportation, commerce, and residential (and other). The drivers for simulating China's energy consumption are growth in GDP and decreasing sectoral energy intensities. To project GDP growth in the model, the user can select one of four scenarios of average annual growth rates for the periods 1996–2005, 2006–2015, and 2016–2025 or create a custom scenario. The user can also use base case assumptions for GDP sector shares or define 10-year sector-share end points. The model uses historical data for calculating energy demand for each sector by primary energy type (coal, oil, natural gas, and electricity) and relies on user-specified end points for calculating future demand. Assumptions regarding electricity fuel shares for nuclear and hydropower can also be changed by the user. Low- or high-infrastructure investment options may be used to calculate future production for each fuel type. Excess demand is calculated in the model as the difference between forecasted demand and production.

For purposes of the results presented in this report, the analysis included generating projections of energy demand and fuel consumption for China through 2025 for the base case (both nuclear and hydropower capture increasing shares in the base case, corresponding with official plans of the Chinese government) and for an alternative scenario with accelerated use of nuclear and hydropower.[18] Energy demand and fuel consumption were also projected for the scenario in which the sector energy intensities remain constant to examine the sensitivity of the results to the base case assumption of decreasing energy intensities over the study period.[19] Excess demand was calculated for low- (base case) and high-infrastructure investment scenarios to examine the sensitivity of the results to the production investment assumptions.[20] The results of the base case simulation were also compared with the results of three recent studies (see "Validity" section for discussion). See Appendix C for a detailed description of the China energy model and the data elements that were used in the analysis.

The Greenhouse Gas Model

Energy production and consumption result in the emission of greenhouse gases, including CO_2, CH_4, and nitrous oxide (N_2O). Agricultural processes serve as both a source and a sink for

[18] The base case assumes that installed nuclear capacity will grow from 2.1 GW in 1994 to 32 GW by 2020 and that hydropower will increase from 36 GW in 1990 to 138 GW in 2020. The alternative scenario assumes that installed nuclear capacity will grow to 86 GW in 2020 (the equivalent of building over ninety-four 900-MW nuclear plants by 2020) and that the installed hydropower capacity will increase by 148 GW, to 286 GW. These numbers correspond to the high-substitution scenario in Johnson et al. (1996).

[19] The base case assumes that the sectoral energy intensities drop significantly over the study period (see Figure C-4 in Appendix C). For the case of constant energy intensities, China's total energy demand increases by a factor of 2.4 by the year 2005, 5.2 by the year 2015, and 9.3 by the year 2025, values that are significantly higher than the energy demand forecasted by the base case.

[20] The base case assumes that the production capacity for coal, oil, and natural gas will grow at the 10-year historic annual growth rate (coal, 4.59%; oil, 1.87%; and natural gas, 3.11%). The high-investment scenario assumes that a higher infrastructure investment will lead to a sustained increase in production capacity at the level of the 5 years with the highest growth in the last 10 years (coal, 6.92%; oil, 2.88%; and natural gas, 3.11%).

greenhouse gases. CO_2 is released as a result of land use changes, mainly deforestation, and is absorbed through uptake during photosynthesis; CH_4 is released from several sources including enteric fermentation in animals, anaerobic decomposition of animal wastes, and flooded rice paddies; and N_2O is released as a result of denitrification in soils, including denitrification of fertilizers. The greenhouse gas model projects emissions of CO_2 and CH_4 generated in the production (extraction), distribution (primarily natural gas pipelines), and consumption (burning) of coal, oil, and natural gas, and CH_4 emissions resulting from the decay of rice paddy biomass and from enteric and anaerobic fermentation in farm animals. The model uses carbon coefficients for Chinese coal, oil, and natural gas in metric tons of carbon (mtC) per metric ton of coal equivalent (mtce) to calculate CO_2 emissions. The model uses the methods outlined by the Intergovernmental Panel on Climate Change (IPCC) for Tier 1 (IPCC, 1994) for calculating national emissions of methane from energy production and consumption and for estimating agricultural emissions. Although N_2O emissions may be modeled in future versions of the model, these emissions were not modeled for the current analysis because significant uncertainties still remain in the existing methodologies that determine levels of N_2O generation and absorption. Additionally, although a methodology for estimating agricultural sinks of CO_2 was to be included in this study, it was not completed in time to be included in this report or version of the model.

The analysis for this report included base case projections of CO_2 and CH_4 emissions from energy production, consumption, and distribution through 2025. CO_2 emissions were also projected for the scenario of accelerated use of nuclear and hydropower (see footnote 18) and for the scenario in which the sectoral energy intensities remain constant over the study period. For agricultural emissions, the model focused solely on methane emitted directly from animals and their waste products and from flooded rice paddies. See Appendix D for a detailed description of the China greenhouse gas model and the data elements that were used in the analysis.

Collaborative Environment

A World Wide Web Internet server was installed with pages that document the results of the China model simulations presented in this report (http://www.igaia.sandia.gov). A Web-based model execution engine was also installed on the server and a graphical user interface was created to provide for remote execution of the integrated model and presentation of the simulation results. Because of its capabilities for real-time communication in the form of textual chat, audio, and video, the Internet provides a collaborative environment for policy planners, decision makers, subject-matter experts, and other interested parties to share information and results and to collaborate on the analysis of data. Analysts and decision makers with access to the Internet can communicate with each other to discuss pertinent issues, review model results, share relevant information, and collectively resolve issues in a timely fashion.

RESULTS

This critical infrastructure analysis of the People's Republic of China successfully combined the four dynamic infrastructure models—water, agronomic, energy, and greenhouse gas—into a comprehensive state-of-the-art integrated model capable of simulating the hydrologic budgetary processes, grain production and consumption, energy demand, and greenhouse gas emissions in China through 2025. The integration consisted of the coupling of the separate models to provide for the exchange of information on available water and water use between the water and agronomic models and to provide information on CH_4 emissions generated in the agricultural sector and CO_2 and CH_4 generated in the energy sector to the greenhouse gas model. The integrated model was developed using the POWERSIM Constructor 2.5 modeling system and allows the user to make adjustments for various "what if" scenarios and policy options concerning available water and water use, water-constrained grain production, caloric consumption, population growth, grain yield, sectoral GDP growth, sectoral energy intensities, fuel shares, energy requirements, and greenhouse gas emissions. The resulting projections, discussed below, provide information about China's critical infrastructures through 2025 in terms of water surpluses and/or deficits, population-driven grain demand, the land and water resources required to meet that demand, energy demand and fuel consumption driven by GDP and by sectoral intensities, and greenhouse gas emissions likely to result from increased energy use and agricultural production. The results are presented below as follows: water resources, agriculture, energy, and, finally, greenhouse gas emissions.

Water Resources

The analysis of China's water resources indicates that, on the basis of regional data, there is a surplus of water in China as a whole. This surplus, however, is not distributed evenly across China, and water deficits are being experienced on a regional basis. On the basis of regional data, 5 of the 10 regions—Chang Jiang, Southeast Coastal, Pearl River, Southwest China, and the Region of Inland Rivers—all located in southern and northwestern China, show a surplus of water throughout the study period. In the five regions located in northeastern China, however, water use requirements exceed the sustainable yield and deficits occur to varying degrees. In three of these regions, the Heilongjiang, Liaohe, and Huaihe, deficits begin to appear late in the study period. Two of the regions in northeastern China, the Haihe and Huanghe, however, experience significant and/or ongoing deficits throughout the study period. The results for these two regions are of particular significance. Serious water shortages have been reported in the area in recent decades (Economy, 1997; World Resources Institute, 1992; Zhang Qishun and Zhang Xiao, 1995). Beijing and Tianjin, two of the four Chinese cities with the greatest populations, are located in the Haihe region. Beijing has faced water shortages since it was founded in the 13th century; it was recently reported that the situation in the city is "extremely serious" (Economy, 1997, citing *Beijing Xinhua* (August 28, 1994) in Foreign Broadcasting Information Service (FBIS), *China Daily Report* (August 29, 1994)). Ocean water intrusion resulting from overextraction of groundwater has also been polluting groundwater reserves in Tianjin (Economy, 1997). Additionally, because the Huanghe region is a significant source for

interbasin transfers into the Haihe region, deficits in either of these regions will play significant roles in water scarcity issues in both regions.

Table 1 presents the expected frequency of each region experiencing a water deficit through the year 2025. As shown in the table, the expected frequencies are "almost always" and "always" for the Huanghe and the Haihe, respectively. This means that any given stochastic realization for these regions will show deficits "almost every year" or "every year" over the duration of the study period, respectively. The five regions located in southern China and in northwestern China—the Chang Jiang, Southeast Coastal, Pearl River, Southwest China, and Region of Inland Rivers—are expected to experience no deficits through the year 2025. The Heilongjiang, Liaohe, and Huaihe, all located in northeastern China, are expected to experience "almost" no deficits during the study period.

Table 1. Expected Frequency of Each Region Experiencing a Water Deficit through the Year 2025 and the End-Use Sector Affected

Region	Location in China	Frequency	End-Use Sector(s) Affected
Heilongjiang	Northeastern	Almost Never	Agricultural
Liaohe	"	Almost Never	Agricultural
Haihe	"	Always	Agricultural
Huanghe	"	Almost Always	Agricultural and Industrial
Huaihe	"	Almost Never	Agricultural
Chang Jiang	Southern	Never	None
Southeast Coastal	"	Never	None
Pearl River	"	Never	None
Southwest China	"	Never	None
Region of Inland Rivers	Northwestern	Never	None

The results for the Haihe and Huanghe regions are discussed below. See Appendix E for the results for the Heilongjiang, Liaohe, Huaihe, Southeast Coastal, Chang Jiang, Pearl River, and Southwest China regions and the Region of Inland Rivers and for figures showing single runs of the model for northwestern, northeastern, and southern China and for all of China based on regional data.

Haihe

Figure 6 presents the results of a single run of the simulation model through 2025 for the Haihe drainage region showing the available water and the breakdown of surface water and

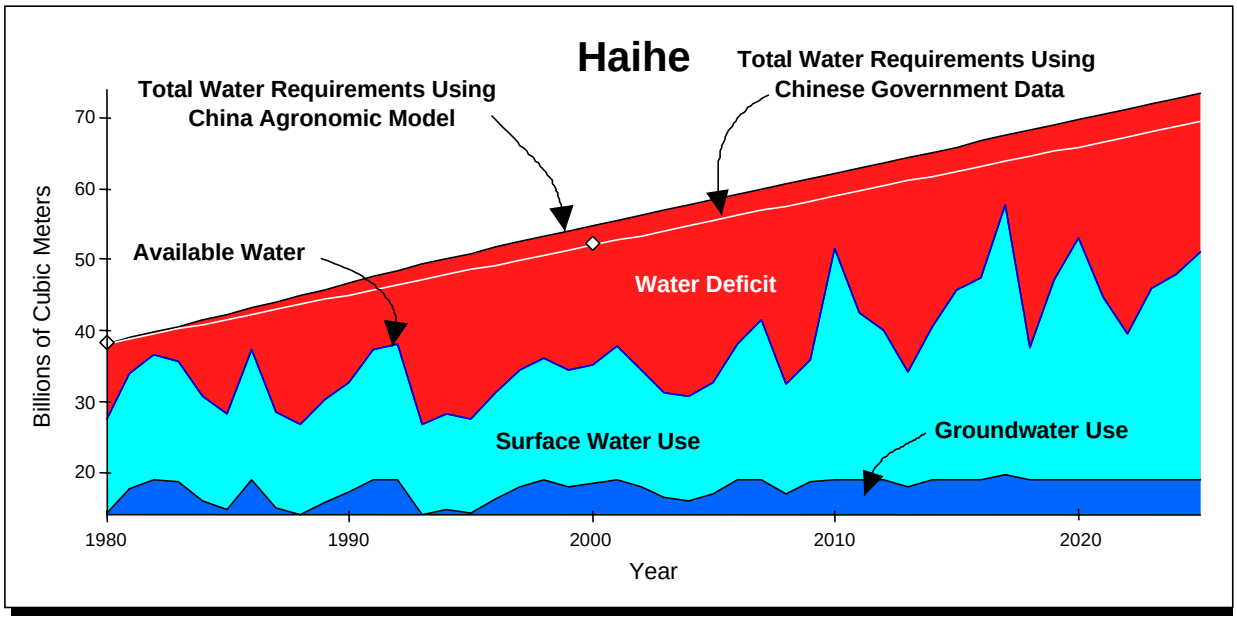

Figure 6. Comparison of the results of a single run of stochastic modeling of available water and surface and groundwater use with two projections of total water requirements in the Haihe region. The two projections of total water requirements were generated using 1) agricultural water requirements computed by the China agronomic model and 2) a linear projection of agricultural water requirements based on data from the China Ministry of Water Resources.

groundwater use. The run generated a series of correlated random values for annual rainfall and runoff using a normal distribution of historic precipitation and runoff data. Figure 6 also presents two projections of total water requirements for the Haihe region, one generated using agricultural water requirements computed by the China agronomic model, the other generated using a linear projection of agricultural water requirements based on data from the China Ministry of Water Resources.

As indicated in Figure 6, the two projections of total water requirements for the Haihe both exceed the combined total of sustainable water available from surface water, groundwater, and interbasin transfers throughout the study period. The difference between the total water requirements and the available water is the water deficit, which, it is assumed, is being met by ongoing groundwater mining, a practice that is not sustainable. The overall increase in available water after the year 2010 is due to additional interbasin transfers that are planned to come on line in that year; the transfers help the situation, but do not eliminate the deficit. Although this figure illustrates a single run of the simulation, it is reasonably representative of the predicted water deficit for this drainage region. Note that the projection that used agricultural water requirements computed by the China agronomic model shows slightly greater total water requirements throughout the study period and thus a larger water deficit than does the projection that used data from the China Ministry of Water Resources.

Figure 7 presents the results of a single stochastic run of the simulation model through 2025 for the Haihe drainage region and the breakdown of water use by sector. Note that the impact of

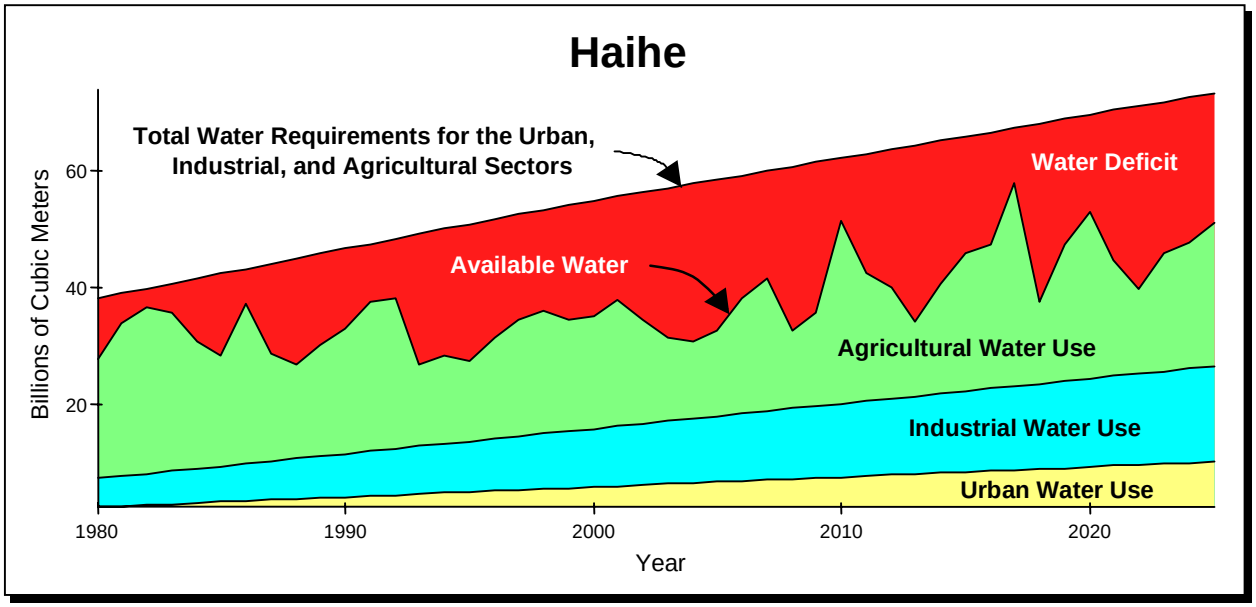

Figure 7. Comparison of the results of a single run of stochastic modeling of total available water and water use in the urban, industrial, and agricultural sectors with projected total water requirements in the Haihe region. Total water requirements include agricultural water requirements generated in the China agronomic model.

the deficit is felt first by the agricultural sector; if the deficit were large enough, the industrial sector would be impacted next and the urban sector last. As shown in Figure 7, the urban and industrial water requirements for the Haihe drainage region are met through the year 2025. The agricultural sector deficit steadily worsens throughout the study period. In 2010, additional interbasin transfers are planned that will bring an additional 10 billion cubic meters of water into the drainage region from the Chang Jiang. Although the interbasin transfers improve the situation, they do not eliminate the deficit. The deficits in the agricultural sector are due not only to the increasing water requirements for agriculture but also to increasing urban and industrial requirements, which receive priority.

Figure 8 illustrates the predicted water deficit for the Haihe drainage region through the year 2025 estimated by generating 100 replications of the simulation model and computing the mean and standard deviation of the water deficit for each year through 2025. The increase in water availability that occurs in 2010 is due to the additional interbasin transfers that are expected to come on line in that year. Calculations based on the assumptions used in the model indicate that there is a probability of 0.68 that the actual water deficit will lie between the upper and lower curves in the figure. For example, the water deficit in the Haihe drainage region is expected to reach 26 billion cubic meters by 2025, and the actual deficit for that year is projected to be between 22 and 30 billion cubic meters, with a probability of 0.68.

As stated above, it is assumed that this deficit is being met by ongoing groundwater mining, that is, the water is being extracted at a faster rate than the aquifer is being recharged. This assumption is confirmed by reports that groundwater mining is already under way in the most intensively cultivated and populated areas of northeastern China, particularly around the Beijing

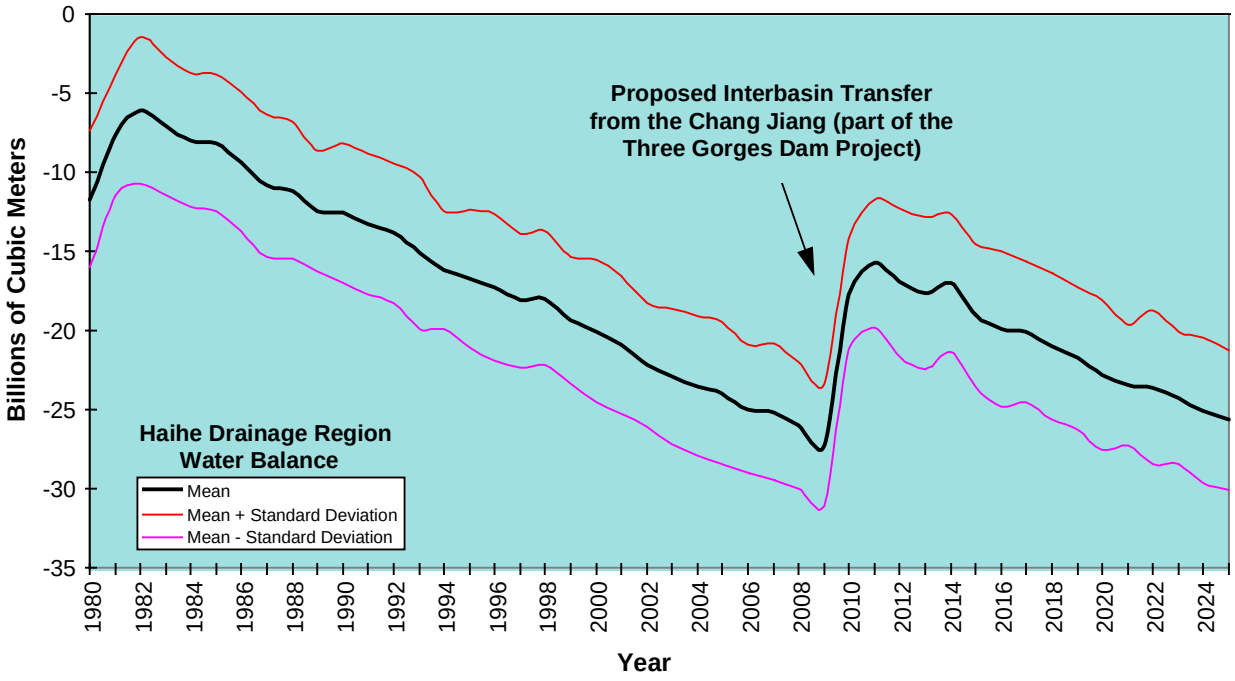

Figure 8. Predicted water deficit for the Haihe region through the year 2025 generated in 100 replications of the simulation model.

area (see, e.g., Economy, 1997; World Resources Institute, 1992; Zhang Qishun and Zhang Xiao, 1995). Groundwater mining in the Haihe cannot continue indefinitely, but is limited to the extent and availability of water in the aquifer. Dropping water tables in the region will make groundwater resources increasingly more difficult and expensive to obtain, until the cost of further extraction is no longer economical. At such a time, users in the Haihe region will be forced to return to extracting water at the sustainable yield. Overextraction is also likely to contribute to a reduction in the quality of the extracted groundwater and a lowered dilution capacity for pollutants.

Huanghe

Figure 9 presents the results of a single run of the simulation model through 2025 for the Huanghe region showing the available water and the breakdown of surface water and groundwater use. The run generated a series of correlated random values for annual rainfall and runoff using a normal distribution of historic precipitation and runoff data. Figure 9 also presents two projections of total water requirements for the Huanghe region, one generated using agricultural water requirements computed by the China agronomic model, the other generated using data from the China Ministry of Water Resources for the years 1980 and 2000.

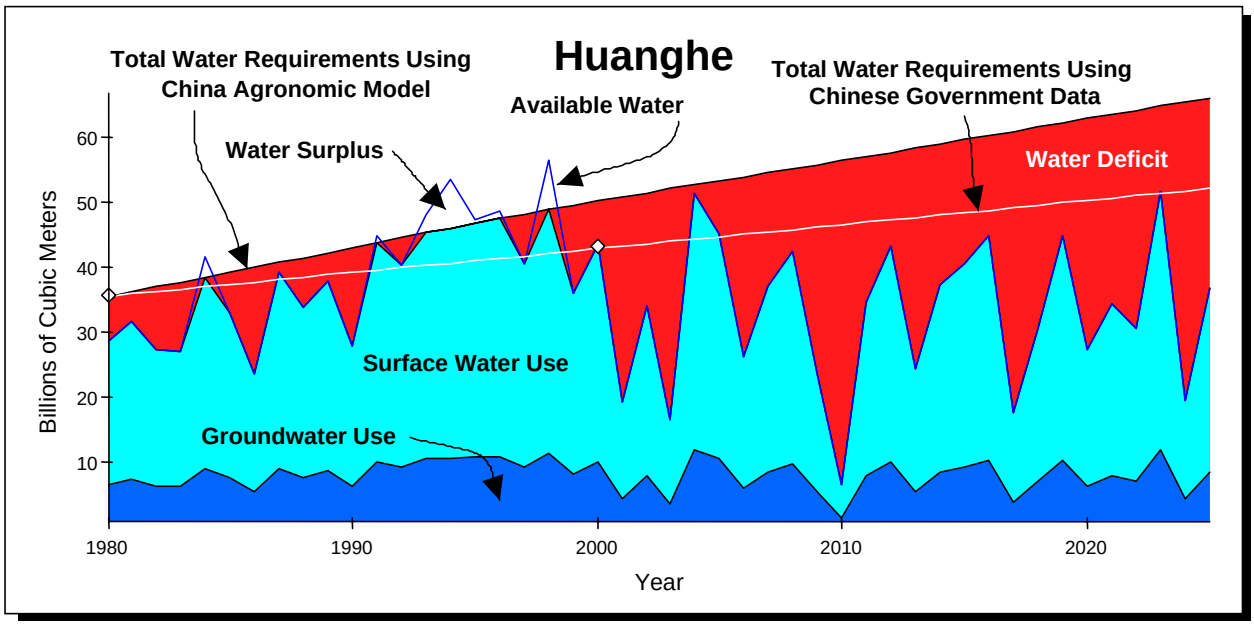

Figure 9. Comparison of the results of a single run of stochastic modeling of available water and surface and groundwater use with two projections of total water requirements in the Huanghe region. The total water requirements were generated using 1) agricultural water requirements computed by the China agronomic model and 2) a linear projection of agricultural water requirements based on data from the China Ministry of Water Resources.

As indicated in Figure 9, comparison of the projected total water requirements with the projection of water available from surface water and groundwater indicates that, although some surplus is indicated in the region in the first half of the study period, the total water requirements exceed the combined total of sustainable water available from surface water and groundwater on an ongoing basis in the second half of the study period. As is the case with the Haihe region, it is assumed that the resulting deficit is being met by groundwater mining, a practice that is not sustainable. Although this figure illustrates a single run of the simulation, it is reasonably representative of the predicted water deficit for this drainage region. The projection generated using the China agronomic model also indicates greater total water requirements and thus a larger water deficit throughout the study period than does the projection generated using data from the China Ministry of Water Resources.

Figure 10 presents the results of a single stochastic run of the simulation model through 2025 for the Huanghe drainage region and the breakdown of water use by sector. As shown in Figure 10, water requirements for the Huanghe region are met in the urban sector throughout the study period; a deficit occurs in the industrial sector, however, at 2010. Water deficits occur in the agricultural sector throughout most of the study period and become severe in the second half of the study period.

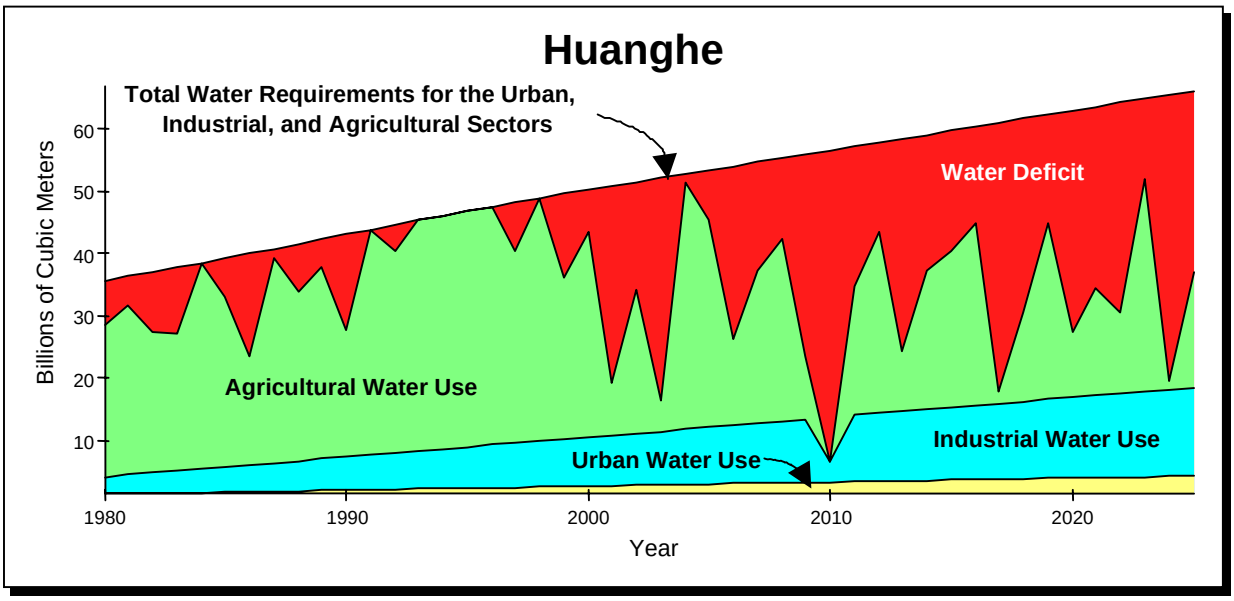

Figure 10. Comparison of the results of a single run of stochastic modeling of total available water and water use in the urban, industrial, and agricultural sectors with projected total water requirements in the Huanghe region. Total water requirements include agricultural water requirements generated in the China agronomic model.

Figure 11 illustrates the predicted water balance for the Huanghe region through the year 2025 estimated by generating 100 replications of the simulation model and computing the mean and standard deviation of the water deficit for each year through 2025. Calculations based on the assumptions used in the model indicate that there is a probability of 0.68 that the actual water deficit will lie between the upper and lower curves in the figure. For example, the water deficit in the Huanghe drainage region is expected to reach 28 billion cubic meters by 2025, and the actual deficit for that year is projected to be between 18 and 38 billion cubic meters, with a probability of 0.68. Note that, although the Huanghe region begins the study period with a much smaller deficit than does the Haihe region, by 2025 the deficit for the Huanghe is expected to be approximately the same as that predicted for the Haihe (compare Figures 8 and 11). This is because interbasin transfers are planned in 2010 for the Haihe that will bring an additional 10 billion cubic meters annually from the Chang Jiang into that region. The Haihe also receives interbasin transfers from the Huanghe region.[21] Deficits in the Huanghe are thus likely to also play significant roles in water scarcity issues in the Haihe region in the coming years.

[21] A total of 8 billion cubic meters has been diverted into the Haihe and Huaihe regions annually from the Huanghe since before 1980. According to the Chinese government, diversions from the Huanghe into the Huaihe will increase by 1 billion cubic meters by the year 2000 (Water Resources and Hydropower Design Institute of the Ministry of Water Resources, 1989). For input to the model, annual transfers of 6 billion cubic meters were assigned to the Haihe and 3 billion cubic meters to the Huaihe from the Huanghe beginning in 1980. See Appendix A for more information.

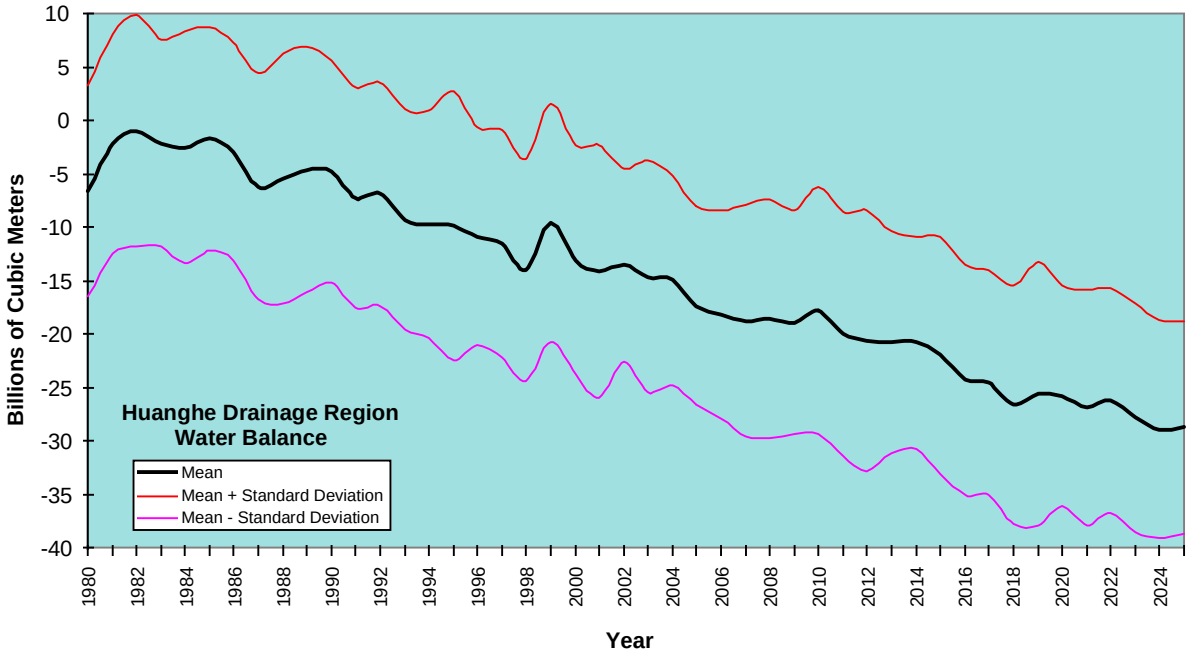

Figure 11. Predicted water balance for the Huanghe region through the year 2025 generated in 100 replications of the simulation model.

Agriculture

The results for the agronomic model are presented below. These include the projected all-China demand for the three major grains (corn, wheat, and rice), meat, and "other" (including other grains and fruits and vegetables) and each region's share of the all-China grain demand (allocated on the basis of each region's share of historic grain production). Comparisons of the amount of land needed in the Haihe and Huanghe regions to meet each region's share of the total demand with initial estimates of arable land in each region are compared, as are the water required to meet the allocated grain demand and the available water in the two regions. The results for the Heilongjiang, Liaohe, Huaihe, Southeast Coastal, Chang Jiang, Pearl River, and Southwest China regions and for the Region of Inland Rivers are presented in Appendix E.

Figure 12 presents the all-China food demand from 1980 to 2025 generated by the agronomic model for the three major grains (corn, wheat, and rice), meat, and "other" (including other grains and fruits and vegetables). The figure includes not only food consumed by humans but also grains and "other" used as feedstock for meat animals that are eventually consumed by humans. These results were generated by apportioning the annual caloric demand for all of China according to historical human consumption data for these food categories for all of China for the years 1994–96 from Crook and Colby (1996). The additional grains and "other" food consumed by meat animals were computed using meat animal feed conversion efficiencies.

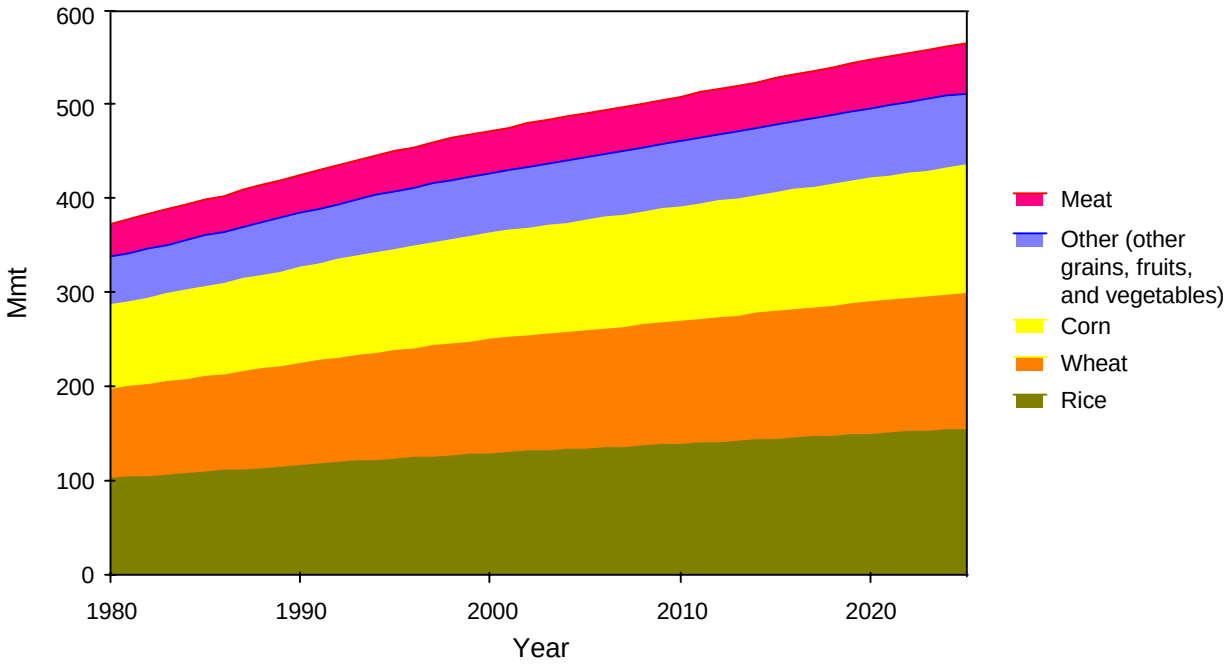

Figure 12. All-China grain, meat, and "other" demand, 1980–2025.

Figure 13 shows the regional all-China grain and "other" demand (excluding meat) allocated by the model on the basis of each region's share of historic grain production. To enable this allocation, agricultural-region production data from the USDA/ERS CPPA Model (Medea Project, 1997) was first transformed to water-drainage-region grain production data (by mapping

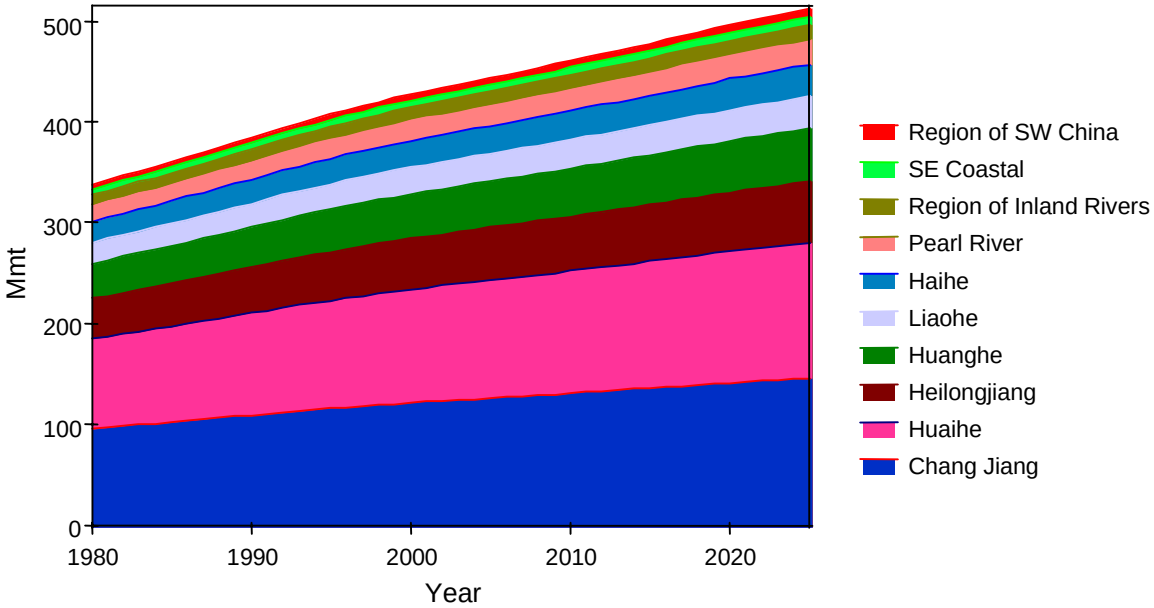

Figure 13. Grain and "other" demand for each water drainage region, 1980–2025.

the USDA/ERS data onto the water drainage regions), and the all-China demand was then apportioned to the regions according to the ratio of each drainage region's historical production to the all-China production.

Figures 14 and 15 present results generated for the Haihe region and the Huanghe region, respectively. (Results for the Heilongjiang, Huaihe, Chang Jiang, Liaohe, Pearl River, Southeast Coastal, Southwest China, and Inland River regions are presented in Appendix E.) Each figure presents the region's projected share of the all-China grain demand (allocated on the basis of each region's share of historic grain production) and the land and water needed to produce the grain to meet that allocated demand. For comparison, the figures also present the estimated total arable land and the total water available for agriculture within each region. The land and water requirements were generated using the deterministic option in the model. The amount of arable land (assumed for this analysis to be a constant) was estimated using a geographic information system (GIS) analysis that identified all land with a slope less than 1%. The available water was computed by concurrently running the China water model in the deterministic mode (average annual precipitation and average annual runoff were used in each time step). Additional figures in Appendix E present the results for the Haihe and Huanghe regions showing land needs and agricultural water requirements generated using the stochastic option for grain yields and water consumption.

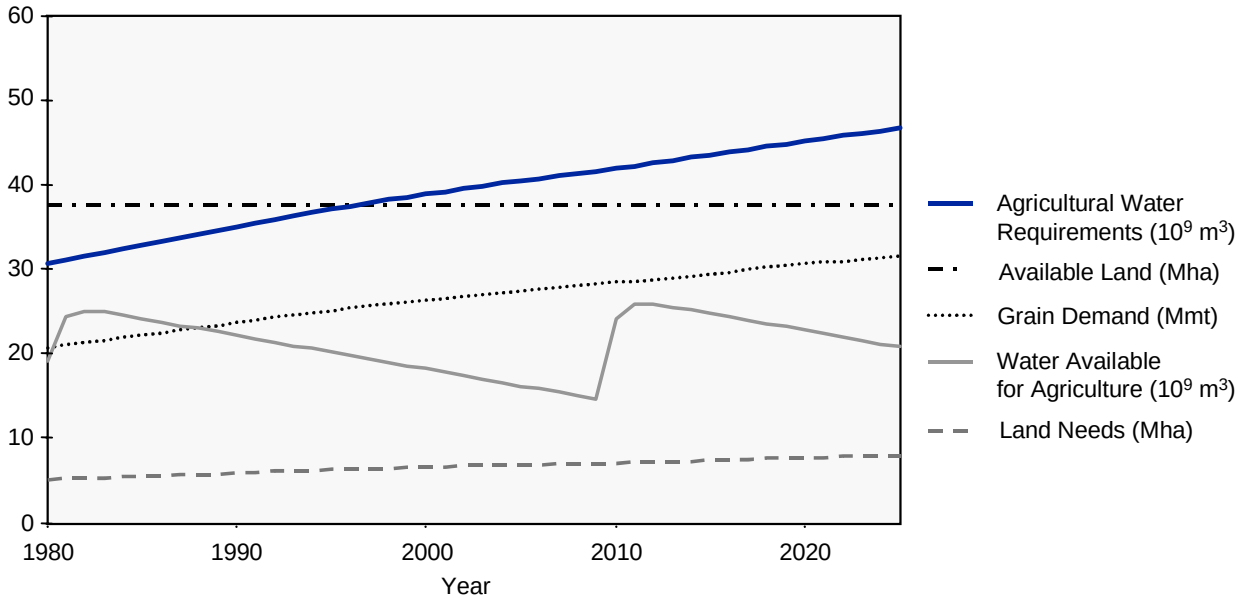

Figure 14. Grain demand and land and water needs and availability for the Haihe region, 1980–2025.

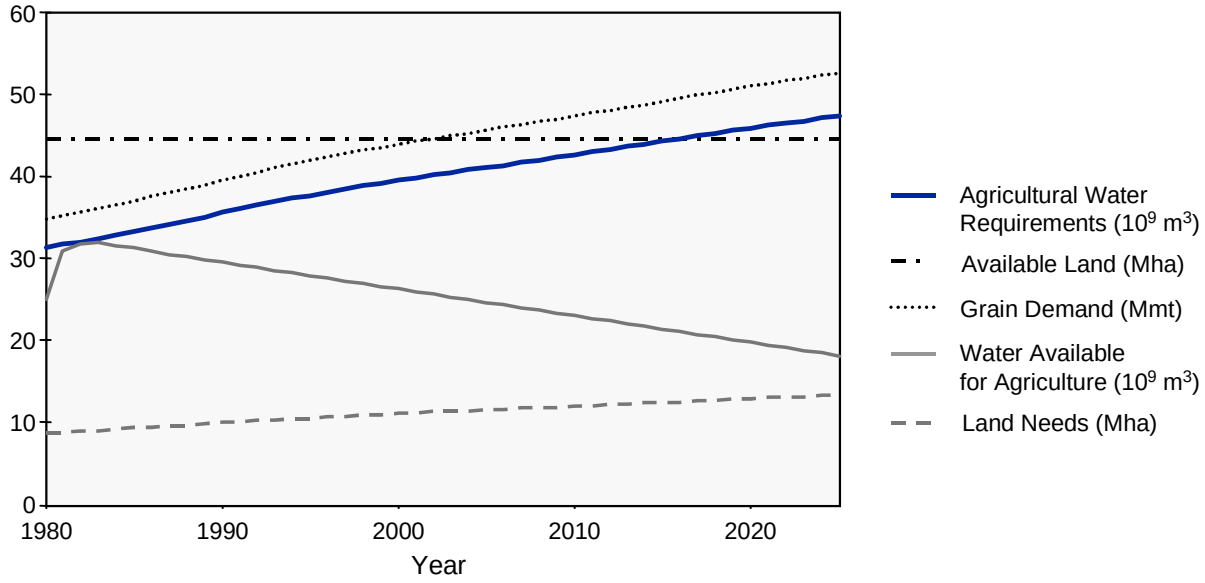

Figure 15. Grain demand and land and water needs and availability for the Huanghe region, 1980–2025.

Energy

The results for the energy model simulation using the base case assumptions are described below. These results are contrasted with the results from the high-growth-nuclear-and-hydropower scenario and the scenario of constant energy intensities. The base case (low-investment scenario) results are further contrasted with the results for the high-investment scenario.

Base Case Simulation

The results for the base case simulation are presented in Table 2 with the corresponding population and GDP for each year in the projection. Figure 16 presents the total energy demand for coal, oil, natural gas, and electricity and the per capita GDP for China through 2025. The percent fuel shares for coal, oil, natural gas, hydropower, and nuclear power through 2025 are presented in Figure 17. Total energy demand increases by a factor of 1.8 (or 80%) from 1995 to 2005, 3.0 (or 200%) from 1995 to 2015, and 4.7 (or 370%) from 1995 to 2025. These factors translate into annual growth rates of 5.9% for the period from 1995–2005, 5.5% for the period from 2006–2015, and 4.4% for the period from 2016–2025. Coal remains the dominant fuel source, growing by a factor of 3.5 by 2025. Coal's relative share, however, decreases from 73.1% in 1995 to 67.6% in 2025 as the shares provided by oil, natural gas, and nuclear increase (see Figure 17).

Table 2. Projected Energy Demand and Fuel Consumption for China through 2025

	Year			
	1995	2005	2015	2025
Population (millions)	1,205	1,312	1,421	1,540
GDP (billion 1978 yuan)	1,173	2,829	5,911	10,490
Per Capita GDP (yuan)	974	2,154	4,157	6,813
Energy Demand (Mmtce*)				
Coal	633	993	1,511	2,222
Oil	204	412	758	1,237
Natural Gas	21	39	76	135
Electricity	369	736	1,377	2,218
Total	1,226	2,179	3,721	5,811
Total Energy Demand (quads)	34.0	60.5	103.4	130.7
Fuel Shares (%)				
Coal	73.1	69.4	68.1	67.6
Oil	19.2	21.8	23.6	24.6
Natural Gas	1.8	1.9	2.2	2.5
Hydropower	5.8	5.5	4.5	3.7
Nuclear Power	<1.0	1.3	1.6	1.6

* Mmtce = million metric tons coal equivalent.

High-Nuclear-and-Hydropower Investment Scenario

Figure 18 compares the results of the high-nuclear-and-hydropower scenario with the base case results. This comparison indicates that a more rapid substitution of hydro and nuclear power for coal would have minimal effects in terms of overall fuel shares.

Constant Energy Intensities

Table 3 summarizes the sensitivity of the results to the base case assumption that sectoral energy intensities drop significantly over the study period. These results demonstrate the potential impact that improvements in overall energy efficiency might have on future energy demand.

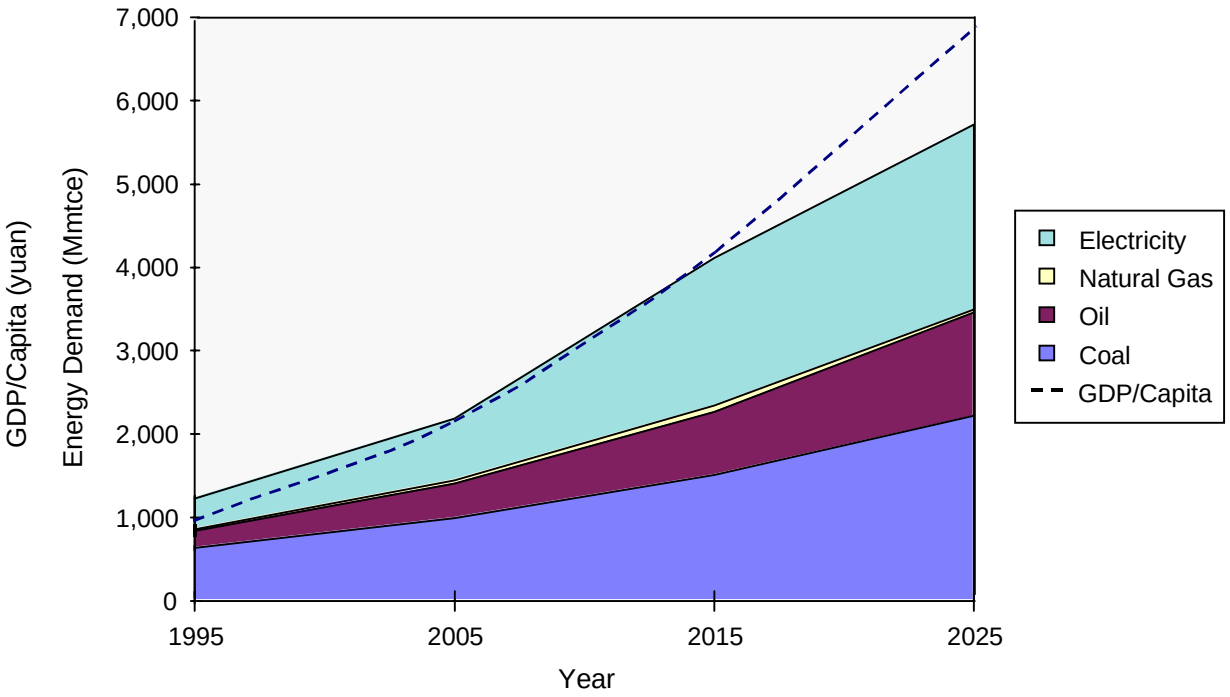

Figure 16. Projected energy demand and per capita GDP for China through 2025.

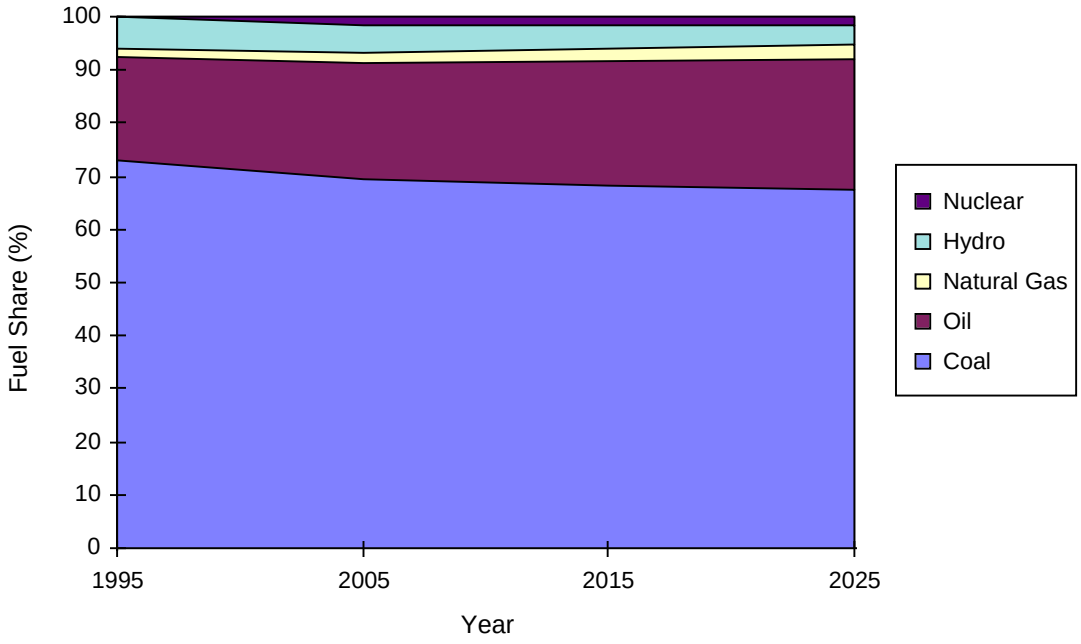

Figure 17. Fuel consumption for China through 2025.

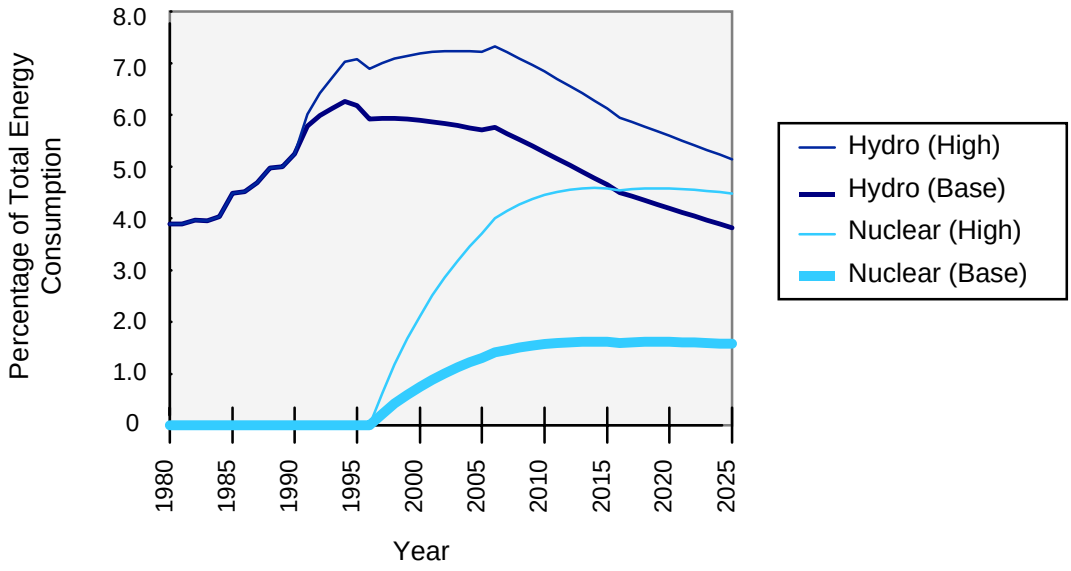

Figure 18. Nuclear and hydropower shares for the base case and for the high-nuclear-and-hydropower scenario through 2025.

Table 3. Results of the Constant-Energy-Intensities Scenario

	Year		
Total Energy Demand (Mmtce)	2005	2015	2025
Base Case	2,179	3,721	5,811
Constant Energy Intensities	2,979	6,367	11,457

Low- (Base Case) Versus High-Infrastructure Investment

Figure 19 demonstrates the sensitivity of the base case results to the production investment assumptions for oil, coal, and natural gas. As shown in Figure 19, demand exceeds production capability in all cases except that of coal under the high-investment scenario. The very large excess production capability for coal is not a surprise given the assumed 6.92% average annual growth for coal production (see footnote 17). This indicates that China will either have to vastly increase oil and natural gas infrastructure investments or that it will have to import oil and natural gas in order to meet the projected demand. For oil, the results translate into required imports of 7.1 to 8.1 million barrels per day by 2015 and 13.1 to 14.9 million barrels per day by 2025 (see Table 4). McCreary et al. (1996) forecast oil shortages of 5.9 to 8.8 million barrels per day by 2015.

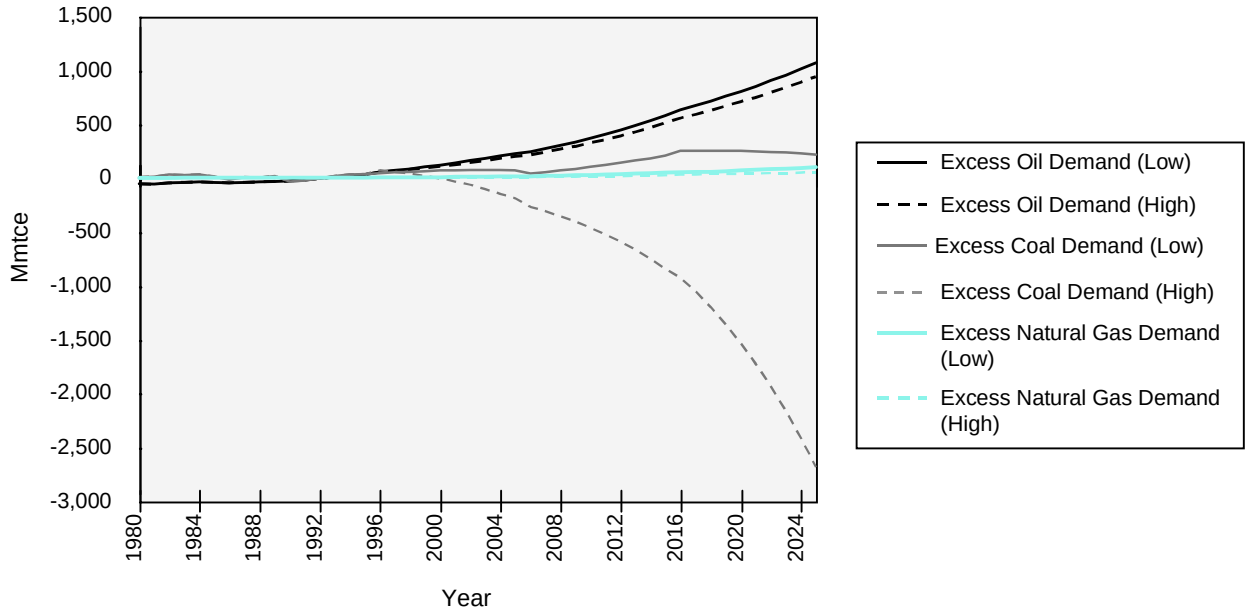

Figure 19. Comparison of excess demand for coal, oil, and natural gas for the low- (base case) and high-production infrastructure investment scenarios.

Table 4. China's Projected Oil Import Requirements

	Oil Import Requirements (million barrels/day)		
Scenario	2005	2015	2025
Low investment	3.1	8.1	14.9
High investment	2.8	7.1	13.1

Greenhouse Gas Emissions

The results for the greenhouse gas model simulation are described below. The base case simulation for CO_2 emissions from energy production, distribution, and consumption are discussed first, followed by the results for CH_4 emissions from the agricultural sector and the energy sector. The results for CO_2 from energy production, distribution, and consumption for the base case simulation are then contrasted with those for the high-growth-nuclear-and-hydropower scenario. The CO_2 base case results are then contrasted with the results for the scenario of constant energy intensities.

CO_2 Emissions From Energy Production, Distribution, and Consumption – Base Case

The large increase in fossil fuel consumption indicated by the base case energy model results presented in Table 2 translates into large increases in greenhouse gas emissions resulting from

the production and distribution of energy, as shown in Table 5. China's total CO_2 emissions increase from 717 million metric tons of carbon[22] (MmtC) in 1995 (11.9% of the total 1995 world emissions of 6,013 MmtC (EIA 1997))[23] to 3,391 MmtC in 2025 (a factor of 4.5, or 350%). By 2025, China will generate CO_2 in an amount that is more than half that of the total current (1995) worldwide CO_2 emissions, demonstrating the potential difficulty of effectively limiting future worldwide emissions without Chinese cooperation (see Figure 20). On a per capita basis, Chinese emissions increase from 0.6 mtC in 1995 to 2.2 mtC in 2025, approximately 38% of current U.S. per capita emissions (5.4 mtC in 1995) (EIA, 1997).

Table 5. Chinese Greenhouse Gas Emissions (CO_2) from Energy Production, Distribution, and Consumption through 2025

	Year			
	1995*	2005	2015	2025
CO_2 Emissions (MmtC)	717	1,260	2,158	3,391
CO_2 Emissions per Capita (mtC)	0.60	0.96	1.52	2.20
CO_2 Emissions (% of 1995 total world emissions)	11.6	20.8	35.6	56.0

* Source: EIA, 1997.

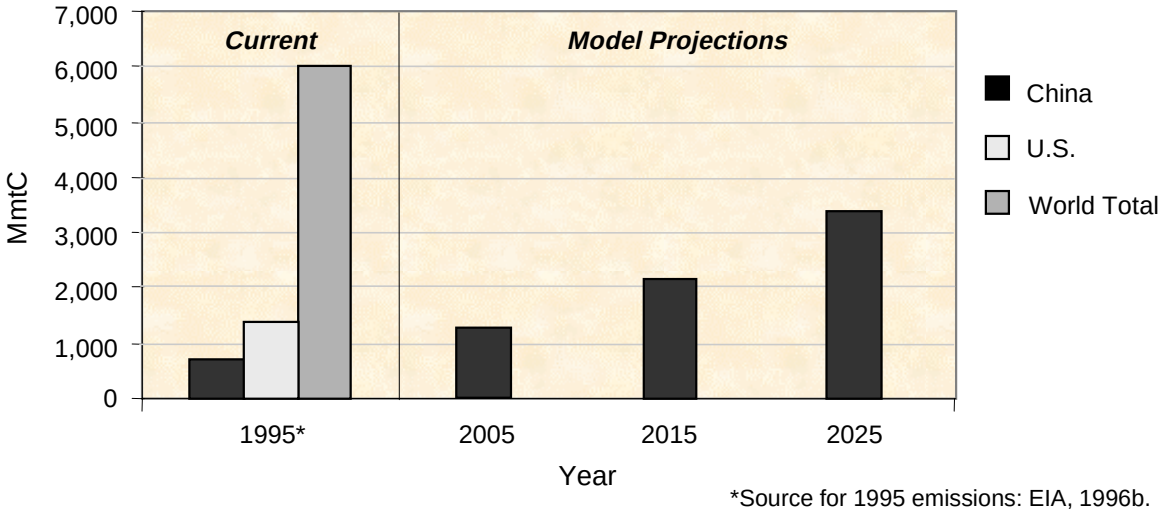

*Source for 1995 emissions: EIA, 1996b.

Figure 20. Projected total Chinese CO_2 emissions for 2005, 2015, and 2025 compared with Chinese, U.S., and total world CO_2 emissions for 1995.

[22] CO_2 emissions are reported in carbon units, defined as the weight of the carbon content of CO_2.

[23] The most current EIA values for worldwide CO_2 emissions at the time of publication were from 1995.

CO_2 Emissions – High-Nuclear-and-Hydropower Investment Scenario

The minimal effect in terms of overall fuel shares of the substitution of hydropower and nuclear power for coal in this scenario (see Figure 18 and accompanying text) also translates to minimal impact on total projected greenhouse gas emissions. In terms of CO_2 emissions, this scenario results in a reduction of 163 MmtC per year by 2025, a 4.8% reduction from the base case emission rate of 3,391 MmtC per year (see Figure 21).

CO_2 Emissions – Constant Energy Intensities

Table 6 summarizes the sensitivity of the results to the base case assumption that sectoral energy intensities drop significantly over the study period. These results demonstrate the potential impact that improvements in overall energy efficiency might have on future greenhouse gas emissions.

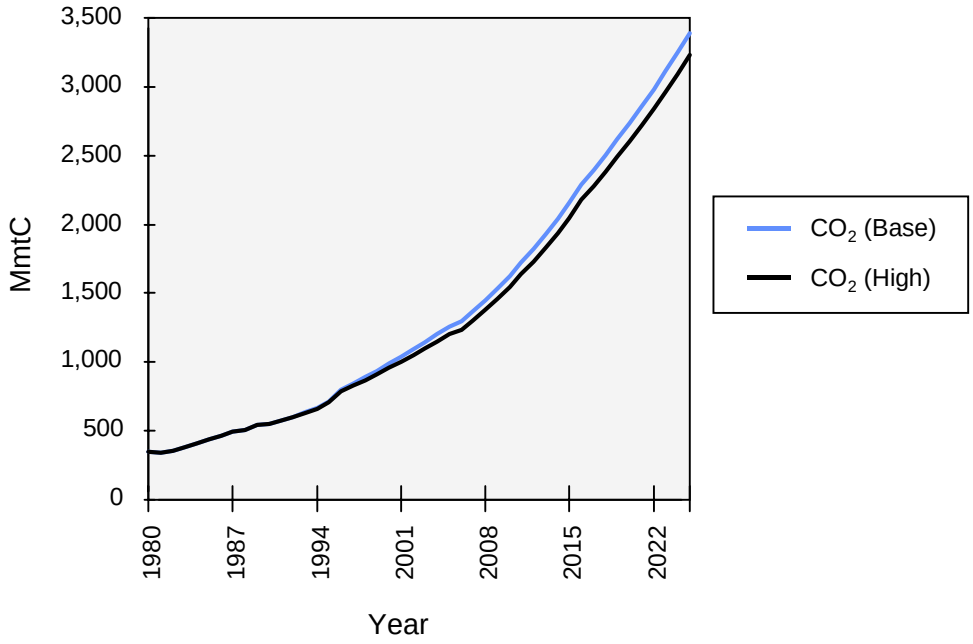

Figure 21. Projected CO_2 emissions for the base case and for the high-nuclear-and-hydropower investment scenario.

Table 6. Results of Constant Energy Intensities Scenario for CO_2 Emissions

	Year		
CO_2 Emissions (MmtC)	2005	2015	2025
Base Case	1,260	2,158	3,391
Constant Energy Intensities	1,761	3,813	6,919

CH_4 from the Agricultural and Energy Sectors – Base Case

The results for CH_4 from energy production, distribution, and consumption and from the agricultural sector for the base case simulation are summarized in Table 7. Based on the initial assumptions, CH_4 emissions from the agricultural sector increase from approximately 26.4 million metric tons of CH_4 ($MmtCH_4$) in 1995 to 37.3 $MmtCH_4$ in 2025 (over 40%). Over the same period, CH_4 emissions from the energy sector increase from 11.3 to 46.0 $MmtCH_4$, a factor of 4.1 (or 307%). Based on these results, total CH_4 emissions from China are expected to increase from approximately 37.7 to 83.3 $MmtCH_4$. The World Resources Institute (WRI) (1996) reported total Chinese CH_4 emissions in 1991 of 46.2 $MmtCH_4$, slightly higher than that estimated by the model. WRI estimates for 1991 (in $MmtCH_4$) include: energy-related, 15.3; livestock, 7.0; and rice, 24.0, values that are also slightly higher than those estimated by the model.

The agricultural sector is currently the primary source of CH_4 in China. However, these initial results indicate that the large growth in the energy sector will result in the energy sector overtaking the agricultural sector as the primary source of CH_4 (see Figure 22).

Table 7. CH_4 Emissions from Energy Production, Distribution, and Consumption and from Agriculture in China through 2025 ($MmtCH_4$)

Source	1995	2005	2015	2025
Livestock				
Enteric	6.8	8.5	10.2	11.9
Anaerobic	2.0	2.4	2.8	3.2
Rice	17.6	19.2	20.7	22.1
Total From Agriculture	26.4	30.1	33.7	37.3
Total From Energy Sector	11.3	18.6	29.3	46.0

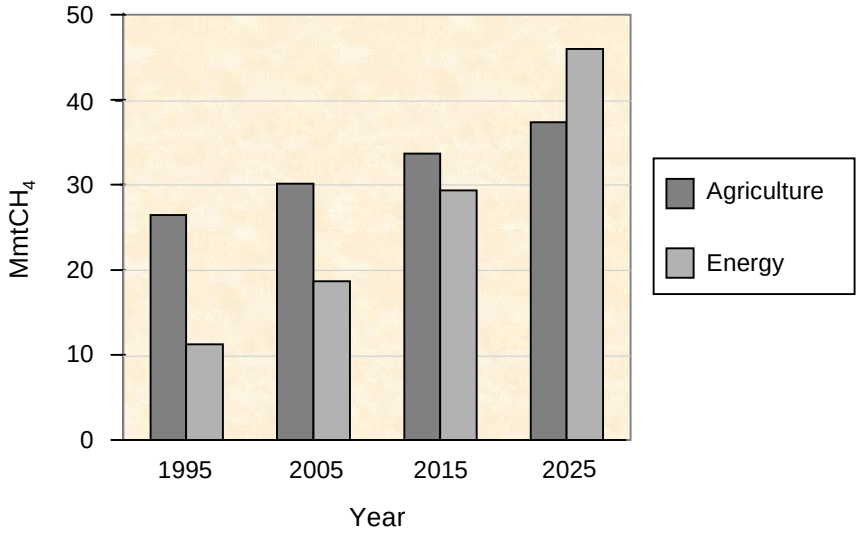

Figure 22. Estimated methane from energy and agriculture, 1995–2025.

VALIDITY

An important question that arises with a projective modeling exercise such as this is "How good are the results?," that is, "Does the model reflect reality or are the projections artifacts of a faulty or inadequate model?" The integrated China model utilizes a dynamic simulation approach, incorporates models of four separate infrastructure systems, and simulates diverse flow networks of commodities between the separate infrastructure models. As such, it more realistically captured the overall dynamics of the infrastructure system and more accurately projected the outcomes of changes in commodity flows than what would have been possible with a model that simulated only one component of the infrastructure system. However, any model is only as good as the data and assumptions that comprise the model.

For the analysis presented in this report, it was not possible to perform formal calibration for the water model because of limited observable and historical data with which to compare the results. The agronomic model was calibrated using USDA/ERS historical production and consumption data. The water model projections are in general agreement with Chinese reports on water distribution and scarcity. The all-China grain and meat demand values generated in the agronomic model agree favorably with grain and meat consumption estimates made by the USDA/ERS. As discussed below, official Chinese government data on energy demand were available for comparison with the China energy and greenhouse gas models.

Discussions on the validity of each infrastructure model are presented below. Ideally, actual historic physical and socioeconomic data would be compared with the results produced by the model to test its historic validity. This approach was followed whenever possible. However, since data on the future does not yet exist, the approach used to evaluate the "projective validity" was to test the *plausibility* of the model results. Plausibility was tested by relying on comparisons of the model results with the intuition of knowledgeable professionals and on comparisons of the results with those of other recent studies. The assumptions and the data that were used in the water and the agronomic models are described first, followed by a comparison of the energy and greenhouse gas model results with those of three other recent studies.

Water Model

Water Model Assumptions

1) The stochastically generated time series for precipitation and runoff are perfectly correlated. The model assumes that years with high precipitation correspond with high runoff years. Neither of these time series is autocorrelated; that is, multiyear patterns of drought and flood are not represented. For the modeling effort, it was assumed that neither precipitation nor runoff is correlated between regions.

2) Annual recharge is calculated to always be proportional to runoff on the basis of the historical recharge/runoff relationship. Surface water reservoir storage is assumed to not hold water from one year to the next, but it is also assumed that, within any year, there is sufficient reservoir storage to hold water until it is needed during that same year.

3) When the water use requirement is greater than the available water, the region is not operating on a sustainable yield basis and groundwater mining is assumed to be occurring. The water deficit is the difference between the total water requirements and the available water. Time to depletion of the groundwater reserves cannot be determined because the exact amount remaining is unknown.

4) When groundwater extraction is less than groundwater recharge and the region is operating on a sustainable yield basis, excess groundwater is discharged to surface water and excess surface water is discharged to the ocean.

5) The proportion of groundwater extraction to surface water extraction is maintained at 1980 levels until groundwater extraction exceeds sustainable yield or surface water extraction exceeds the available surface water.

6) Water use requirements for the three sectors are met in the following order of priority: urban receives first priority, industrial receives second priority, and agricultural receives last priority. The agricultural sector returns water to both the groundwater system and the surface water system, whereas the urban and industrial sectors return water only to the surface water system. Return flows are assumed to be proportional to the water use within each of these sectors.

Water Model Data

The data used in the water model are from several sources, but most of the data were taken from one source, *Water Resources Assessment for China* (Department of Hydrology, Ministry of Water Resources, 1992). This source was originally prepared in Chinese and was translated into English at Hohai University, Nanjing. In the absence of any evidence to the contrary, it was assumed that all data, no matter what the source, were derived in a manner that is consistent with the data descriptions provided in *Water Resources Assessment for China.* There were a number of instances, however, where these descriptions were insufficient. As a result, significant uncertainty remains about whether the water model has been properly parameterized.

For example, the description of evapotranspiration data from *Water Resources Assessment for China* states that runoff is subtracted from precipitation and that the remainder is assumed to have been removed from the system through evapotranspiration. The document, however, does not indicate whether agricultural evapotranspiration, especially that portion of agricultural evapotranspiration from irrigation water, is included as part of the evapotranspiration term or whether it is considered to be a water withdrawal from the surface water and/or groundwater systems.

Additionally, for data that were collected, translated, and summarized from Chinese government agency data tables, it was not possible in all cases to interpret accompanying text that might have explained how the data were derived or their intended use. The data that came from *Water Resources Utilization in China* (Water Resources and Hydropower Design Institute of the Ministry of Water Resources, 1989), in particular the data for water use requirements, fell into this category. In general, it could not be determined whether the water use requirements from *Water Resources Utilization in China* are net requirements (which would not include any return flows) or gross requirements (which would include return flows). It also could not be

determined whether the data summarizing the agricultural water use requirements were restricted solely to irrigation water or whether the definition of agricultural water use also includes water consumed in dryland farming.

Agronomic Model

Assumptions for the Agronomic Model

1) The value used for daily caloric requirements was a constant 2,250 calories per capita, the median of the generally accepted range for the United States, which is 2,000–2,500 calories per capita per day (National Research Council, 1989). This value will be revised when a better estimate for China becomes available. The model will also account for the increase in caloric intake that is likely to occur in China as a result of increasing affluence and changed consumption patterns.

2) The all-China projected caloric requirements for each year were apportioned between the three major grains (rice, wheat and corn), meat, and "other" (other grains and fruits and vegetables) in accordance with Chinese historical grain and meat consumption patterns from the USDA (Crook and Colby, 1996).

3) The category "other" (or "other grains and fruits and vegetables"), as used in the demand projection segment of the agronomic model, was defined as "all foods other than the three major grains and meat." It was assumed that this category constituted 10% of the total human food consumed. The data for "other" that were obtained later on in the modeling process from the USDA/ERS CPPA Model (Medea Project, 1997) and that were used in the production transformation segment of the agronomic model, included barley, sorghum, millet, oats, and rye, but not fruits and vegetables. According to the USDA/ERS model, this "other grain" constituted 8% of total grain produced in China in 1980 and 4% in 2000. Because fruits and vegetables were not included in the USDA data, it was considered acceptable to consider the two categories equivalent, within the accuracy of the model, for purposes of computing regional production allocations.

4) To account for the caloric inefficiency of meat production, the caloric requirements value apportioned to meat consumption was converted to grain-equivalent caloric requirements using an assumed grain-to-meat conversion efficiency ratio of 4:1. The assumption was made that, in the aggregate, meat animals consume grains and grain equivalents in the following proportions: rice–15%, wheat–15%, corn–50%, and other–20%.

5) Values used for the average caloric content for each grain type and for meat, in calories per gram, were as follows: rice–3.63, wheat–3.35, corn–3.65, other–3.54, and meat–3.48. These values were obtained from the *USDA Nutrient Database for Standard Reference* (1997).

6) The following values for yield coefficients, in metric tons per hectare, were obtained from the USDA (Crook and Colby, 1996): rice–4.1, wheat–3.41, corn–4.74. An average of these, 4.0, was assumed for "other." It was assumed that factors for same-grain multiple cropping were implicitly captured to the first order in the grain yields obtained from the USDA. Future refinements to the model are planned for computations for multiple cropping of different grains.

7) An alternate source, the Decision Support System for Agrotechnology Transfer (DSSAT) crop model, was used to obtain statistical yield coefficients for the three major grains to permit investigation of the effects of stochastic yield variations on the computation of sown areas.

8) The DSSAT crop model was also used as the source for both nominal average and stochastic water consumption rates for the three major grains. The nominal average rates were calibrated, on a regional basis, to make them consistent with historical agricultural water consumption data obtained from *Water Resources Utilization in China* (Water Resources and Hydropower Design Institute of the Ministry of Water Resources and Electric Power, 1989).

9) To allow for the computation of production estimates, land requirements, and water consumption estimates on a regional basis, the all-China grain demand computed by the agronomic model was apportioned to the ten Chinese drainage regions according to historical production data taken from the USDA/ERS CPPA Model (Medea Project, 1997).

Data for the Agronomic Model

Table 8 presents a comparison of the all-China grain and meat demand values for 1995 that were generated in the agronomic model with grain consumption data for 1994-96 obtained from Crook and Colby (1996). As shown in the table, the demand values generated by the model agree favorably with the USDA consumption data. The demand values for meat are somewhat lower than those from the USDA; planned extensions to the model that will account for rising caloric intake are expected to close the difference.

The projections of agricultural land requirements generated by the model also agree favorably with the agricultural production land data in Crook and Colby (1996) to the extent that the model's grain demand compares with USDA data on historical grain production. The projections of agricultural water requirements generated by the model also agree favorably with water usage data from *Water Resources Utilization in China* (Water Resources and Hydropower Design Institute of the Ministry of Water Resources and Electric Power, 1989). This is to be expected because the yields were obtained from Crook and Colby (1996), and the water consumption rates that were used to generate the agricultural water requirements were calibrated on the basis of historical data from *Water Resources Utilization in China*.

Energy and Greenhouse Gas Models

Values generated in the energy and greenhouse gas models for total energy demand and energy consumption by fuel type for the years 1980 to 1995 correlate closely with the official Chinese government statistics for these years obtained from various years of the *China Statistical Yearbook* (State Statistical Bureau, 1996).

Table 8. Comparison of the 1995 Projected Grain and Meat Demand Values Generated by the Agronomic Model with 1994–96 Consumption Data from the USDA/ERS

	Agronomic Model 1995 Grain and Meat Demand Values	USDA/ERS* 1994–96 Consumption Estimates	Difference (% of USDA Value)
Rice			
Total (Mmt†)	123.62	128.48	-3.8
Per Capita (kg)	101.31	105.70	-4.2
Wheat			
Total (Mmt)	117.20	111.68	+4.9
Per Capita (kg)	96.05	89.30	+7.6
Corn			
Total (Mmt)	106.25	105.86	+0.4
Per Capita (kg)	87.08	87.10	<0.1
Other			
Total (Mmt)	61.83	not available	not available
Per Capita (kg)	50.67	not available	not available
Meat			
Total (Mmt)	42.62	52.50	-18.8
Per Capita (kg)	34.93	43.50	-19.7

*Crook and Colby, 1996.

†Mmt = million metric tons.

Comparison with Other Studies

Table 9 presents a comparison of the results of the base case energy and greenhouse gas simulation with the results of three other studies ((EIAa, 1996), Zhang Zhong Xiang (1996), and McCreary et al. (1996)). The results of the base case are consistent with these other studies. While the base case results forecast higher total energy demand and carbon emissions in 2015 than indicated by the high-growth EIA scenario, using the EIA GDP reference case growth assumptions in this model provides a forecast that is similar to that of the base case. Specifically, applying GDP growth rates of 9.2% per year from 1990–2000 and 7.6% from 2001–2015 results in a forecasted energy demand of 3,016 Mmtce in 2015, compared with the EIA prediction of 2,944 Mmtce.

Table 9. Comparison of Base Case Energy and Greenhouse Gas Results to Other Studies

	Year		
	2005	2010	2015
Base Case Results			
Energy Demand (Mmtce)	2,179	2,819	3,721
Carbon Emissions (MmtC)	1,260	1,629	2,158
EIA 1996a			
Energy Demand (Mmtce)			
Reference Case	1,951	2,401	2,944
High Economic Growth	2,120	2,717	3,463
Carbon Emissions (MmtC)			
Reference Case	1,204	1,462	1,780
High Economic Growth	1,307	1,654	2,093
Zhang Zhong Xiang (1996)	– –	– –	– –
Energy Demand (Mmtce)	– –	2,560	– –
Carbon Emissions (MmtC)	– –	1,441	– –
McCreary et al. (1996)	– –	– –	– –
Energy Demand (Mmtce)			
Business-as-Usual Scenario	– –	– –	4,075
Energy-Efficiency Scenario	– –	– –	3,687

COMMENTARY

Summary and Conclusions

The integrated China infrastructure model is a comprehensive state-of-the-art model that successfully combines four dynamic infrastructure models—water, agronomic, energy, and greenhouse gas—to simulate, respectively, hydrologic budgetary processes, grain production and consumption, energy demand, and greenhouse gas emissions in China through the year 2025. The integrated model operates on a platform that generates results quickly (within minutes rather than hours or weeks), presents the results visually, demonstrates the relationships between the key variables, and allows the user to make adjustments for various "what if" scenarios and policy options concerning available water and water use, caloric consumption, population growth, grain yield, sectoral GDP growth, sectoral energy intensities, fuel shares, energy requirements, and greenhouse gas emissions. The model's architecture is also sufficiently robust to make it reusable in analyses of other geographic regions that may be of interest.

The results of the modeling of China's water resources show that, based on regional data, there is a surplus of water in China as a whole. In five of the regions, however, all of which are located in northeastern China, water use requirements exceed the sustainable yield and deficits are occurring to various degrees. Because of the water use priority scheme imposed by the model, the impact of a deficit is felt first by the agricultural sector. In two of these regions, the Haihe and the Huanghe, significant and/or ongoing deficits occur in the agricultural sector throughout the study period. In the Huanghe, a deficit also appears in the industrial sector in the second half of the period. In Heilongjiang, Liaohe, and Huaihe, less severe deficits appear late in the period in the agricultural sector. Based on 100 replications of the water model, the expected frequencies of experiencing a water deficit through the year 2025 for the Haihe and the Huanghe are "always" and "almost always," respectively. The other eight regions are expected to experience no or almost no deficits through 2025.

Given the model assumptions and available data, the agricultural sector deficit for the Haihe is likely to reach between 22 and 30 billion cubic meters by the year 2025. Although the Huanghe region begins the study period with a much smaller agricultural water deficit than that in the Haihe region, by 2025 the deficit for the Huanghe region is likely to reach between 18 and 38 billion cubic meters. Because the Haihe receives interbasin transfers from the Huanghe region, deficits in either region are also likely to play a significant role in water scarcity issues in both regions in the coming years. Moreover, because water use requirements exceed the sustainable yield in all regions experiencing a deficit, it is assumed that the deficit must be met by mining groundwater. This assumption is confirmed by reports that groundwater mining is already under way in the most intensively cultivated and populated areas of northeastern China, particularly around the Beijing area (Economy, 1997; World Resources Institute, 1992; Zhang Qishun and Zhang Xiao, 1995).

Comparisons of available land with the amount of land needed in the Haihe and Huanghe regions to meet each region's projected share of the all-China grain demand generated in the China agronomic model indicate that the amount of available land is more than sufficient to meet land needs in both regions. The availability of water for agriculture in these regions appears to be the limiting factor in meeting this allocated grain demand.

The China energy model results indicate that total energy demand will increase by a factor of 4.7 (or 370%) from 1995 to 2025. Although the demand for coal will decrease slightly relative to oil, natural gas, and nuclear energy (73.1% of all fuel consumed in 1995 compared with 67.6% in 2025), coal will remain the dominant fuel source in China, growing by a factor of 3.5 (or 250%) by the year 2025. Minimal changes are predicted in terms of overall fuel shares if installed nuclear capacity grows to 86 GW in 2020 (the equivalent of building over ninety-four 900-megawatt (MW) nuclear plants by 2020) and if installed hydropower capacity increases by 148 gigawatts (GW).

The greenhouse gas model results indicate that total CO_2 emissions will increase by a factor of 4.5 (or 350%) from 1995 to 2025, indicating a potential difficulty in effectively limiting future worldwide emissions without Chinese cooperation. CH_4 emissions from the energy sector will increase from 11.3 to 46.0 MmtCH_4 (a factor of 4.1, or 307%), and CH_4 emissions from the agricultural sector will increase from approximately 26.4 MmtCH_4 in 1995 to 37.3 MmtCH_4 in 2025 (over 40%). Although the agricultural sector is currently the primary source of methane in China, the energy sector will overtake the agricultural sector as the primary source by the year 2025. Finally, the minimal effect in terms of overall fuel shares of the substitution of hydropower and nuclear power for coal also translates to minimal effect in total projected greenhouse emissions.

The results of the modeling effort have several implications, if the country is to remain on its current course of rapid economic growth and expanding population. In particular:

1) The future availability of water in the northeastern provinces may depend on additional transfers of water from southern China and the Chang Jiang (Yangtze) (cost and feasibility will play a role);

2) Agricultural production may need to move from northeastern China to the water-plentiful provinces in southern China;

3) China may need to concentrate on growing fruits and vegetables while relying on imports to satisfy increasing grain requirements.

4) China's energy demand will continue increasing at an annual rate of approximately 5.3% despite improvements in overall energy intensities. This is likely to result in increased oil imports.

5) Chinese greenhouse gas emissions will continue growing at a rapid rate, even if the country is able to meet its ambitious plans for increasing reliance on both hydro and nuclear power.

Recommendations

The analysis of the four critical infrastructures—water, agriculture, energy, and greenhouse gas—was conducted by modeling the nonlinear dynamics of hydrologic budgetary processes, grain production and consumption, energy demand, and greenhouse gas emissions in China through the year 2025. An integrated model for all of China was constructed to capture the interrelationships between these critical infrastructures. Recommendations, discussed below,

include refining and improving the four models and expanding the integrated model to include policy-gaming capabilities.

Model Integration

Additional commodity flows between the models are needed to provide a more complete integrated model and to improve its fidelity. Figure 23 illustrates the flows modeled in the analysis with additional flows that would increase the model's capabilities. The agricultural sector is not only a source of greenhouse gases (CO_2, CH_4, and N_2O) but is also a sink for CO_2. This has not yet been modeled. Changes in the animal population are related to changes in the population-driven demand for meat, and projections should be included in the agronomic model. These projections can also be used to calculate enteric and anaerobic greenhouse gas emissions from farm animals. N_2O is generated in the transportation sector as a byproduct of fossil fuel combustion, in the agricultural sector during fertilizer application, and in the industrial production of adipic and nitric acids. The impact of N_2O on global warming has been calculated to be as much as 310 times that of CO_2 (IPCC, 1996), making it a potentially significant contributor. Additionally, water projects that rely on significant energy to pump water were not modeled. The impacts of these projects on the agriculture sector, in terms of water availability and use, and on greenhouse gas emissions, should also be included. These links would provide better modeling capabilities, allow for the evaluation of a greater variety of system scenarios, and improve the fidelity of the current scenarios.

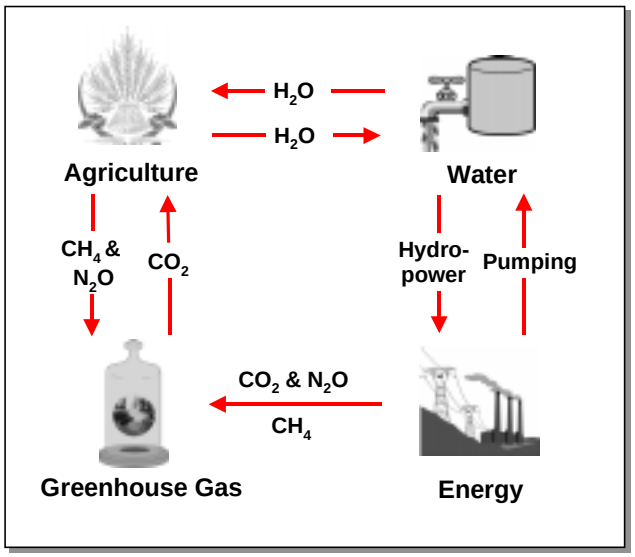

Figure 23. Enhanced integration of commodity exchange between critical infrastructures.

Water Model

It is recommended that the water model be refined so that it accounts for water quality problems and groundwater storage.

Identify Water Quality Problems: A component of the model should be developed that would allow for the consideration of water quality constraints. This effort would address both surface

water and groundwater quality. It would also require refining the model to the subregion level of analysis because water quality problems are commonly localized. Each region would be divided into spatial components (called subregions) (such as tributaries and reaches of the main river) that represent distinct hydrologic sections of the region. Each subregion would be represented by a unique model that would include interactions with other subregions (in the form of water transfers). If such a component is developed, the effects of seasonality are also likely to be considered (by reducing the time step from yearly to monthly), and optimal surface water management may also be incorporated (by including reservoirs and their operating rules).

Quantifying Groundwater Storage: For the analysis reported in this document, information on the quantities of groundwater reserves in each region was not available. Initially, data on the quantity of water in each aquifer will be needed; ultimately, data on the depth and the quality of these reserves will be required. An initial survey will be performed to determine if the data exist; a pilot survey for the Haihe region is planned. Including quantitative information on groundwater reserves will make it possible to calculate what proportion of these reserves remain and to predict when the reserves will be depleted.

Additional refinements suggested for the China water model include the following:

1) Sensitivity analyses to identify critical parameters.
2) The development of more accurate data on water use requirements for each of the major end-use sectors (agricultural, urban, and industrial).
3) The improvement of return-flow algorithms to better reflect Chinese water management practices specific to the 10 regions and sectoral use within each region.
4) Augmentation of the stochastic generation of precipitation and runoff to include interbasin correlation of weather patterns and drought and flood patterns across China.

Agronomic Model

The initial objective in designing the agronomic model was to provide first-order estimates of both China's grain consumption requirements and the land area and water volumes necessary to produce those grains. For the analysis presented in this report, the model was expanded to provide initial estimates of arable land and to address water resources as well as historical production levels for the 10 water drainage regions. Regional land- and water-constrained production components of the model have been planned but have not yet been completed. A number of further extensions and refinements are recommended to carry the model beyond a first-order prototype.

The underlying premise of the agronomic model is based upon fulfilling the caloric energy demand of the population. The individual daily caloric consumption value that was used by the model to generate the results presented in this report is the median of the range for the U.S. This value should be adjusted not only to accurately reflect caloric consumption for the Chinese population, but to reflect the inevitable increase in caloric consumption that will result from increasing economic prosperity. This refinement will directly and proportionately affect the projected grain and meat demands.

Refinements to the grain demand submodel should include accommodating the effects of rising economic trends as well as increasing meat consumption and changing grain consumption patterns. Seed grain consumption and inventory losses should be included as well.

Refinements to the meat animal submodel should include 1) disaggregating the individual animal species' grain consumption and feed conversion efficiencies; 2) incorporating animal forage, grazing, and hay consumption; 3) incorporating feed demand for exported meat animals; and 4) accounting for fish and seafood consumption by the population. The relationship between meat demand and livestock populations should also be incorporated to allow more realistic animal population data to be provided to the greenhouse gas model.

Grain production capacity trends and influences should also be incorporated into the model. This includes 1) refining the estimates of regional arable land, and 2) including the effects of pesticide and fertilizer use; land loss due to urbanization, industrialization, inundation by reservoirs, and salinization; as well as the effects of investment in agronomic/agricultural research.

Finally, data should be obtained on China-specific regional crop cultivars, soils, weather, solar radiance, photoperiod, etc., to drive the DSSAT crop model. This will allow more accurate computations of local yields and water use made by DSSAT, which will in turn improve the accuracy of regional land and water needs that are projected by the agronomic model.

Energy and Greenhouse Gas Models

The energy and greenhouse gas models were constructed with three objectives in mind: 1) to provide methodologies consistent with other models currently in use, 2) to provide models consistent with the two other China infrastructure models, and 3) to build models capable of being further expanded and refined to the provincial level of analysis. Both models provide results that are consistent with other models currently in use (see discussion under the "Validity" section and EIA, 1996; Zhang Zhong Xiang, 1996; and McCreary et al., 1996). The models also provide flexibility in changing various assumptions and answering various "what-if" questions such as: 1) What might be the impact of China rapidly developing its internal reserves of natural gas or proceeding with plans to build large natural gas pipelines originating in other countries rather than further exploiting its vast coal resources? 2) What if China succeeds in achieving energy intensity levels comparable to those of industrialized countries? 3) What if China's economy grows at an even faster pace than projected or rapidly moves from an industrialized economy to a more service-oriented one? 4) What are the potential impacts of changes in Chinese greenhouse gas emissions in terms of the successful implementation of the recently negotiated Kyoto Protocol?[24] While the models are capable of providing information for addressing these questions, further refinements could provide more complete insights. Including regional- and provincial-level analysis will help with identifying and pinpointing options for improving energy efficiency or limiting future greenhouse gas emissions. Other refinements include:

[24] The Kyoto Protocol, adopted December 11, 1997, limits overall greenhouse gas emissions between 2008 and 2012 to at least 5% below 1990 levels.

- Coupling a provincial level version of the model to a GIS that contains specific information regarding location and quantities of existing energy and infrastructure reserves and resources.
- Further analysis of the potential for improvements in sectoral energy intensities.
- Broadening the model to incorporate existing and potential renewable resources.
- Development of an infrastructure investment submodule that calculates the potential magnitudes of investments necessary to achieve various demand scenarios, such as a "high-energy-efficiency" scenario that would demonstrate the potential impacts of moving towards the most efficient energy-producing and -consuming technologies. Such a scenario might also be useful for identifying which areas would have the largest payback in terms of overall effectiveness per monetary investment.
- Incorporating energy pricing into the overall model framework.

Expanding the Models

The models used in this analysis were developed with an eye toward adapting the analysis to countries other than China and toward expanding the models to incorporate input from submodels of other critical infrastructures such as finance and of environmental impacts and natural disasters such as droughts and floods. The models can also be expanded to include optimization techniques (which find optimal solutions, such as cost or food-shortage minimization, through multiattribute decision analysis or linear optimization). Work is already under way to include policy-gaming capabilities. It is further recommended that uncertainty analyses and data value calculations be performed to identify additional data that should be collected before policy actions are initiated or modified and to track the consequences of policy decisions.

REFERENCES

Brown, L. R., *Who Will Feed China?*, W.W. Norton & Company, New York & London, 1995.

Crook, F. W., and W. H. Colby, *The Future of China's Grain Market*, U.S. Department of Agriculture/Economic Research Service (USDA/ERS), Agricultural Information Bulletin (AIB) No. 730, October 1996.

Department of Hydrology, Ministry of Water Resources, *Water Resources Assessment for China*, China Water and Power Press, Beijing, 1992.

Economy, E., *Environmental Scarcities, State Capacity, Civil Violence: The Case of China*, Committee on International Security Studies, American Academy of Arts and Sciences, 1997.

Energy Information Administration (EIA), *International Energy Outlook 1996*, U.S. Department of Energy, DOE/EIA-0484(96), May 1996a.

Energy Information Administration (EIA), *Annual Energy Outlook 1997*, U.S. Department of Energy, DOE/EIA-0383(97), December 1996b.

Energy Information Administration (EIA), Office of Integrated Analysis and Forecasting, *Emissions of Greenhouse Gasses in the United States*, U.S. Department of Energy, DOE/EIA-0573(96), October 1997.

ERIM Geographic Information Systems and Applications Department, Earth Sciences Group, *GIS Database of China Land Use*, 1997.

Framework Convention on Climate Change, United Nations, A/AC.237/18, May 15, 1992.

Intergovernmental Panel on Climate Change (IPCC), *Greenhouse Gas Inventory Reference Manual*, First Draft, Volume 3, 1994.

Intergovernmental Panel on Climate Change (IPCC), *Climate Change 1995: Impacts, Adaptations and Mitigation of Climate Change*, Cambridge University Press, 1996.

Johnson, Todd M., Li Junfeng, Jiang Zhongxiao, and Robert P. Taylor, *China: Issues and Options in Greenhouse Gas Emissions Control*, World Bank Discussion Paper No. 330, The World Bank, Washington, DC, 1996.

McCreary, E. I, A. Y. Gu, V. Loose, and J. Roop, *China's Energy: A Forecast to 2015*, Office of Energy Intelligence, U.S. Department of Energy, La-UR-96-2972, September 1996.

Medea Project (2/10/97) Base Scenario Area and Production Estimates Using New 1995 Estimates (Harvested Area and Grain Production for Years 1980-2010, by region): LOTUS Spreadsheet from the U.S. Department of Agriculture/Economic Research Service (USDA/ERS) Country Projections and Policy Analysis (CPPA) Model (attachment to e-mail from F. Crook and W.H. Colby, USDA, to D. Jeppesen, Sandia National Laboratories, February 10, 1997).

National Research Council, *Recommended Dietary Allowances*, 10th ed. National Academy of Sciences, Washington, DC, 1989.

REFERENCES (cont.)

State Statistical Bureau, *China Statistical Yearbook 1996*, China Statistical Publishing House, People's Republic of China, 1996 (various other years used to derived data estimates as well).

Thomas, R. P., S. H. Conrad, D. M. Jeppesen, and D. Engi, *Understanding the Dynamics of Water Availability and Use in China,* SAND97–1626. Sandia National Laboratories, Albuquerque, NM, 1997.

United Nations Department of International Economic and Social Affairs, *World Population Prospects,* United Nations, New York, 1993.

Water Resources and Hydropower Design Institute of the Ministry of Water Resources and Electric Power, *Water Resources Utilization in China,* Beijing: Water and Power Press, February 1989.

World Resources Institute, *World Resources Institute 1992–93: A Report by the World Resources Institute in Collaboration with the United Nations Environment Programme and the United Nations Development Programme,* Oxford University Press, Oxford, 1992.

World Resources Institute, *World Resources 1996–7,* Oxford University Press, New York, NY, 1996.

USDA Nutrient Database for Standard Reference, http://www.nal.usda.gov/fnic/cgi-bin/nut_search.pl, 1997.

Zhang Qishun and Zhang Xiao, "Water Issues and Sustainable Social Development in China," *Water International*, vol. 20, pp. 122–128, 1995.

Zhang Zhong Xiang, Integrated Economy-Energy-Environment Policy Analysis: A Case Study for the People's Republic of China, Ph.D. dissertation, University of Gronigner, The Netherlands, 1996.

APPENDIX A – THE CHINA WATER MODEL

Intentionally Left Blank

APPENDIX A – THE CHINA WATER MODEL

The China water model, a dynamic computer model of the hydrologic budgetary processes in the People's Republic of China, was developed by Sandia National Laboratories to analyze China's water resources. It is a component of the China critical infrastructure model, which integrates four infrastructure models (water, agronomic, energy, and greenhouse gas) to allow for the exchange of information between the separate models and to capture the overall dynamics of the integrated system. The China water model was used to dynamically simulate the available water resources and expected water use in ten river drainage regions representing 100% of the country's mean annual runoff. The model, a mass balance model of the hydrologic cycle, was constructed to simulate connections between the natural hydrologic systems in each region and water consumption systems incorporating water use requirements in the urban, industrial, and agricultural sectors. The model computes the effects of changes in agricultural, urban, and industrial water use requirements on the availability of water in each region. Figure A-1 shows the movement of water in the hydrologic cycle simulated in the model.

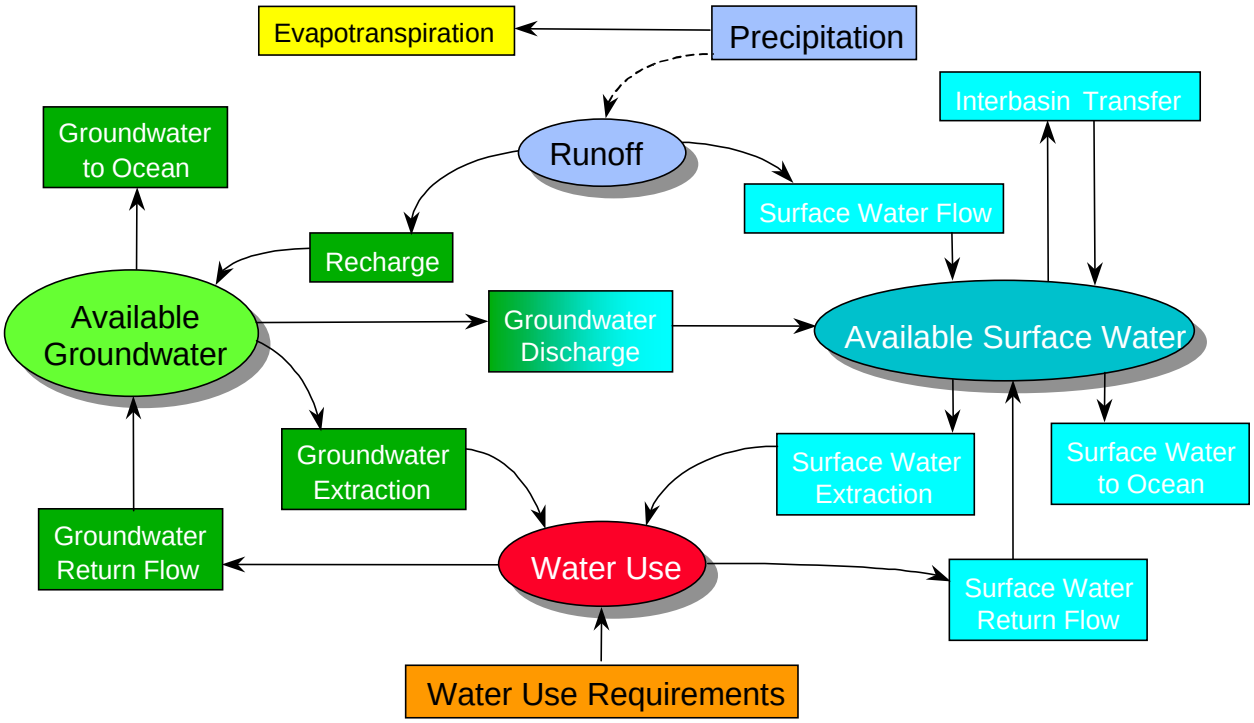

Figure A-1. Conceptual model of the hydrologic cycle as simulated in the China water model.

The Water Model

The hydrologic processes are modeled using the POWERSIM Constructor 2.5 modeling system, a dynamic simulation tool that allows tracking of the flow or movement of a commodity, such as water, through time. The POWERSIM system provides feedback mechanisms so that both the internal and external dynamics of the system being modeled can be simulated. In the China

water model, the movement of water in each drainage region was modeled by simulating changes to both the availability and use of water through time.

The model was specifically designed to:

1) Track the movement of water through each region on an annual basis;

2) Allow the user to adjust certain major parameters affecting flow in the natural system and in a set of simple water management scenarios; and

3) Provide an interface so that the user can observe the simulation, modify parameters both before and during model computation, and investigate policy options.

There are two main simulation components to the China water model: 1) a model of the hydrologic system that quantifies the amount of extractable water available within each water region and 2) a model for water use requirements. The hydrologic model covers the main components of the hydrologic cycle—precipitation, surface water, and groundwater—and the movement of water to and from these components via runoff, groundwater recharge, groundwater discharge, evapotranspiration (direct evaporation and evaporation through plants), and discharge to the ocean (from both surface water and groundwater), as well as the transfer of water from one region to another by way of canal (interbasin transfers). The water-use component of the model covers the extraction of water from both surface water and groundwater and its division between the agricultural, industrial, and urban sectors. Total available water and total water use requirements can then be compared to determine the likelihood of each region's water needs being met.

The model can be adjusted using simulation controls as follows:

1) *Deterministic versus stochastic switch:* In the deterministic setting, average annual precipitation and average annual runoff are used in each time step. In the stochastic setting, a series of correlated random values are generated for annual rainfall and runoff using a normal distribution, mean, and standard deviation for each of these parameters.

2) *Water-use requirements – slope delta slider bars:* Users can adjust the slope of the water-use requirements curves for each region and for each use sector: agricultural, urban, and industrial.

3) *Return flow – slider bars:* For each region, users can adjust the percentage of return flow from the agricultural sector to both groundwater and surface water, and can adjust the percentage of return flow from the industrial and urban sectors to surface water.

Data

Data for the water model were obtained from several sources, as follows:

1) Data were collected, translated, and summarized from Chinese government agency publications and maps by Jim Nickum, one of the study team members, who traveled to China during August and September 1996.

2) Data were also obtained from *Water Resources Assessment for China* (Department of Hydrology, Ministry of Water Resources, 1992), which was loaned to the study team by Jim Condon of the Defense Intelligence Agency.

3) Spatial data were obtained from the Consortium for International Earth Science Information Network (CIESIN) (University of Washington and CIESIN, 1996) and the Australian Centre of the Asian Spatial Information and Analysis Network (ACASIAN) (Crissman, 1996).

Hydrologic Basins

The ten major drainage regions that were modeled for this study include 37 major river basins and represent 100% of the country's mean annual runoff. Table A-1 identifies the river basins in each region.

The data elements summarized in Table A-2 were used to simulate precipitation, total evapotranspiration, surface water runoff, interbasin transfers, ocean discharge (average and minimum), groundwater recharge, groundwater extraction, surface water extraction, and water-use requirements. The sources for each data element are also listed in Table A-2.

Precipitation Data

Annual precipitation and mean annual discharge are the primary drivers for the hydrologic portion of the model. Average annual precipitation and an approximation of the standard deviation of average annual precipitation are used to randomly generate a time series of annual precipitation.

Average annual precipitation was obtained from Table 3-1 in *Water Resources Assessment for China*. The standard deviation for annual precipitation was computed from mean annual precipitation and a coefficient of variation for precipitation that was assumed to be equal to the coefficient of variation computed for mean annual runoff.

Surface Water Data

Surface water runoff: Annual averages for surface water runoff for each region are from *Water Resources Assessment for China,* Table 3-3. Table A-3 presents the annual averages and the standard deviations derived from these values.

Return Flow: A return flow of 40% for the agricultural sector was based on the assumption that at least one-third of the water applied to the crop will be returned and the other two-thirds is lost to evapotranspiration. A minimum of one-third of the water is needed to flush salts from the system (Hernandez, 1997); 40% was thus used as a conservative estimate. A return flow of 50% for the urban sector is based on the return flow percentage for water to U.S. municipalities. A return flow of 10% for the industrial sector is based on the assumption that most industries will reuse their water until it is virtually used up, leaving very little return flow (Hernandez, 1997).

Table A-1. River Basins in Each Drainage Region

Drainage Region	River Basin
Heilongjiang	1. Heilongjiang 2. Suifenhe 3. Baicheng 4. Wuyur
Liaohe	5. Liaohe 6. Tumen 7. Yalu 8. Liaodong Peninsula 9. West Liaoning Coastal
Haihe	10. Haihe 11. Luanhe
Huaihe	12. Huaihe 13. Shandong Peninsula
Huanghe	14. Huanghe
Chang Jiang	15. Chang Jiang
Southeast Coastal	16. SE Coastal 17. Taiwan
Pearl River	18. Zhujiang 19. Hainan 20. Guangdong-Guangxi
Southwest China	21. Gyirong 22. Indus 23. Irrawaddy 24. Lancang 25. Nujiang 26. Yadong 27. Yarlung Zangpo 28. Yuanjiang
Region of Inland Rivers	29. Ili 30. Junggar 31. Tarim 32. Qaidam 33. Ordos 34. Northern Tibet 35. Hexi Corridor Alxa 36. Nei Mongol 37. Ertix

Table A-2. Sources for Hydrologic Data Used in the China Water Model*

Data Element	Source
Precipitation – Average	*Water Resources Assessment for China* (Department of Hydrology, Ministry of Water Resources, 1992), Table 3-1
Precipitation – Maximum, Minimum, and Standard Deviation	*Map Collection of China's Climatic Resources* (China Meteorological Bureau, 1994)
Evaporation – Distribution	*Water Resources Assessment for China* (Department of Hydrology, Ministry of Water Resources, 1992), Table 2-18
Evaporation – Annual	*Water Resources Assessment for China*, (Department of Hydrology, Ministry of Water Resources, 1992), Figure 2-19
Surface Water – Initial Storage	*Almanac of China Water Resources 1991* (Editorial Committee for the Almanac of China Water Resources, 1992)
Surface Water – Interbasin Transfer	*Water Resources Utilization in China* (Water Resources and Hydropower Design Institute of the Ministry of Water Resources and Electric Power, 1989)
Groundwater Recharge Rate	*Water Resources Assessment for China*, (Department of Hydrology, Ministry of Water Resources, 1992), Table 4-15
Ocean Discharge	*Water Resources Assessment for China*, (Department of Hydrology, Ministry of Water Resources, 1992), Table 3-24
Ocean Discharge – Minimum	*Water Resources Utilization in China* (Water Resources and Hydropower Design Institute of the Ministry of Water Resources and Electric Power, 1989)
Urban, Industrial, and Agricultural Water Supply and Use Requirements	*Water Resources Utilization in China* (Water Resources and Hydropower Design Institute of the Ministry of Water Resources and Electric Power, 1989)
Agricultural Return Flow	Dr. John Hernandez, New Mexico State University (1997)
Spatial Data – City Locations, Province Boundaries	Consortium for International Earth Science Information Network (CIESIN) (University of Washington and CIESIN, 1996)
Spatial Data – River Basin Delineation	Australian Centre of the Asian Spatial Information and Analysis Network (ACASIAN) (Crissman, 1996)

*See the References section for a complete listing of these sources.

Table A-3. Surface Water Runoff

Drainage Region	Average Annual Flow (10^9 m^3)	Derived Standard Deviation (10^9 m^3)
Heilongjiang	116.6	40
Liaohe	48.7	16
Haihe	28.8	13
Huaihe	74.1	36
Huanghe	66.1	14
Chang Jiang	951	140
Southeast Coastal	255.7	60
Pearl River	468.5	75
Southwest China	585.3	60
Inland Rivers	106.4	8

Interbasin Transfer: Values for interbasin transfers in Table A-4 were derived from a summary by Jim Nickum of information obtained from *Water Resources Utilization in China* (Water Resources and Hydropower Design Institute of the Ministry of Water Resources and Electric Power, 1989) and supplemented by his expert knowledge. For purposes of modeling China's water resources, the following interbasin transfers were assumed to have started at or before the beginning of the study period (1980):

Table A-4. Interbasin Transfer Rates

From	To	Beginning Year	Amount of Transfer (10^9 m^3/yr)
Chang Jiang	Huaihe	1980	17.5
Huanghe	Haihe	1980	6
Huanghe	Huaihe	1980	3
Chang Jiang	Haihe	2010	10
Chang Jiang	Huaihe	2010	5
Heilongjiang	Liaohe	2020	2

- 10 billion cubic meters per year of water have been diverted from Chang Jiang into the Huaihe region since prior to 1980. Supplemental diversions from Chang Jiang to Huaihe began in 1980 at about 4 billion cubic meters and increased to 7.5 billion cubic meters by 1990. As a simplifying approximation for input to the model, an additional 7.5 billion cubic meters was assigned to each transfer beginning in 1980, making the total transfer 17.5 billion cubic meters per year.

- 8 billion cubic meters have been diverted from the Huanghe into the Haihe and Huaihe drainage regions since prior to 1980. Nickum is of the opinion that most of this water gets diverted into the Haihe region. Therefore, for input to the model, 75% of the water (6 billion cubic meters) was assigned to the Haihe with the remainder (2 billion cubic meters) going to the Huaihe. In *Water Resources Utilization in China* (Water Resources and Hydropower Design Institute of the Ministry of Water Resources and Electric Power, 1989), it was stated that diversions from the Huanghe would increase between 1980 and 2000. Most of this increase would be provided by a first-stage diversion of about 1 billion cubic meters into the Shandong peninsula (included as part of the Huaihe basin in the model). This diversion has been operating since 1985. As a simplifying approximation for input to the model, transfers of an additional 1 billion cubic meters from the Huanghe were assigned to the Huaihe beginning in 1980, bringing the total to 3 billion cubic meters. Since the Huanghe has been running dry in its lower reaches, it is not clear how much more water can be diverted in subsequent stages.

Future interbasin transfers were modeled as follows:

- By reinforcing the Danjiangkou Reservoir, an additional 15 billion cubic meters could be diverted from the Chang Jiang to the Haihe (10 billion cubic meters) and the Huaihe (5 billion cubic meters). This plan, which is referred to as the south-north transfer, is linked to the Three Gorges Dam project, so implementation will take some time. As a reasonable estimate, the model begins these additional transfers in 2010.

- Two stages are being considered for the north-south transfer (also known as the Songhua transfer). The first would divert 2 billion cubic meters from the Nen Jiang into the Liaohe. The second would divert 4 billion cubic meters from the Second Songhua Jiang into the Liaohe. (Both the Nen Jiang and the Second Songhua Jiang are included within the Heilongjiang basin for the purpose of our modeling.) It is estimated that the first stage will not be completed until sometime after 2010. For modeling purposes, it was assumed that the first stage of the north-south transfer would be completed by 2020. It was anticipated that the second stage would not be completed within the time frame of the modeling, which extends to 2025.

Ocean Discharge: The values for ocean discharge (Table A-5) are allowed to fluctuate in the model but are compared to the historical mean and are constrained by minimum discharges needed to flush silt into the sea.

Table A-5. Discharge to the Sea by Drainage Region

Region	Annual Mean Discharge to Sea (10^9 m^3)	Minimum Discharge to Flush Silt (10^9 m^3)
Heilongjiang	0	not available
Liaohe	21.3	not available
Haihe	16	8
Huaihe	59.3	not available
Huanghe	41	20
Chang Jiang	890.8	not available
Southeast Coastal	240.9	not available
Pearl River	455	not available
Southwest China	0	not available
Inland Rivers	0	not available

Groundwater Data

Recharge to Groundwater: Values used to compute groundwater recharge for each region (Table A-6) were based on values defined as the total groundwater recharge for the plains areas within each region (from Table 4-15, *Water Resources Assessment for China*). Base flow from the mountains was not included in these recharge values.

Table A-6. Groundwater Recharge

Drainage Region	Recharge (Plains) (10^9 m^3)
Heilongjiang	22.39
Liaohe	11.04
Haihe	19.23
Huaihe	16.42
Huanghe	31.32
Chang Jiang	26.09
Southeast Coastal	5.19
Pearl River	9.36
Southwest China	not available
Inland Rivers	49.25

Groundwater and Surface Water Extraction: The initial values for groundwater and surface water extraction are based on the groundwater and surface water use values for 1980 presented in *Water Resources Utilization in China* (Water Resources and Hydropower Design Institute of the Ministry of Water Resources and Electric Power, 1989). The 1980 water use values (Table A-7) and estimated values for the year 2000 (Table A-8) were used to calculate linear relationship for available water and water use. These relationships were then used to estimate values for all other years between 1980 and 2025. These projections proved to be similar to water use projections based on population growth.

Table A-7. Water Sources and Water Use in Ten Chinese Water Drainage Regions, 1980*

	Water Sources (10^9 m^3)			Water Use (10^9 m^3)			
Region	**Surface**	**Ground**	**Total**	**Urban†**	**Industry**	**Agriculture**	**Total**
Heilongjiang	16.41	3.65	20.06	0.49	3.38	16.19	20.06
Liaohe	10.48	4.84	15.31	0.78	3.01	11.53	15.31
Haihe	18.14	20.24	38.38	2.57	4.87	30.94	38.38
Huaihe	40.23	12.89	53.13	3.25	3.84	46.03	53.13
Huanghe	27.40	8.44	35.84	1.61	2.80	31.44	35.84
Chang Jiang	128.63	6.70	135.33	9.72	20.88	104.73	135.33
Southeast Coastal	28.34	3.52	31.86	2.41	2.91	26.54	31.86
Pearl River	65.45	0.61	66.06	6.33	4.59	55.15	66.06
Southwest China	4.33	0.07	4.39	0.37	0.07	3.95	4.39
Inland Rivers	51.93	3.95	55.87	0.99	0.71	54.16	55.86

* Source: Water Resources and Hydropower Design Institute of the Ministry of Water Resources and Electric Power, 1989.

† Urban includes rural drinking water.

Table A-8. Projected Water Sources and Water Use Requirements for the Year 2000*

	Water Sources (10^9 m^3)			Water Use Requirements (10^9 m^3)				
Region	**Surface**	**Ground**	**Total**	**Urban†**	**Industry**	**Agriculture**	**Total**	**Deficit (10^9 m^3)**
Heilongjiang	32.28	10.76	43.03	3.80	9.11	31.13	44.04	1.01
Liaohe	16.9	7.87	24.76	3.08	8.28	17.85	29.20	4.44
Haihe	22.37	17.56	39.93	6.00	10.01	36.25	52.26	12.33
Huaihe	58.53	16.05	74.58	5.62	14.43	62.31	82.36	7.78
Huanghe	32.01	8.99	41.00	2.91	7.87	32.44	43.22	2.22
Chang Jiang	236.22	7.58	243.79	23.93	57.81	169.97	251.71	7.91
Southeast Coastal	31.45	1.01	32.46	3.38	6.75	22.39	32.52	0.06
Pearl River	94.98	0.41	95.39	11.38	12.80	75.15	99.33	3.94
Southwest China	6.53	0.07	6.59	0.66	0.38	5.84	6.88	0.29
Inland Rivers	54.80	11.47	66.27	1.76	2.77	63.55	68.08	1.81

* Source: Water Resources and Hydropower Design Institute of the Ministry of Water Resources and Electric Power, 1989.

† Urban includes rural drinking water.

Modeling of Available Water and Projections of Water Use

The total available water is calculated in terms of potentially extractable groundwater and surface water by simulating the hydrologic balance within each region. The water model, represented schematically in Figure A-2, is driven by precipitation, runoff, and water use requirements.

Available Water

Rainfall, Runoff, and Evapotranspiration: The model can be run either in a deterministic mode, in which annual averages for rainfall and runoff are used, or in a stochastic mode, in which a random time series of both rainfall and runoff are computed using a normal distribution, mean, and standard deviation for each of these parameters. A time series of total evaporation, which includes evaporation from water bodies, evapotranspiration, and groundwater evaporation, is simulated by subtracting runoff from rainfall. These values are then checked for

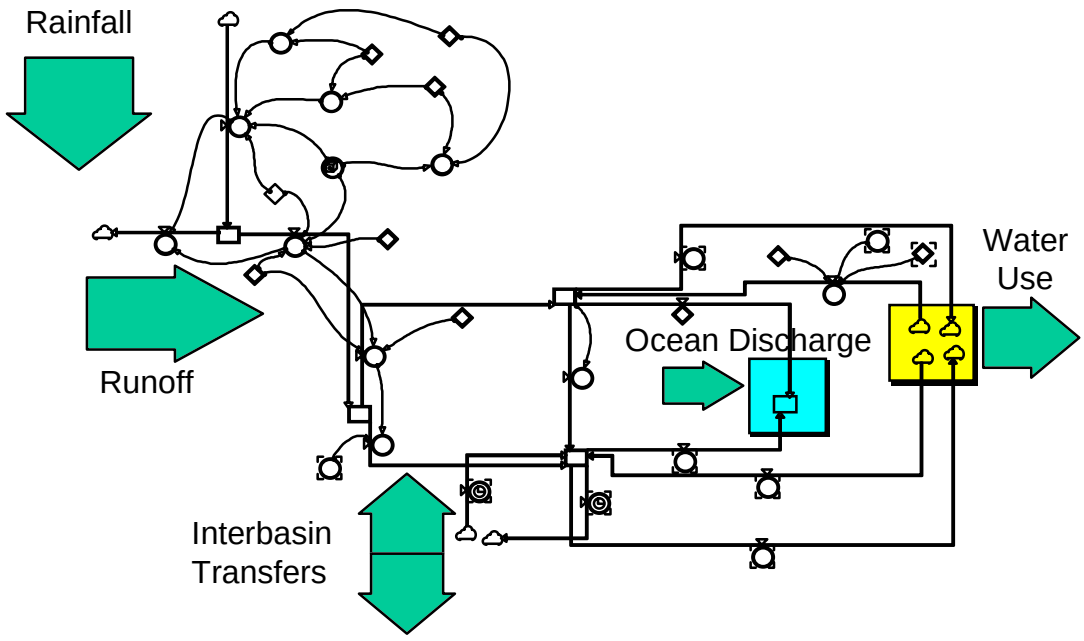

Figure A-2. Overview schematic representation of the China water model.

reasonableness against values of annual average total evaporation. Runoff is then apportioned between groundwater recharge and surface water flow. Figure A-3 shows a schematic representation of the rainfall/runoff portion of the water model.

Groundwater Recharge and Surface Water Flow: Groundwater recharge and surface water flow are calculated in the following manner. Groundwater recharge is computed in proportion to average runoff and average recharge values (from *Water Resources Assessment for China),* as follows; surface water flow is the remainder:

$$\text{recharge} = \text{runoff} \times (\text{average recharge} \div \text{average runoff}).$$

The Quantity of Potentially Extractable Water: The potential water supply is a function of mass balance considerations and is equal to the inflows to each region's hydrologic system minus the outflows. Figure A-4 is a schematic representation of the elements involved in the computation of available surface water and available groundwater in the model. Groundwater recharge and surface water flow plus any return flows constitute the inflows, while discharges to the ocean and consumption constitute the outflows. Water transfers between regions can be either inflows or outflows depending on the direction of the transfer. (Outflows due to evapotranspiration are accounted for prior to this point in the model.) The potential drought-mitigating effects of surface water storage in reservoirs are not included in the model because stored water is considered more important for leveling out seasonal variations in precipitation than for leveling out year-to-year variations. Although water supplied from reservoir storage may turn out to be nonnegligible in forestalling drought over a time frame of a year or two, limited quantities of water held in surface water storage become relatively inconsequential over the long term once the requirements for water consistently exceed the extractable amount. Moreover, since there was insufficient data to develop temporal correlation in annual

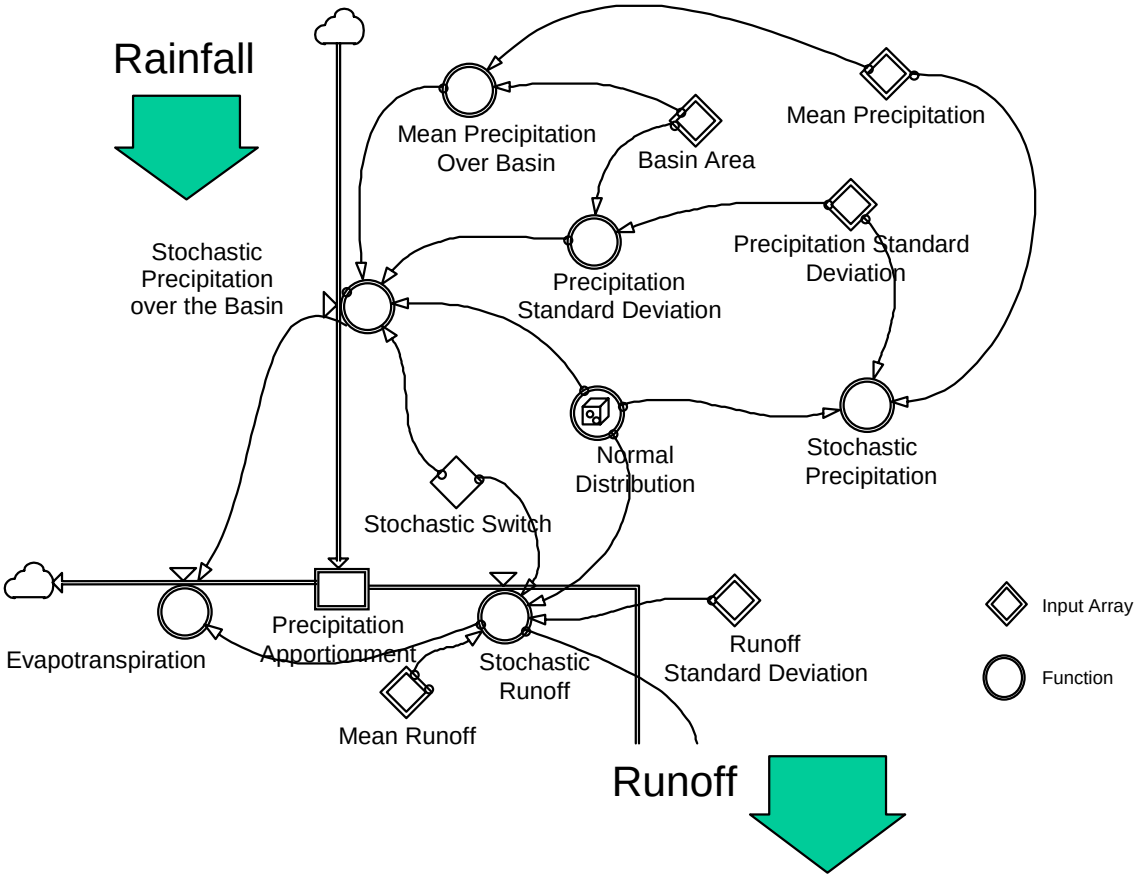

Figure A-3. Schematic of the rainfall/runoff portion of the China water model.

precipitation, drought years are typically simulated as isolated events. If droughts were realistically simulated (i.e., extending over several years), then the limited surface water storage in reservoirs would surely be depleted.

Surface Water and Groundwater Extraction: Extraction from groundwater is constrained to not exceed an amount equal to the average recharge plus agricultural return flows to the groundwater system minus any groundwater discharges to the ocean that may be required to prevent salt water intrusion. Groundwater extraction below this amount occurs at a proportion to surface water extraction that is equivalent to the 1980 proportion. Any unused groundwater is discharged to the surface water system. It is assumed that when water use requirements exceed sustainable water supply, groundwater mining will occur. The impact of groundwater mining is not accounted for because estimates of groundwater reserves were not obtained. Similarly, the depletion of economically recoverable groundwater reserves could not be computed. Groundwater mining is already under way in Haihe, particularly around the Beijing area, and in other parts of northern China (see, e.g., Zhang Qishun and Zhang Xiao, 1995). Groundwater mining cannot continue indefinitely, but is limited to the extent and availability of water in the aquifer. In most situations, groundwater mining will continue until the cost of further extraction is no longer economical. In these cases, the users will be forced to return to extracting water at the sustainable yield.

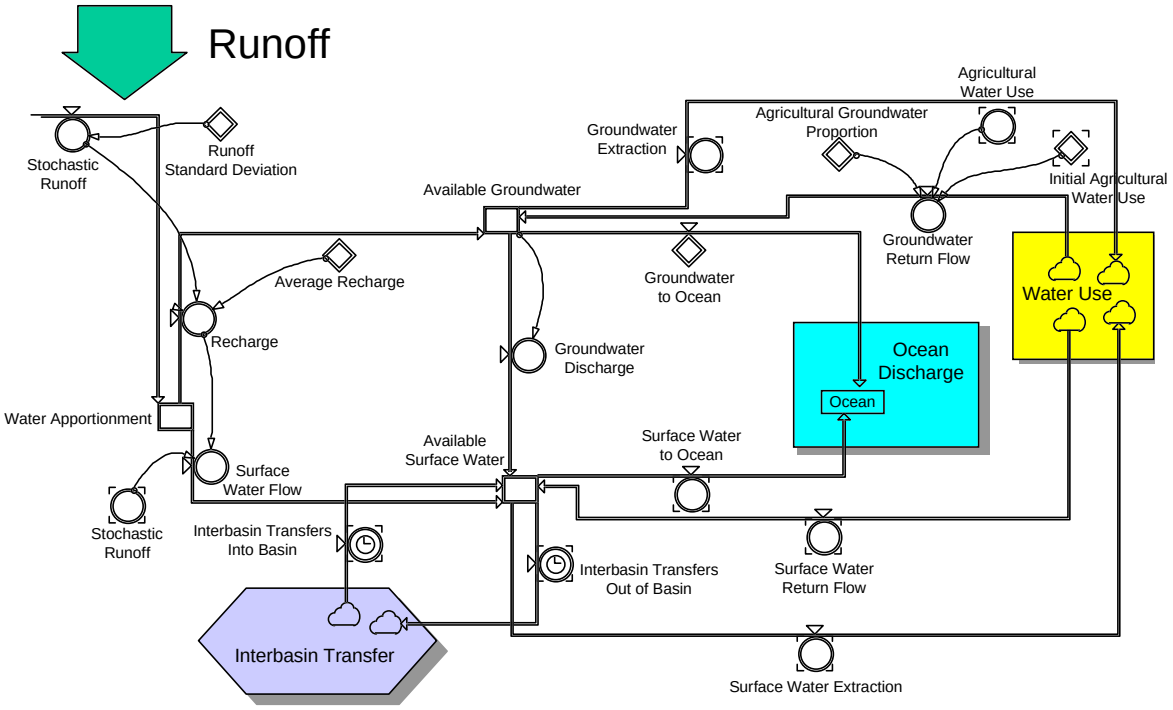

Figure A-4. Schematic representation of the China water model showing the elements involved in the computation of available surface water and available groundwater.

Extraction from available surface water is equal to the difference between the total amount of water to be extracted and that supplied from groundwater, if the water use requirements do not exceed the total available surface water. If the water use requirements exceed the amount of available surface water and the sustainable yield of groundwater, all available surface water will be extracted (all inflows minus any interbasin transfers out and the minimum required surface water discharge to the ocean). Any unused water is discharged to the ocean. See Figure A-5, a schematic representation of the China water model showing the elements involved in the computation of extractable surface water.

Water Use Requirements

Water use requirements for each region were computed in the China agronomic model and entered directly into the water model. Water use requirements for the industrial and urban sectors are based on linear functions using values for 1980 water use and for expected water use in the year 2000. These data were obtained from the *Water Resources Utilization in China* (Water Resources and Hydropower Design Institute of the Ministry of Water Resources and Electric Power, 1989). The values appear in Tables A-7 and A-8. A water use priority scheme was imposed as follows: Urban sector requirements were met first, industrial requirements were met second, and agricultural requirements received the lowest priority. See Figure A-6 for a schematic representation of the China water model showing the elements involved in the computation of the maximum amount of extractable water, water use requirements per sector,

and water use per sector. The arrows "From Ag Model" and "To Ag Model" in Figure A-6 show the interface with the agronomic model.

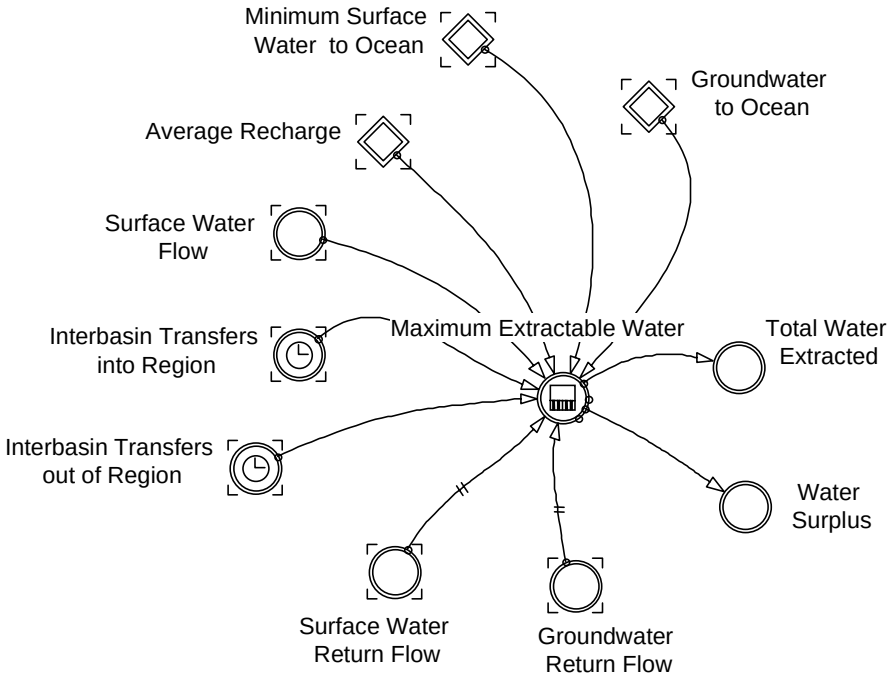

Figure A-5. Schematic of the China water model showing the elements involved in the computation of extractable surface water.

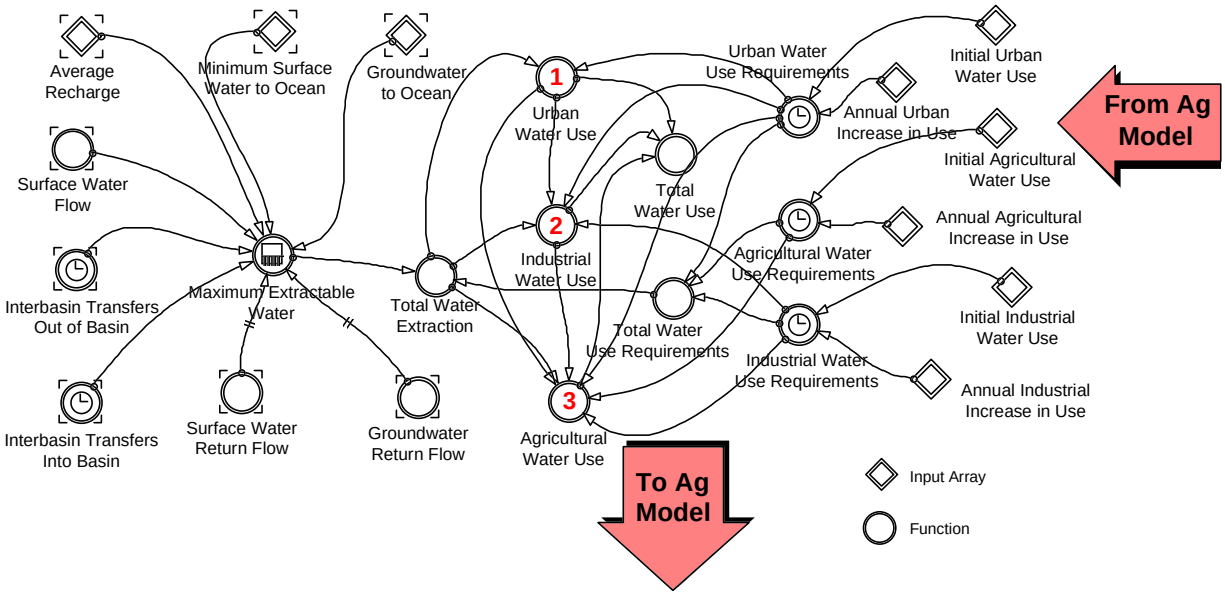

Figure A-6. Schematic of the China water model showing the elements involved in the computation of the maximum amount of extractable water, water use requirements per sector, and water use per sector.

References

China Meteorological Bureau, ed., *Map Collection of China's Climatic Resources*, Beijing: China Cartography Press, October 1994.

Crissman, L. W., *DRAINAGE Data Layer* (used by permission), Australian Centre of the Asian Spatial Information and Analysis Network (ACASIAN), China Geographical Information System (GIS) Project (www.asian.gu.edu.au/chinagis.html), Griffith University, Brisbane, Australia, 1996.

Department of Hydrology, Ministry of Water Resources, *Water Resources Assessment for China,* China Water and Power Press, Beijing, 1992.

Editorial Committee for the Almanac of China Water Resources, ed., *Almanac of China Water Resources 1991*, Beijing: Water and Power Press, May 1992.

Hernandez, J. W., Department of Civil, Agricultural, and Geological Engineering, New Mexico State University, telephone conversation with Richard P. Thomas, Sandia National Laboratories, February 1997.

University of Washington and CIESIN (Consortium for International Earth Science Information Network), *Digital Chart of the World for China prepared by CITAS (China in Time and Space),* downloaded August 1996 from CIESIN Web site, www.ciesin.org.

Water Resources and Hydropower Design Institute of the Ministry of Water Resources and Electric Power, *Water Resources Utilization in China*, Beijing: Water and Power Press, February 1989.

Zhang Qishun and Zhang Xiao, "Water Issues and Sustainable Social Development in China," *Water International,* vol. 20, pp. 122-128, 1995.

Intentionally Left Blank

APPENDIX B – THE CHINA AGRONOMIC MODEL

Intentionally Left Blank

APPENDIX B – THE CHINA AGRONOMIC MODEL

The China agronomic model, a dynamic computer model of grain production and consumption in the People's Republic of China, was developed by Sandia National Laboratories. It is a component of the China critical infrastructure model, which integrates four infrastructure models (water, agronomic, energy, and greenhouse gas) to allow for the exchange of information between the separate models and to capture the overall dynamics of the integrated system.

The China Agronomic Model was designed to:

- Generate population-driven projections of China's grain and meat demand;
- Generate projections of regional and all-country land and water resources required to meet the grain demand;
- Generate projections of each drainage region's contribution to China's total grain production;
- Compare China's projected grain demand with projected grain production to estimate grain surpluses and deficits;
- Provide projections of agricultural water requirements to the water model; and
- Provide both projections of the total land area cultivated in rice and estimates of livestock population to the greenhouse gas model.

The China agronomic model is composed of two segments, a *demand projection segment* and a *production transformation segment*. The demand projection segment computes population-driven all-China projected grain and meat demand and apportions the grain demand among the 10 water drainage regions to permit an assessment of each region's production capability. The demand projection segment also interfaces bidirectionally with the China water model to provide for the exchange of data on projected agricultural water requirements and available water. It provides computed values for agricultural water requirements to the water model for that model's use in the water balance computations and receives in return computed values for available water for use in the agronomic model in projecting water-constrained agricultural production levels. The demand projection segment also provides projections of the total land area cultivated in rice and estimates of livestock population to the greenhouse gas model, which is used to model China's greenhouse gas emissions balance.

The production transformation segment of the model is used to convert the Chinese agricultural regional grain production data obtained from the U.S. Department of Agriculture/Economic Research Service (USDA/ERS) Country Projection and Policy Analysis (CPPA) Model (Medea Project, 1997) to water drainage regional grain production data by mapping the USDA/ERS agricultural regional data onto the water drainage regions. This region-to-region transformation is necessary because the China water model simulates hydrologic budgetary processes on the basis of river drainage regions rather than agricultural regions or political provinces, and converting the data makes it possible for the model to compute the production-based agricultural water requirements and the water-constrained grain production by water drainage region.

Demand Projection Segment

The demand projection segment of the agronomic model is represented schematically in Figure B-1. This segment of the model is population driven, that is, the all-China food requirements are computed on the basis of population growth, per capita caloric demand, and the caloric content per gram of grains and meats, as follows:

1) Two options are provided for entering population growth into the model: a) a standard exponentially increasing constant-annual-percentage-rate method, and b) an annually varying percentage rate method. The second method permits the use of population projections made by agencies such as the United Nations and the USDA (see United Nations Department of International Economic and Social Affairs, 1993; Crook and Colby, 1996). The projected yearly caloric demand for all of China is generated by multiplying an average annual per capita caloric demand by the population size for each year in the simulation. The value used for daily caloric demand was 2,250 calories per capita, the median of the accepted range for the United States: 2,000–2,500 calories per capita per day (National Research Council, 1989).[1]

2) The model then apportions the all-China projected caloric demand for each year between the three major grains (rice, wheat and corn), meat, and "other" (which includes other grains and fruits and vegetables) in accordance with Chinese historical grain and meat consumption data for these food categories for all of China for the years 1994-96 obtained from the USDA (Crook and Colby, 1996). Meat animals also consume grain and "grain equivalents." To account for the caloric inefficiency of meat production, the caloric demand value apportioned to meat consumption is converted to grain-equivalent caloric demand using a grain-to-meat ratio coefficient of 4:1.[2] The assumption was made that, in the aggregate, meat animals consume grains and grain equivalents in the following proportions: rice–15%, wheat–15%, corn–50%, and other–20%. The adjusted grain-equivalent caloric demand values are then multiplied by human meat consumption caloric demand, and the resulting values are added to the corresponding human grain caloric demand to obtain the all-China total grain caloric demand for each grain type, in billions of calories. As indicated in Figure B-1 by the dashed arrow between "meat demand" and "livestock populations," the relationship between these two elements has not yet been modeled. Historic livestock populations were therefore modeled as a near-term proxy in order to generate projections for the greenhouse gas model.

---

[1] This figure will be revised when a better estimate for the China population becomes available.

[2] Meat animals are inefficient producers of calories for human consumption. For example, 7 kilograms of grain equivalents are required to produce 1 kilogram of beef, and 2 kilograms of grain are required to produce 1 kilogram of poultry (see *The Economist*, November 16, 1996; and Pond, Church, and Pond, 1995). The ratio of 4 kilograms of grain equivalents to 1 kilogram of meat is an intermediate value between the values for beef and poultry. It was used in the model as an aggregate approximation for all meat consumed in China. This value will be disaggregated into individual meats in future refinements of the model.

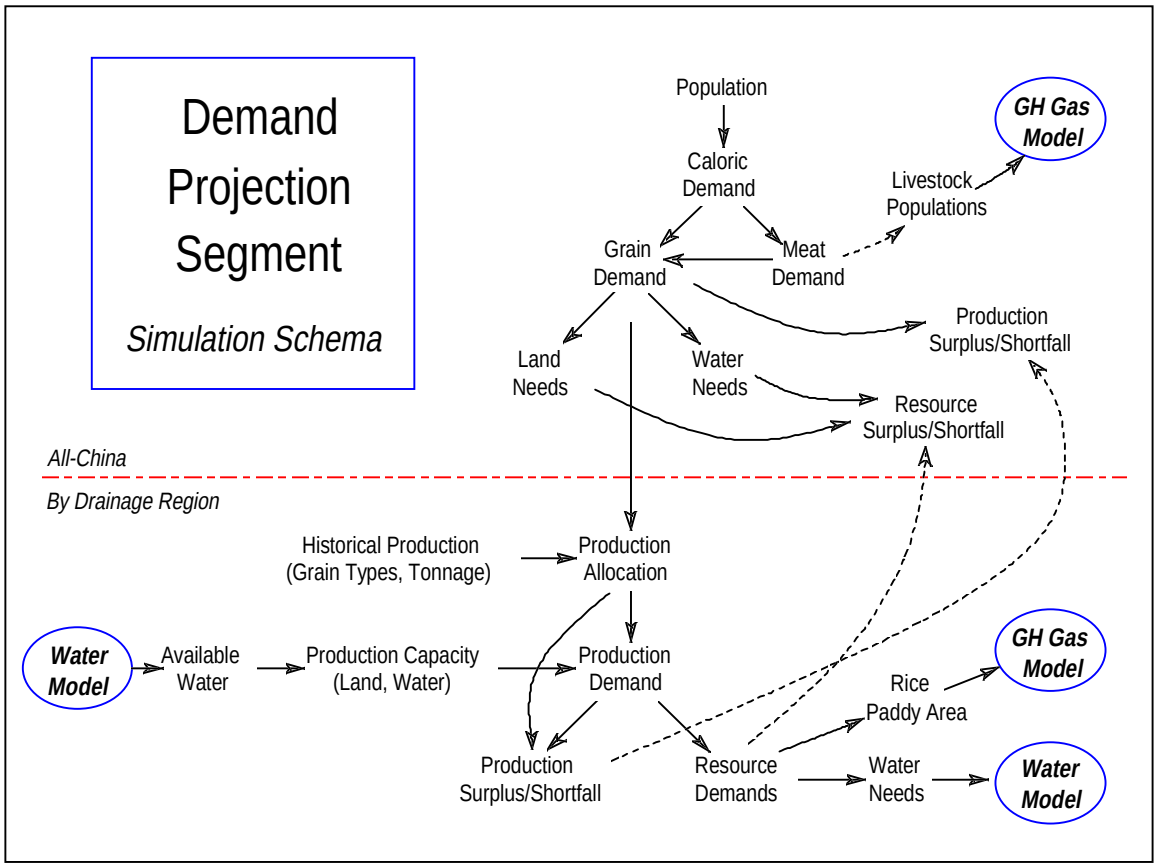

Figure B-1. The demand projection segment of the China agronomic model.

3) The total projected yearly all-China demand by weight for each grain type[3] and for meat is obtained by dividing the total grain caloric demand for each by a coefficient in calories per gram corresponding to the average caloric content for each as follows: rice–3.63, wheat–3.35, corn–3.65, meat–3.48. These average values were obtained from the *USDA Nutrient Database for Standard Reference* (1997). The average of the three grains, 3.54, was assumed as the value for "other."

4) Estimates of the total land required to produce the grain to meet the total projected yearly all-China demand are then calculated as follows: The all-China yearly demand values by weight for each grain type are divided by the corresponding yield coefficients obtained from the USDA (Crook and Colby, 1996) (in metric tons per hectare): rice–4.1, wheat–3.41, corn–4.74, and other–4.0 (an intermediate value). When summed over all grains, this provides an estimate of sown area, which is in turn a conservative maximum estimate for cultivated area. It is assumed that factors for same-grain multiple cropping have been implicitly captured in the yield coefficients to the first order; future refinements of the model are planned that will allow computations for multiple-cropping of different grains. For later applications of the model, an alternate set of grain yield coefficients, obtained

[3] As a validity check, these totals are divided in the model by total population to obtain per capita demand figures, which were then compared with historical consumption data from Crook and Colby (1996).

from the Decision Support System for Agrotechnology Transfer (DSSAT) model, was also incorporated. The approach that uses these coefficients is described below under "DSSAT Crop Model."

5) The corresponding total water volume required to produce the grain to meet the projected yearly all-China demand for each grain type is computed on a water drainage regional basis (see description in paragraph 8 below).

6) Once the population-driven all-China grain demand by weight is computed, the next step is to allocate this demand among the water drainage regions in order to assess each region's ability to meet the demand with its available land and water resources. The all-China demand is allocated among the drainage regions by apportioning this demand according to the ratio of each drainage region's historical production of each of the grains to the all-country historical production of each of the grains. For simplicity, a first-order approximation of historical production was chosen to be that of the year 1990. The all-country production for the year 1990 was obtained from Crook and Colby (1996). The derivation of the corresponding 1990 production for each drainage region is described below under "Production Transformation Segment."

7) After computing the grain demand allocations for each drainage region, the cultivated land requirements for each of the drainage regions are estimated by dividing the yields per hectare for each grain into the respective regional grain demands. These land requirements for each grain, summed over all grains for a drainage region, provide that region's total sown area requirement, a conservative maximum estimate for its cultivated land area requirement.

8) Similarly, each drainage region's total agricultural water requirement is obtained by summing over all grains, each drainage region's water requirement for each of the grains. To ensure consistency with Chinese historical records of agricultural water consumption, this computation is performed with an iterative calibration. First, estimated nominal values of water consumption, in millimeters per unit of cultivated area, are obtained from the DSSAT model for each of the grains. These figures are then multiplied by the corresponding cultivated areas for each grain, as computed above, to obtain the nominal water volume consumed for each of the grains. Summed over all grains, these provide the nominal agricultural water consumption for a drainage region. Because each drainage region has different climatic and soil growing conditions, the actual water use will vary from the nominal values. This variation is accommodated by calibrating the nominal water consumption rates for each grain, as estimated by DSSAT, for each drainage region, by multiplying the rates by the ratio of historical agricultural water consumption for each drainage region to the nominal agricultural water consumption for each drainage region. Thus calibrated, the actual agricultural water consumption values calculated for each drainage region are consistent with the historical Chinese records for the year 1980 that were obtained from *Water Resources Utilization in China* (Water Resources and Hydropower Design Institute of the Ministry of Water Resources and Electric Power, 1989). These water requirement values, by drainage region, are then provided to the water model.

9) At this point, graphs can be produced by the agronomic model to show how well each of the drainage regions is likely to fare in the future in meeting its allocation of the all-China grain demand, within the constraints of its estimated arable land and agricultural water. The projected available agricultural water for each drainage region is obtained from the water model, and the regional arable land is estimated using a geographical information system (GIS) analysis that identifies all land with a slope that is less than 1%. Spatial data for this analysis were obtained from the ACASIAN (Crissman, 1996).

10) The final step in the demand projection segment of the model is to compare the sum of all drainage region productions for each grain with the all-China demand for each grain, and the sum of regional land and water requirements with the all-China land and water requirements to determine the grain production and resource surpluses and/or shortfalls. Because the regional land- and water-constrained production portion of the model has not yet been completed, these simulation flows are shown as dashed arrows in Figure B-1.

Production Transformation Segment

There are three objectives for the production transformation segment of the China agronomic model, which is represented in Figure B-2. The first purpose is to transform the Chinese agricultural regional grain production data obtained from the USDA/ERS into water drainage regional grain production data. Converting this data provides estimates of historical drainage region production that can be used in the demand projection segment of the agronomic model to permit allocation of the all-China grain demand among the drainage regions. The second purpose of the production transformation segment is to assess the magnitude of agricultural water surpluses or deficits in each drainage region when the drainage regions are producing grain at officially projected levels. The third purpose is to determine the potential effects of placing drainage region constraints on agricultural water availability on each drainage region's grain production capability.

As with the demand projection segment of the agronomic model, converting the data from agricultural regions to water drainage regions permits the transfer of data between the production transformation segment and the water model. To achieve the three objectives stated above, several transformations are necessary, which are governed by the available data sources and their choices of geographic data representation. The grain production data are first transformed from agricultural regions to provinces, then to water basins, and then to water drainage regions. Once this final conversion has been completed, the water-related computations can be performed.

1) First, an array was developed that defines the relationship for mapping between agricultural regions and provinces (based on information provided via e-mail from W.H. Colby, USDA/ERS, to D. Jeppesen, Sandia National Laboratories, February 11, 1997). An array of provincial cultivated areas was then developed based on data obtained from Crook and Colby (1996). These two arrays, when multiplied together and summed by agricultural region, produce an array of cultivated areas for each agricultural region. An array of regional agricultural production data for each of the grains is then introduced. This array is based upon grain production data from 1980 to 2010 from the USDA/ERS CPPA Model (Medea Project, 1997). Provincial production data for each grain are then

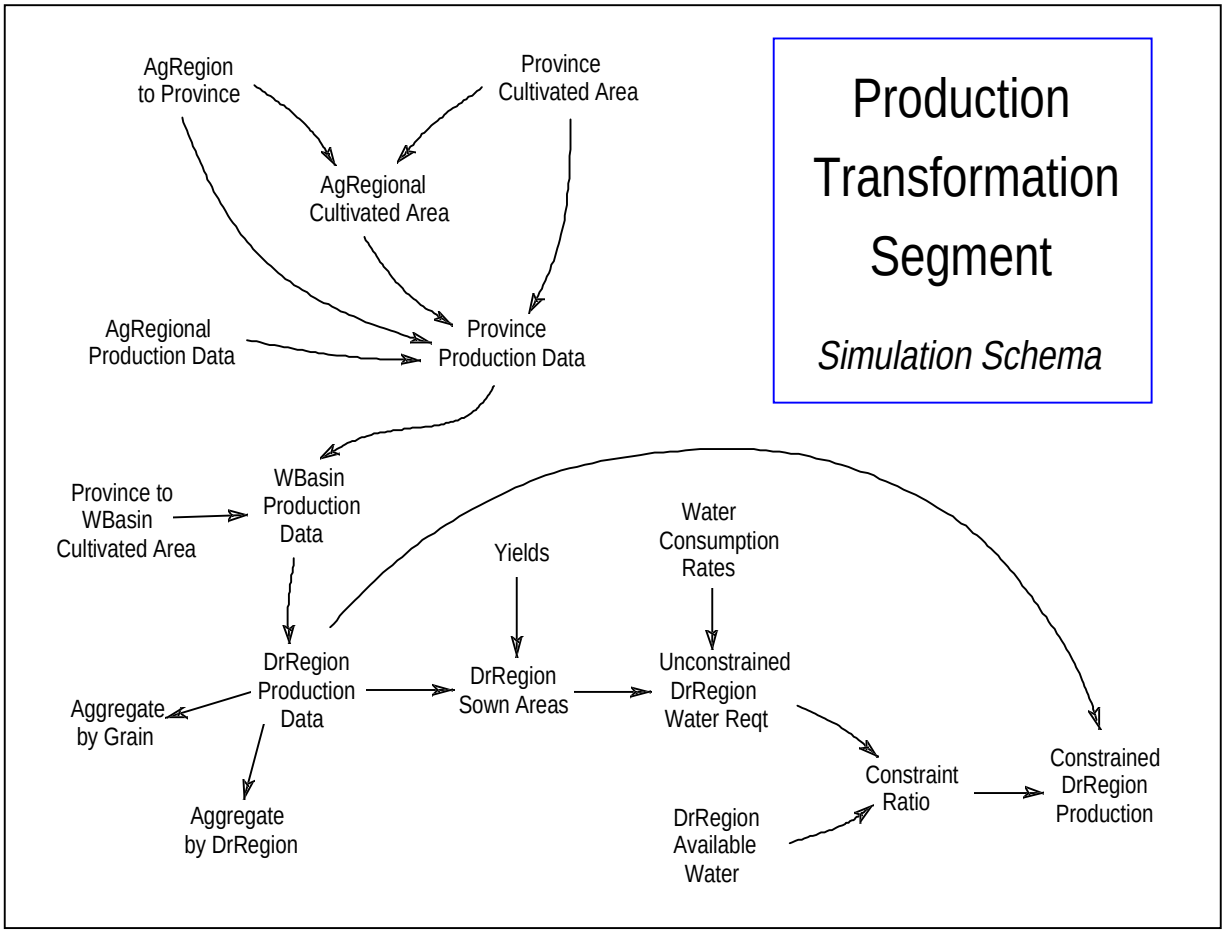

Figure B-2. The production transformation segment of the China agronomic model.

obtained by multiplying the array of data for regional production of each grain by the corresponding ratio of provincial cultivated areas to the cultivated area of the region that contains the province under consideration.

2) An array that defines the relationship between provinces and water basins is introduced next. Unlike the array that maps entire provinces to agricultural regions, described in paragraph 1, this array accounts for portions of provinces that lie in more than one water basin. To create this province-to-basin array, a GIS analysis was performed on ERIM satellite images of China's cultivated lands (ERIM, 1997) to map the provincial cultivated areas onto the appropriate water basins. Multiplying the resulting array by the provincial production data array produces an array of grain production data for each water basin.

3) The grain production data are next transformed from water basins to water drainage regions. Several of the drainage regions encompass multiple water basins. This transformation is accomplished by simply summing the grain production data for each water basin to obtain its respective drainage region production.

4) Once the production data by drainage region are obtained, the water consumption assessments may be made. This first requires computing the sown areas by grain type;

these values are obtained, as in the demand projection segment, by dividing the regional production for each grain by the yield for that grain. The resulting sown areas for each grain are then multiplied, as in the demand projection segment, by the calibrated water consumption rates, in millimeters per crop season, for that grain. The resulting water consumption volumes, summed over all grains produced in a drainage region, provide the total grain production water requirement for that drainage region. This regional total water requirement can now be compared with the water available for each region obtained from the water model, either graphically or by differencing, to assess water deficits and surpluses.

5) For those drainage regions in which a water deficit is found, it is of interest to estimate the effects of these deficits as constraints upon the grain production for those regions. This is accomplished by first defining a "water-constraint ratio" array, by dividing the unconstrained water usage for each drainage region, as computed above, into the available water for that drainage region obtained from the water model. This water-constraint ratio array is then multiplied by the regional grain production array to obtain the water-deficit-constrained production of each grain for each drainage region.

In conclusion, it should be noted that all of the steps described above, for both segments of the agronomic model, are repeated for each year in a simulation. In the demand projection segment, the simulation begins with a population that increases each year; in the production transformation segment, the simulation begins with agricultural regional production that changes each year.

DSSAT Crop Model

As explained in the previous sections, computing land and water use requirements for the production of individual grains requires some measure of the yields per unit of crop area and of water consumption rates per unit of grain weight or per unit of crop area for each of the grains. For the initial build of the agronomic model, for expedience, approximations for yields were obtained from Crook and Colby (1996) and approximations of water use coefficients were obtained from Dr. Joe Ritchie, University of Michigan Agronomy Department, who based them on his experience with field crop experiments.

To allow the agronomic model to better reflect local rather than aggregated average crops and growing conditions, the DSSAT crop model was engaged. DSSAT was selected because it is an internationally recognized crop modeling software system. DSSAT originated during the 1970s with the research models of several independently funded scientific efforts that were studying the growing processes of different grains. These individual models were consolidated into a single system, revised, and extended under a 10-year program funded by the U.S. Agency for International Development. DSSAT now carries the credibility and acceptance of over 25 years of modeling development in agronomic sciences (see *The IBSNAT Decade*, 1993, for a historical perspective). The input drivers for the DSSAT model are comprehensive and include local weather, soil, and solar conditions; crop genetics; and pest and crop management practices. The model produces as outputs, among many other crop parameters, yields in kilograms per hectare and the three components of water usage—evapotranspiration, drainage and runoff—in millimeters per hectare.

To permit the generation of stochastic variation in grain yields and water requirements within the agronomic model, DSSAT was used as the basis for developing a Monte Carlo generator that is now operational as an option within the demand projection segment of the agronomic model.

Complete integration of the DSSAT model into the China agronomic model has not yet been accomplished. This is primarily because *in situ* Chinese crop field data with which to drive DSSAT have not yet been obtained. Instead, data obtained from several field experiments conducted in other countries that were modeled in the DSSAT were used as the basis for calculating nominal crop water usage in both segments of the agronomic model. Because yields are more cultivar-specific and geographically sensitive than water uses, USDA average yields will continue to be used in the model (except for runs with the stochastic Monte Carlo option enabled) until Chinese field data become available.

Data

The following data elements were used in the China agronomic model: population growth rate; caloric content of grains and meats; grain-to-meat conversion efficiencies; grain yields per hectare; grain production and consumption; agricultural water availability; grain water consumption coefficients; grain water use efficiency rates; provincial cultivated areas; and province-to-agricultural region relationships. A summary of the data elements used and their sources appears in Table B-1.

Table B-1. Sources of Data for the China Agronomic Model*

Data Element	Source
Population Growth Rate	*The Future of China's Grain Market* (Crook and Colby, 1996) *World Population Prospect* (United Nations, 1993)
Caloric Content of Grains and Meats	*USDA Nutrient Database for Standard Reference* (1997)
Grain-to-Meat Conversion Efficiencies	*Basic Animal Nutrition & Feeding* (Pond, Church, & Pond, 1995) *Will the World Starve?,* The Economist, November 16, 1996 *Chinese Grain Economy and Policy* (Chen Xian Yu & Buckwell, 1971)
Grain Yields per Hectare	*The Future of China's Grain Market* (Crook and Colby, 1996) DSSAT V3 Crop Model
Grain Production and Consumption	*The Future of China's Grain Market* (Crook and Colby, 1996) *Chinese Grain Economy and Policy,* (Chen Xian Yu & Buckwell, 1971) USDA/ERS CPPA Model (Medea Project, 1997)
Agricultural Water Availability	*Water Resources Utilization in China* (Water Resources and Hydropower Design Institute of the Ministry of Water Resources and Electric Power, 1989)
Grain Water Consumption Coefficients (Estimated Ranges)	Dr. Joe Ritchie, Department of Agronomy, Michigan State University, 1997
Grain Water Use Efficiency Rates	DSSAT V3 Crop Model
Provincial Cultivated Areas	*The Future of China's Grain Market* (Crook and Colby, 1996)
Province-to-Agricultural-Region Relationships	W. H. Colby, USDA/ERS

*See the References section for a complete listing of these sources.

References

Chen Xiang Yu and A. Buckwell, *Chinese Grain Economy and Policy,* CAB International, Wallingford, Oxon, UK, 1971.

Colby, W. H., USDA/ERS, e-mail correspondence to D. Jeppesen, Sandia National Laboratories, February 11, 1997.

Crissman, L. W., *DRAINAGE Data Layer* (used by permission), Australian Centre of the Asian Spatial Information and Analysis Network (ACASIAN), China Geographical Information System (GIS) Project (www.asian.gu.edu.au/chinagis.html), Griffith University, Brisbane, Australia, 1996.

Crook, F. W., and W. H. Colby, *The Future of China's Grain Market,* U.S. Department of Agriculture/Economic Research Service (USDA/ERS), Agricultural Information Bulletin (AIB) No. 730, October 1996.

ERIM Geographic Information Systems and Applications Department, Earth Sciences Group, *GIS Database of China Land Use Data*, provided by Christopher Chiesa, 1997.

International Benchmark Sites Network for Agrotechnology Transfer, *The IBSNAT Decade.* Department of Agronomy and Soil Science, College of Tropical Agriculture and Human Resources, University of Hawaii , Honolulu, HI, 1993.

Medea Project Base Scenario Area and Production Estimates Using New 1995 Estimates (Harvested Area and Grain Production for Years 1980–2010, by region): LOTUS Spreadsheet from USDA/ERS Country Projections and Policy Analysis (CPPA) Model (attachment to e-mail from F. Crook and W.H. Colby, USDA, to D. Jeppesen, Sandia National Laboratories, February 10, 1997).

National Research Council, *Recommended Dietary Allowances,* 10th ed., National Academy of Sciences, Washington, DC, 1989.

Pond, W. G., D. C. Church, and K. R. Pond, *Basic Animal Nutrition & Feeding,* John Wiley & Sons, New York, 1995.

Ritchie, J., Department of Agronomy, Michigan State University, e-mail messages to D. Jeppesen, Sandia National Laboratories, February 2–8, 1997.

The Economist, Will the World Starve?, Vol. 341, no. 7992, pp. 21–23, November 16, 1996.

United Nations Department of International Economic and Social Affairs, *World Population Prospects,* United Nations, New York, 1993.

USDA Nutrient Database for Standard Reference, http://www.nal.usda.gov/fnic/cgi-bin/nut_search.pl, 1997.

Water Resources and Hydropower Design Institute of the Ministry of Water Resources and Electric Power, *Water Resources Utilization in China,* Beijing: Water and Power Press, February 1989.

APPENDIX C – THE CHINA ENERGY MODEL

Intentionally Left Blank

APPENDIX C – THE CHINA ENERGY MODEL

The China energy model is a dynamic computer model of energy consumption in the People's Republic of China developed by Sandia National Laboratories.[1] It is a component of the China critical infrastructure model, which integrates four infrastructure models (water, agronomic, energy, and greenhouse gas) into a single critical infrastructure model for all of China to allow for the exchange of information between the separate models and to capture the overall dynamics of the integrated system.

The drivers for simulating China's energy consumption are growth in gross domestic product (GDP) and decreasing sectoral energy intensities. Energy consumption is calculated for each sector (i = 1, 2, ... , 6) in each time period (t) based on GDP (GDP_t), sector GDP share ($S_{i,t}$), and sector-specific energy intensities ($I_{i,t}$). Total energy consumption in time period t is calculated as

$$E_t = \sum_{i=1}^{6} (I_{i,t} S_{i,t} GDP_t). \quad (1)$$

GDP Growth

Growth in GDP averaged about 7% per year for the period 1978–1995, as shown in Figure C-1.[2] GDP growth during the 1980s averaged 5.4% per year; it averaged 11.2% during the 1990s.

To simulate future economic growth, future GDP is incorporated into Equation (1) simply as a product of past GDP and a time period growth rate r_j:

$$GDP_t = GDP_{t-1}(1 + r_j), \quad (2)$$

where j = 1996–2005, 2006–2015, 2016–2025.

---

[1] Two other models that calculate China's energy demand and greenhouse gas emissions are the Edmonds, Reilly, and Barns (ERB) model, developed at Pacific Northwest Laboratory (Edmonds et al., 1994), and the MARKAL-MACRO model, developed at Brookhaven National Laboratory (Goldstein, 1994). The ERB model calculates supply and demand for each of six major primary energy categories in each of nine global regions; China is one of nine regions. Supply and demand for each region depends on several exogenous variables and energy prices. Demand is a function of population, labor productivity, energy intensity, energy prices, including exogenously specified taxes, subsidies, and tariffs. The ERB model is often run as part of a larger integrated assessment model, the Global Change Assessment Model. The ERB model does not, at present, contain any provincial-level detail on China.

The MARKAL-MACRO model consists of two component models, MARKAL and MACRO. MARKAL is a cost-minimization linear programming model. The user specifies available supply options, demand options, and other constraints, such as a 20% carbon dioxide emission for a country or region. The model then calculates the option that minimizes the total system costs for that particular country or region. The MACRO component is a macroeconomic growth model that is used to calculate the economic impacts of scenarios used in the MARKAL component. MARKAL-MACRO has gained widespread use in the U.S. and in many other countries.

[2] GDP is deflated by the GDP index in *China Statistical Yearbook* (State Statistical Bureau, 1996), Table 2-10, p. 42.

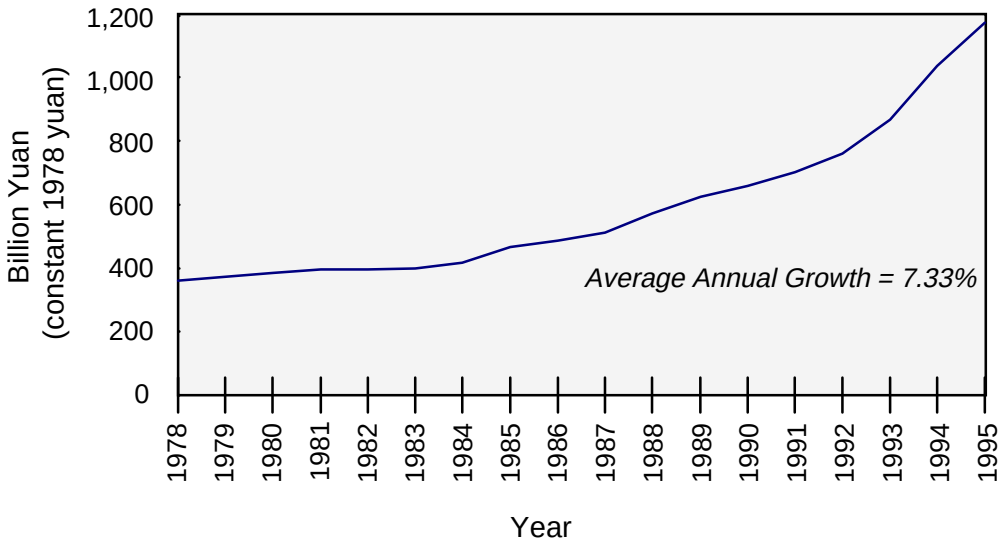

Figure C-1. China's GDP, 1978–1995.

To project GDP growth in the model, the user can choose one of the scenarios outlined in Table C-1 or create a custom scenario. The base case growth rates in Table C-1 are the averages of the high and low growth rates of the World Bank GDP scenarios.

Table C-1. GDP Growth Scenarios

	Average Annual Growth Rates (percent per year)		
Scenario	1996–2005	2006–2015	2016–2025
World Bank*			
High growth	9.5	8.0	6.5
Slow growth	8.5	6.5	5.0
OECD†	8.5	7.0	6.5
Base Case	9.0	7.25	5.75

* Johnson et al. (1996), p. 19. These growth rates were adapted from reported 10-year growth periods of 1990–2000, 2000–2010, and 2010–2020.

† OECD (1996), Table 2, p. 99. The 1996–2005 and 2006–2015 growth rates were adapted from rates reported for the intervals 1993–2000 and 2000–2010; the growth rate for 2016–2025 is an extrapolation.

GDP Sector Shares

GDP is assumed to originate from each of six historically significant economic sectors—transportation, construction, commerce, residential (and other), agriculture, and industry. Figure C-2 presents the GDP shares for these six sectors for the years 1978 to 1995.[3] Not surprisingly, as China continued to develop during this period, the agricultural sector's share declined while that of other sectors increased; agriculture's share declined from a high of 34% in 1982–83 to just 20.6% in 1995. The industrial sector share has remained fairly flat, having increased only slightly in the 1990s. In general, the residential, commerce, and construction sectors have increased their contribution to the national GDP as China has modernized and begun the move from an agrarian to an industrial society.

The base case GDP sector share assumptions appear in Table C-2. It is assumed that as GDP grows, agriculture's share will decline.[4] Other sector percentages slope to 10-year period end points (see Table C-2) that reflect China's industrial saturation and continued shift to a service-oriented economy, or to user-defined end points.

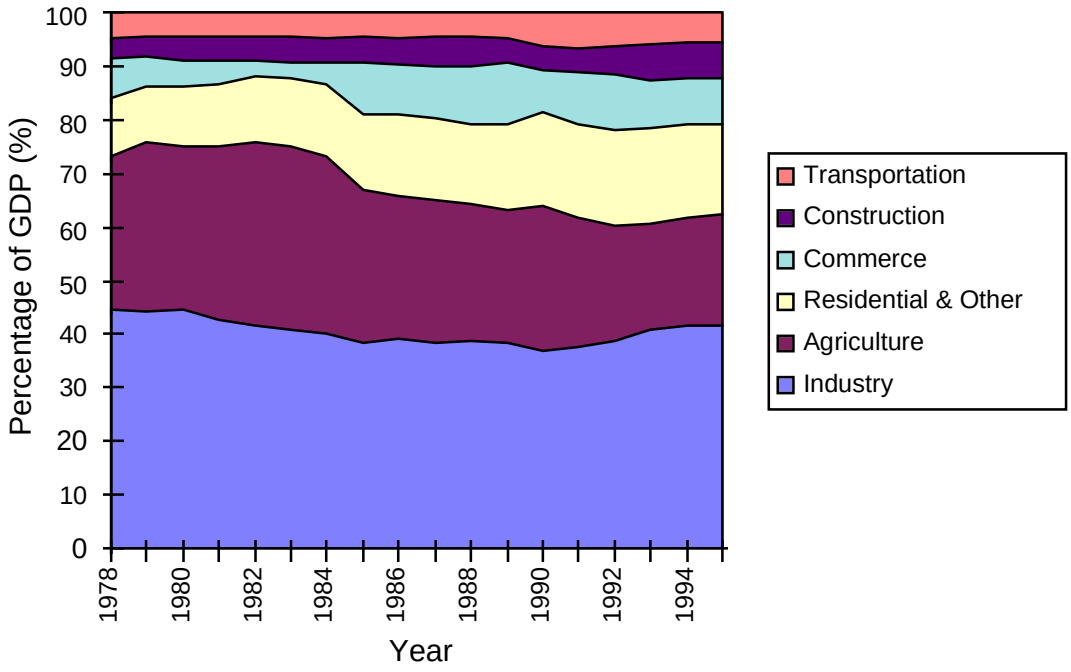

Figure C-2. GDP sector shares, 1978–1995.

[3] Shares were calculated at current year prices.

[4] In the simulation, agriculture's share of GDP is not explicitly defined, but rather is computed as 100% minus the sum of the shares of the other sectors.

Table C-2. GDP Sector Share Assumptions, Base Case

	Sector Share (%)			
		End of Time Period		
Economic Sector	1995*	2005	2015	2025
Industry	41.8	42	43	44
Residential	16.8	17	18	18
Commerce	8.7	10	12	15
Construction	6.5	7	7	7
Transportation	5.6	6	6	6
Agriculture	20.6	18	14	10

* Source: China Statistical Yearbook (1996), Table 2-10, p. 42. Residential GDP is calculated as the total for tertiary industry less the transportation and commerce sectors.

Energy Intensity

The second driver used in the model to simulate Chinese energy consumption is energy intensity. Figure C-3 plots average energy intensity for the Chinese economy in kilograms of coal equivalents (kgce) per yuan from 1978 to 1995 and shows a rapid decline from the mid-1980s; however, the average energy intensity is still well above industrial country averages and the energy intensities of comparable developing countries. For example, China's energy intensity is 4.42 times that of Japan, 3.80 times that of Brazil, and 1.65 times that of India (see Nilsson (1993), for a comparison of the energy intensities of 31 countries from 1950 to 1988). Sector-specific energy intensities ($I_{i,t}$) are plotted in Figure C-4.

Much has been written on the source of China's energy intensity decline and its implications for future energy savings, particularly within the industrial sector. Through the decomposition of energy intensity decline into structural change (i.e., due to shifting industry and sector dominance) and technological change, recent researchers have concluded that the majority of decline has been due to improved technology within individual industries (Huang, 1993; Sinton and Levine, 1994; Zhang Zhong Xiang, 1995).

For the base case, it was assumed that energy intensity will continue to decline over the study period, as shown in Table C-3. Whether China can continue to lessen its dependence on energy while continuing to increase GDP will depend on a number of dynamic factors. Perhaps most important is the continued technology transfer to and foreign investment in the industrial and power sectors. Also, if China begins to make the transition to a more service-oriented economy, as many other developing nations have, then the structural impact on energy intensity improvements that have been limited in the past may increase.

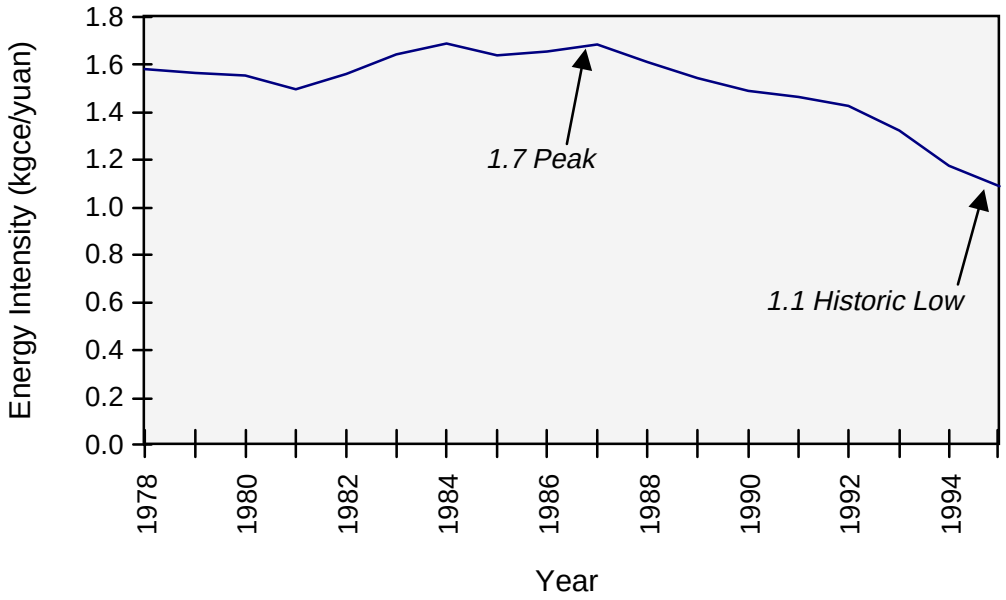

Figure C-3. Chinese average energy intensity, 1978-1995.

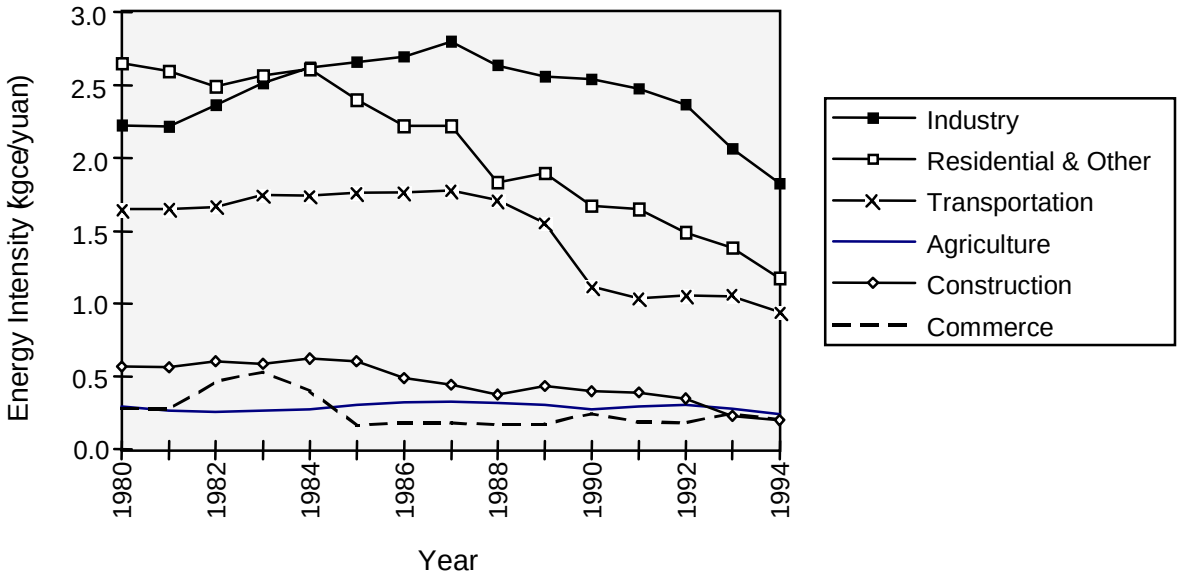

Figure C-4. Sector-specific energy intensities, 1980-1994.

Table C-3. Assumed Sectoral Energy Intensities

	Base Case Sectoral Energy Intensities* (kgce/Yuan)			
Sector	1995	2005	2015	2025
Agriculture	0.204	0.13	0.10	0.086
Industrial	1.75	1.13	0.88	0.72
Construction	0.192	0.169	0.160	0.154
Transportation	0.93	0.82	0.78	0.74
Commerce	0.165	0.145	0.137	0.132
Residential (and Other)	1.15	0.97	0.90	0.857

*1995 sectoral energy intensities were derived from the *China Statistical Yearbook*. Values for the year 2025 for agriculture, industrial, and other are derived from Lu (1993), Table 3.19, on the basis of his estimates for efficiency improvements between 1980–2020. For the construction, transportation, and commerce sectors, values for the year 2025 are 20% lower than those for 1995; the energy intensity for these sectors has already dropped to close to the levels forecasted by Lu for 2020. For all sectors, it is assumed that 60% of the improvement will occur between 1995–2005 and that 60% of the remainder will occur between 2005–2015.

Sectoral Fuel Shares

Once total energy demand by sector ($E_{i,t}$) has been calculated (see Equation 1), the next step is to determine sectoral demand by primary energy type (coal, oil, natural gas, and electricity). The model uses historical data for calculating sectoral primary energy demand shares and relies on user-specified end points for calculating future demand. Table C-4 summarizes base case assumptions regarding fuel shares. Coal shares are not directly input into the model, but are calculated as one hundred percent minus the sum of the other shares. In other words, it is assumed for this model that, if, for example, electricity's share in the industrial sector increases over time, then coal's share will decrease. However, because coal is a primary fuel type for electricity, the *direct* use of coal in the industrial sector will increase.

Assumptions regarding electricity fuel shares can also be changed in the model. The base case assumption is that coal will remain the dominant fuel choice for generating electricity. Both nuclear and hydropower capture increasing shares in the base case, corresponding with official plans of the Chinese government. Specifically, the base case assumes 32 GW of installed nuclear capacity by 2020, up from the current 2.1 GW, and 138 GW of installed hydropower capacity, up from 36 GW in 1990 (Johnson et al., 1996). As hydropower and nuclear capacities increase, the percentage of electricity generated by coal will decline. The base case further assumes that oil and natural gas play a minor role (8.7% and 0.5%, respectively) in future electricity generation plans. Because of increasing international interest in natural gas as an environmentally superior alternative to coal, future versions of this model will explore the impact of increasing natural gas use for electricity generation.

Table C-4. Assumed Sectoral Fuel Shares

	Base Case Sectoral Energy Shares (%)*			
Sector Primary Energy	1995	2005	2015	2025
Agriculture				
Coal	26	20	17	16
Oil	31	34	34	34
Natural Gas	0	0	0	0
Electricity	43	46	49	50
Industrial				
Coal	54	51	48	47
Oil	13	13	13	13
Natural Gas	2	2	2	2
Electricity	31	34	37	38
Construction				
Coal	28	25	24	24
Oil	26	30	30	30
Natural Gas	0	1	1	1
Electricity	46	45	45	45
Transportation				
Coal	25	17	13	12
Oil	62	69	72	73
Natural gas	0.3	0.3	0.3	0.3
Electricity	12	14	15	15
Commerce				
Coal	41	26	18	15
Oil	18	25	28	29
Natural Gas	0.3	0.5	0.5	0.5
Electricity	41	49	54	56
Other				
Coal	58	45	37	33
Oil	14	18	20	21
Natural Gas	2	2	3	4
Electricity	27	35	40	42

* Energy shares for each sector do not total 100%, due to rounding.

Excess Demand Calculations

The excess demand submodule of the China energy model determines whether historical production growth is sufficient to meet future demand. A relatively simplistic, but insightful, methodology was used to calculate excess demand. Specifically, the model uses either low or high infrastructure investment assumptions to calculate future production for each fuel type. Excess demand is then calculated as the difference between forecasted demand and production. Positive excess demand implies that assumed average production increases are sufficient to meet future demand growth. Negative excess demand implies that domestic production will not be sufficient to meet forecasted demand, indicating the need to either import energy or increase infrastructure investment in order to increase production.

Low infrastructure investment is defined as achieving an annual production increase by fuel type comparable to the 10-year historical growth pattern. High infrastructure investment is defined as achieving an annual production increase comparable to the average growth achieved in the 5 years with the highest growth in the last 10-year period. For example, oil production in China averaged 1.87% per year for the period 1985–1995 (low investment assumption). However, the 5-year high average is 2.88% (high investment assumption). For coal, the assumed production growth rates for the low- and high-investment options are 4.59% and 6.92%. For natural gas, the low- and high-investment-option assumptions are 3.11% and 5.10%.[5]

[5] These estimates are calculated from the *China Statistical Yearbook 1996* (State Statistical Bureau, 1996).

References

Edmonds, J. A., M. A. Wise, and C. N. MacCracken, *Advanced Energy Technologies and Climate Change: An Analysis Using the Global Change Assessment Model (GCAM)*, Pacific Northwest Laboratory, Richland, WA, 1994.

Goldstein, G., "MARKAL-MACRO: A Policy Assessment Tool to Support Decision Making", Brookhaven National Laboratory, October 2, 1994.

Huang Jin-ping, "Industry Energy Use and Structural Change: A Case Study of the People's Republic of China," *Energy Economics*, April, pp. 131–136, 1993.

Johnson, Todd M., Li Junfeng, Jiang Zhongxiao, and Robert P. Taylor, *China: Issues and Options in Greenhouse Gas Emissions Control*, World Bank Discussion Paper No. 330, The World Bank, Washington, D.C., 1996.

Lu Yingzhong, *Fueling One Billion: An Insider's Story of Chinese Energy Policy Development*, Washington Institute Press, Washington, D.C., 1993.

Nilsson, Lars J., "Energy Intensity Trends in 31 Industrial and Developing Countries 1950–1988," *Energy*, Vol. 18, No. 4, pp. 309–322, 1993.

Organisation for Economic Co-operation and Development (OECD), *China in the 21st Century: Long-term Global Implications*, Organisation for Economic Co-operation and Development, Paris, France, 1996.

Sinton, Jonathan E. and Mark D. Levine, "Changing Energy Intensity in Chinese Industry: The Relative Importance of Structural Shift and Intensity Change," *Energy Policy*, pp. 239–255, March 1994.

State Statistical Bureau, *China Statistical Yearbook 1996*, China Statistical Publishing House, People's Republic of China, 1996 (various other years used to derived data estimates as well).

Zhang Zhong Xiang, "Energy Conservation in China: An International Perspective," *Energy Policy*, vol. 23, no. 2, pp. 159–166, 1995.

Intentionally Left Blank

APPENDIX D – THE CHINA GREENHOUSE GAS MODEL

Intentionally Left Blank

APPENDIX D – THE CHINA GREENHOUSE GAS MODEL

The China greenhouse gas model, a dynamic computer model of greenhouse gas emissions in the People's Republic of China, was developed by Sandia National Laboratories. It is a component of the China critical infrastructure model, which integrates four infrastructure models (water, agronomic, energy, and greenhouse gas) into a single critical infrastructure model for all of China to allow for the exchange of information between the separate models and to capture the overall dynamics of the integrated system.

Energy production and consumption result in the emission of several greenhouse gases, including carbon dioxide (CO_2), methane (CH_4), and nitrous oxide (N_2O). CO_2 is generated as a results of fossil fuel consumption, CH_4 is released during coal mining and oil and natural gas production and distribution, and N_2O is generated in the transportation sector as a byproduct of fossil fuel combustion. Agricultural processes serve as both a source and a sink for greenhouse gases. CO_2 is released as a result of land use changes, mainly deforestation. CO_2 is also absorbed through uptake during photosynthesis. CH_4 is generated from enteric fermentation in animals, anaerobic decomposition of animal manure, and anaerobic decomposition of vegetation in rice paddies. N_2O is released as a result of denitrification in soils, including denitrification of fertilizers.

The greenhouse gas model forecasts emissions of CO_2 and CH_4 generated in the production (extraction), distribution (primarily natural gas pipelines), and consumption (burning) of coal, oil, and natural gas, and CH_4 emissions resulting from the decay of rice paddy biomass and from enteric and anaerobic fermentation in farm animals. N_2O was not included in the model because significant uncertainties still remain in the existing methodologies for measuring N_2O emissions. Additionally, although a methodology for estimating agricultural sinks of CO_2 was to be included in this study, it was not completed in time to be included in this report or version of the model.

CO_2 Emissions from the Energy Sector

Combustion of fossil fuels is the largest anthropogenic source of CO_2. The carbon content of fossil fuels varies by fuel type: coal is the most carbon intensive, natural gas the least. The model assumes carbon coefficients for Chinese coal, oil, and natural gas of, respectively, 0.651, 0.543, and 0.404 metric tons of carbon (mtC) per metric ton of coal equivalent (mtce) (Zhang Zhong Xiang, 1996). China emitted approximately 717 million metric tons of carbon (MmtC)[1] in 1995, 13.1% of total world emissions in 1995 (6,013 MmtC) (EIA, 1997).[2] However, on a per capita basis, Chinese emissions were approximately 0.66 mtC in 1995, compared to a world average of 0.95 mtC/capita and a U.S. average of 5.4 mtC/capita.

---

[1] CO_2 emissions are reported here in units of metric tons of carbon (mtC). To convert metric tons of carbon to metric tons of CO_2, multiply by 3.667.

[2] The most current EIA values for worldwide CO_2 emissions are from 1995.

CH_4 Emissions from the Energy Sector

CH_4 is released during the mining of coal and during the production and distribution of oil and natural gas. The greenhouse gas model uses the methodology outlined by the Intergovernmental Panel on Climate Change (IPCC, 1994) for Tier 1 calculations of national emissions of CH_4 from energy production and consumption.

CH_4 from Coal Mining

CH_4 is released as a by-product of coal mining. Factors contributing to the amount of CH_4 include depth, coal rank, gas content, and mining methods (IPCC, 1994). An estimated 23 to 39 teragrams (Tg) of CH_4 were released from coal mining in 1990 (IPCC, 1994, p. 1.89), approximately 5.9–9.9% of the total estimated anthropogenic emissions (392 MmtCH_4/year).[3]

The China greenhouse gas model relies on the simplest of recommended methods for calculating emissions, referred to by the IPCC as the Tier 1 Methodology: the Global Average Method. This methodology is recommended "in cases where total coal production from underground mines is available but more detailed data on mining emissions, geological conditions, coal characteristics, and the like are not" (IPCC, 1994, p. 1.93). This Tier 1 approach assumes emissions of 10–25 m^3/ton coal mined from underground mines and 0.3–2.0 m^3/ton coal mined from surface mines (IPCC, 1994, pp. 1.93–1.97). To account for emissions from post-mining activities, the IPCC recommends emission factors of 0.9–4 m^3/ton for underground mined coal and 0–0.2 m^3/ton for surface mined coals (IPCC, 1994, p. 1.99). The China greenhouse gas model uses average values for all emission factors. Approximately 96% of Chinese coal comes from underground mines (McCreary, et al., 1996, p. II-6).

CH_4 from Oil and Natural Gas Production and Distribution

CH_4 is released during the production, processing, and distribution of oil and natural gas. Estimates of total worldwide emissions from these sources range from 30 to 60 Tg per year (IPPC, 1994, p. 1.103), which is 7.7–15.3% of total estimated anthropogenic emissions. The IPCC (1994) has formulated a three-tier approach for estimating emissions from these sources, with each successive tier requiring more detailed information. The China greenhouse gas model relies on the most generic estimation methodology recommended, Tier 1–"Production Based Average Emission Factors."

Emission factors for the various production and distribution steps are listed in Table D-1. The China greenhouse gas model assumes average values for each range given in Table D-1. Emissions associated with crude oil transportation and refining were not included in this initial phase of the modeling effort as they do not constitute a major source of CH_4 compared to the production and distribution processes.

---

[3] The IPCC (1996) estimates total CH_4 emissions of 560 ± 90 Mt/year, of which 70% is from anthropogenic sources and 30% from natural sources.

Table D-1. CH_4 Emission Factors from Oil and Gas Production*

Emissions Type	Emissions Factor (kg/petajoule)
Oil and Gas Production	
Oil	290–4,670 of oil produced
Gas	39,590–96,000 of gas produced
Crude Oil Transportation and Refining	
Transportation	745 of oil tankered
Refining	90–1,400 of oil refined
Storage Tanks	20–260 of oil refined
Natural Gas Processing, Transportation, and Distribution	116,610–340,000 of gas consumed

* Source: IPCC, 1994, p. 1.119.

CH_4 Emissions From the Agricultural Sector

The model considers CH_4 emissions from beef cows, dairy cows, buffalo, sheep, and pigs. Using the IPCC Tier 1 methodology, enteric emissions are calculated by multiplying the animal populations by animal-specific emission factors. Anaerobic emissions from waste management systems are calculated by multiplying the population of animals by the estimated emission factors for temperate regions.[4] Enteric and anaerobic emission factors and initial animal population assumptions for China are summarized in Table D-2. Future animal population growth rates are derived from a linear regression of growth rates for 1980-1995.

Emissions from rice paddies are calculated as a function of growing temperature, whether or not the rice paddy is flooded, and the length of the growing season. The total hectares of rice is estimated by the agronomic model. Table D-3 summarizes the IPCC recommended emission factors for each temperature. For the base case, the model assumes that the percentage of rice grown in flooded paddies remains constant at 93%, the current estimated percentage, and assumes an average growing season of 115 days (IPCC, 1994, Table 4-6). For the purposes of this model, emission factors were assigned to each water region by estimation using July average temperatures listed in *The Times Atlas of China* (Geelan and Twitchett, 1974).

[4] The IPCC methodology also includes anaerobic emission factors for cool and warm regions. For this initial phase, the factors for temperate regions were used.

Table D-2. Animal Populations and CH_4 Emission Factors

	1980 Population[a] (millions)	1995 Population[a] (millions)	Enteric Emission Factors[b] (kg/head)	Anaerobic Emission Factors[c] (cool/temperate/warm) (kg/head)
Beef cows	50.6	96.9	44	1/1/2
Dairy cows	1.9	3.6	56	7/16/27
Buffalo	18.4	22.9	55	1/2/3
Sheep	102.6	117.4	5	0.1/0.16/0.21
Pigs	325.1	424.7	1	3/4/6

[a] Animal population numbers are from the Food and Agriculture Organization of the United Nations (FAO) (1997).

[b] Enteric emission factors are derived from Tables 4-3 and 4-4 in IPCC (1994).

[c] Anaerobic emission factors are derived from Tables 4-5 and 4-6 in IPCC (1994).

Table D-3. Emission Factors for CH_4 from Rice Paddies (as a Function of Temperature)

Growing Season Average Temp. (C°)	Emission Factor (kg/ha/day)*	
	Continuously Flooded	*Intermittently Flooded*
15	2.91	1.75
16	3.09	1.85
17	3.28	1.97
18	3.48	2.09
19	3.68	2.21
20	3.91	2.34
21	4.14	2.49
22	4.39	2.64
23	4.66	2.80
24	4.94	2.97
25	5.24	3.15
26	5.56	3.34
27	5.90	3.54
28	6.25	3.75
29	6.63	3.98
30	7.03	4.22

* Source: IPCC (1994).

References

Energy Information Administration (EIA), *Annual Energy Review 1996,* U.S. Department of Energy, DOE/EIA-0384(96), July 1997.

Food and Agriculture Organization of the United Nations (FAO), *FAOSTAT Statistics Database*, available at http://apps.fao.org/cgi-bin/nph-db.pl?subset= agriculture, 1997.

Geelan, P. J .M. and D. C. Twitchett, *The Times Atlas of China.* New York Times Book Co., 1974.

Intergovernmental Panel on Climate Change (IPCC), *Greenhouse Gas Inventory Reference Manual*, First Draft, Volume 3, 1994.

Intergovernmental Panel on Climate Change (IPCC), *Climate Change 1995: Impacts, Adaptations and Mitigation of Climate Change*, Cambridge University Press, 1996.

McCreary, E. I, A. Y. Gu, V. Loose, and J. Roop, *China's Energy: A Forecast to 2015*, Office of Energy Intelligence, U.S. Department of Energy, La-UR-96-2972, September, 1996.

Zhang Zhong Xiang, *Integrated Economy-Energy-Environment Policy Analysis: A Case Study for the People's Republic of China*, Ph.D. dissertation, University of Gronigner, The Netherlands, 1996.

APPENDIX E – ADDITIONAL CHINA INFRASTRUCTURE MODEL RESULTS

Intentionally Left Blank

APPENDIX E – ADDITIONAL CHINA INFRASTRUCTURE MODEL RESULTS

China Water Model – Additional Results

Figures E-1 through E-10 present the results of a single run of the China water model through the year 2025 for each of 10 water drainage regions, the Heilongjiang, the Haihe, the Huaihe, the Huanghe, the Chang Jiang, the Liaohe, the Pearl River, Southeast Coastal, Southwest China, and the Region of Inland Rivers. Figures E-11 through E-14 present the results of single runs using regional data for all of China and for three geographic regions, northeastern China, northwestern China, and southern China. These figures also compare two projections of total water requirements for each region. The first was generated using agricultural water requirements that were computed in the China agronomic model. The second was generated using linear projections of agricultural water requirements based on data from *Water Resources Utilization in China*, consisting of water use for 1980 and projected agricultural water use for the year 2000 (Water Resources and Hydropower Design Institute of the Ministry of Water Resources and Electric Power in Beijing, 1989). The water requirements for the industrial and urban sectors were generated in both sets of projections using data from *Water Resources Utilization in China*.

When the total water requirements from the agronomic model for a region exceed the combined total of sustainable water available from both surface water and groundwater, a deficit results. These results indicate that the Haihe region (Figure E-3) is in a serious and ongoing deficit situation. The Huanghe region shows some surplus in the first half of the study period; after the year 2000, however, the total water requirements continuously exceed the combined total of sustainable water available from surface water and groundwater (see Figure E-5). Deficits also appear in the Liaohe and Huaihe regions late in the study period (Figures E-2 and E-4). At the other extreme, the Chang Jiang drainage region will have a substantial surplus of water through 2025 (see Figure E-6). The other five drainage regions (Figures E-1, E-7, E-8, E-9, and E-10) generally fall between these extremes.

Figures E-15 through E-24 present the results of single runs of the China water model through the year 2025 for each of the 10 drainage regions. The figures show the water use by sector and the indicated water deficit. As shown in Figure E-17, the urban and industrial water requirements for the Haihe drainage region are met through the year 2025. A large deficit occurs in the agricultural sector, however, that steadily worsens throughout the study period. The overall increase in available water after 2010 is due to additional interbasin transfers that are planned to come on line in that year. Although the transfers help the situation, the deficit is not eliminated. Figure E-19 shows that the urban water requirements are met in the Huanghe region through the year 2025. A deficit appears in the industrial sector, however, at 2010. Water deficits in the agricultural sector in that region appear throughout the study period, although they become more severe in the second half of the period. Water requirements in the urban and industrial sectors are also met in the Liaohe and Huaihe regions through 2025, as shown in Figures E-16 and E-18, but water deficits begin to appear in the agricultural sector late in the study period. Finally, as shown in Figures E-15, E-16, E-20, E-21, E-22, E-23, and E-24, the water requirements are met for all three sectors in the remaining regions through the year 2025.

Figures E-25 through E-34 present the predicted water deficits or surpluses for the 10 Chinese drainage regions through the year 2025 estimated by generating 100 replications of the simulation model and computing the mean and standard deviation of the water deficit for each year through 2025. Based on the assumptions used in the simulation, there is a probability of 0.68 that the actual water deficit for each drainage region will lie between the upper and lower curves in each figure.

Figure E-35 presents the aggregated all-China differences between the total water requirements generated using agricultural water requirements computed by the China agronomic model and total water requirements that were generated using the Ministry of Water Resources data for 1980 water use and for expected water use in the year 2000. This curve, which represents the sum of the differences for all of the regions over the study period, shows that this difference ranges from 0% in 1980 to less than 4% in 2025.

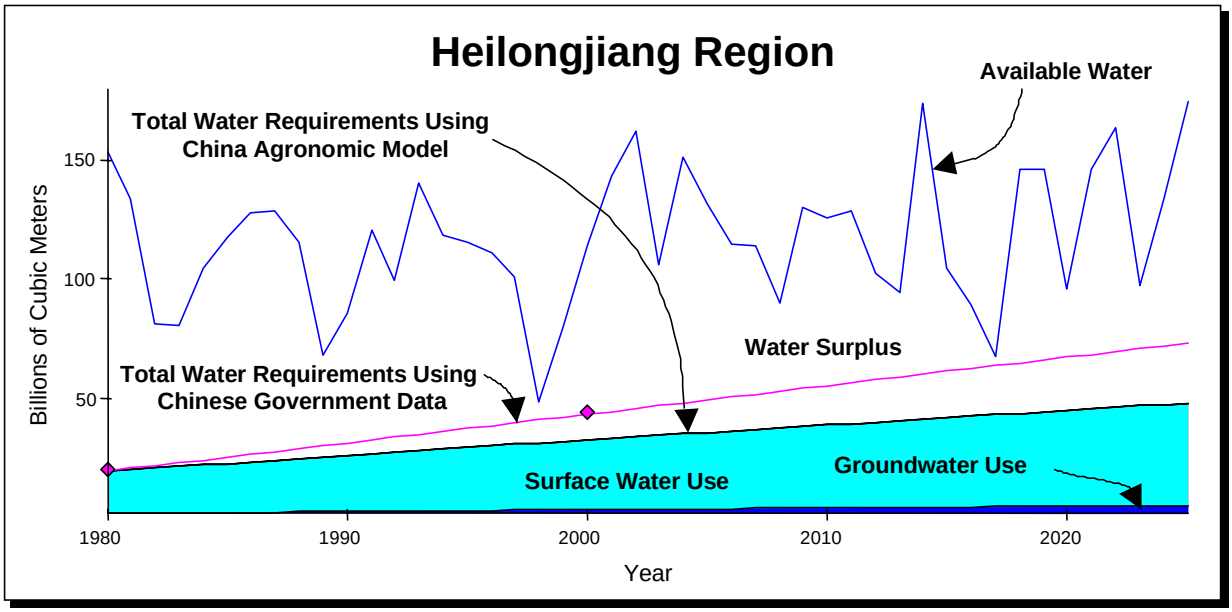

Figure E-1. Comparison of the results of a single run of stochastic modeling of available water with projected total water requirements in the Heilongjiang drainage region. The total water requirements were generated using 1) agricultural water requirements computed by the China agronomic model and 2) a linear projection of agricultural water requirements based on data from the China Ministry of Water Resources.

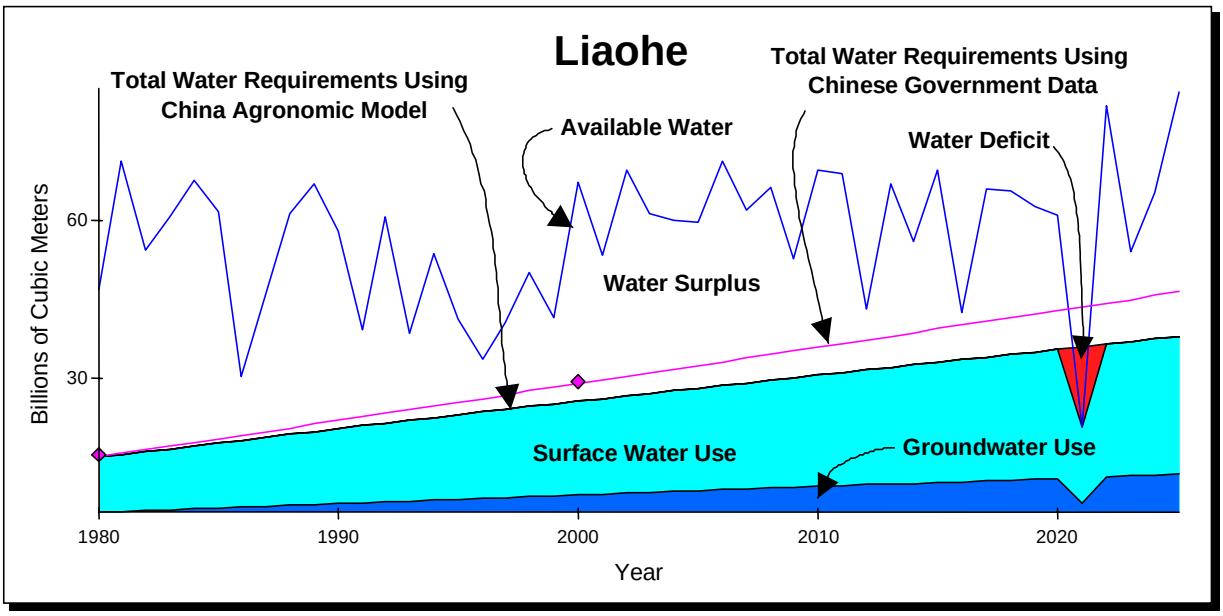

Figure E-2. Comparison of the results of a single run of stochastic modeling of available water with projected total water requirements in the Liaohe drainage region. The total water requirements were generated using 1) agricultural water requirements computed by the China agronomic model and 2) a linear projection of agricultural water requirements based on data from the China Ministry of Water Resources.

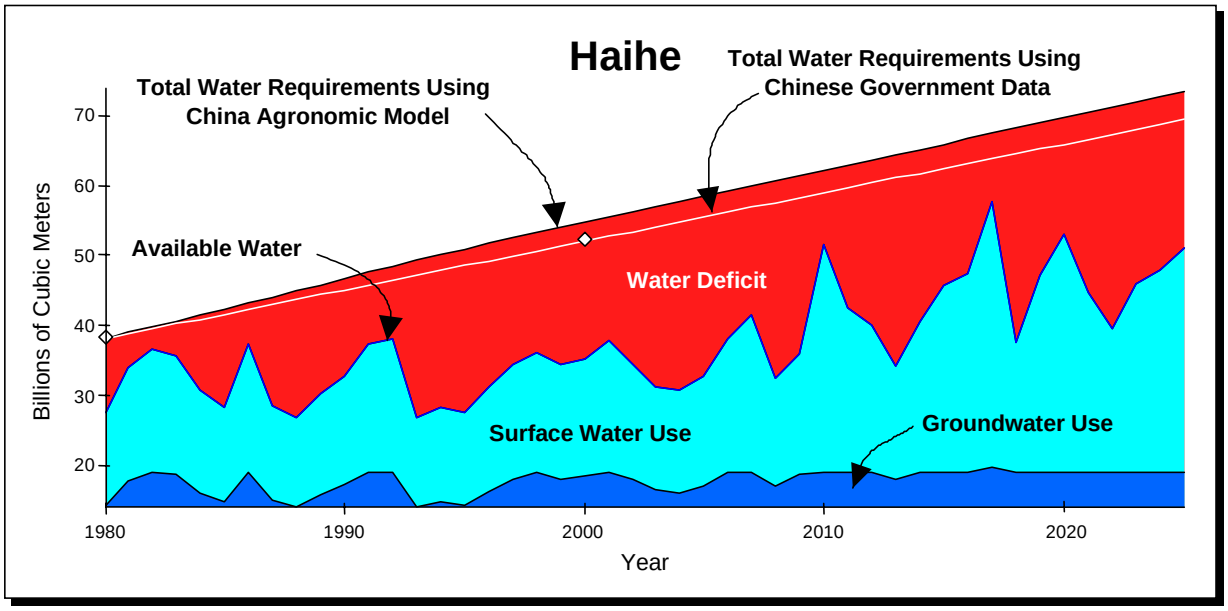

Figure E-3. Comparison of the results of a single run of stochastic modeling of available water with projected total water requirements in the Haihe drainage region generated using 1) agricultural water requirements computed by the China agronomic model and 2) a linear projection of agricultural water requirements based on data from the China Ministry of Water Resources.

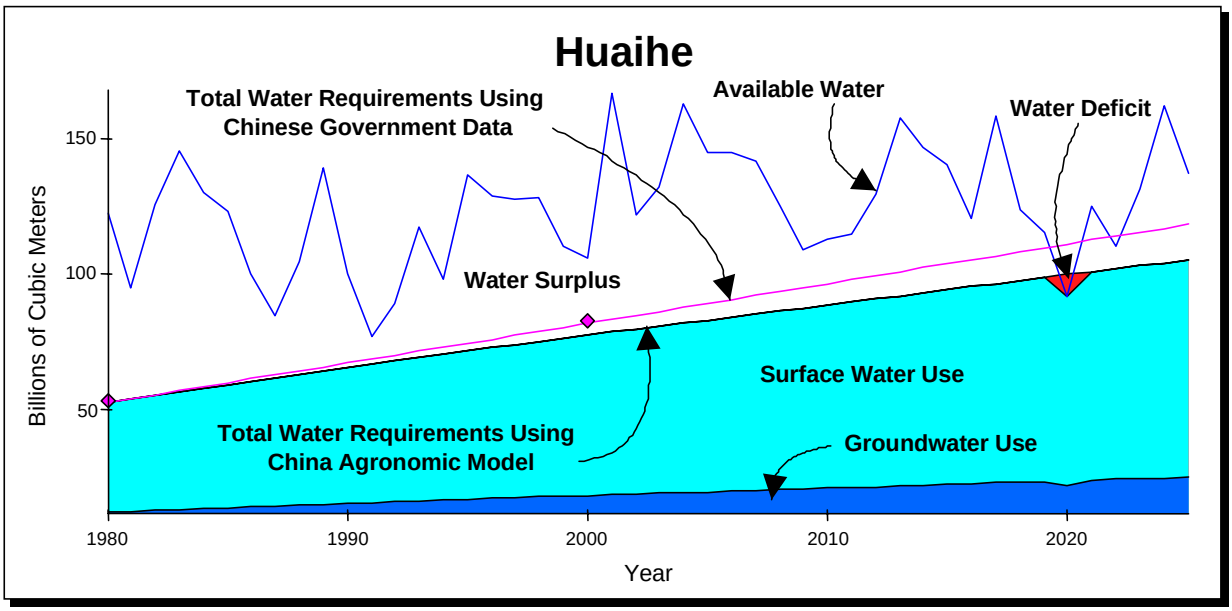

Figure E-4. Comparison of the results of a single run of stochastic modeling of available water with projected total water requirements in the Huaihe drainage region. The total water requirements were generated using 1) agricultural water requirements computed by the China agronomic model and 2) a linear projection of agricultural water requirements based on data from the China Ministry of Water Resources.

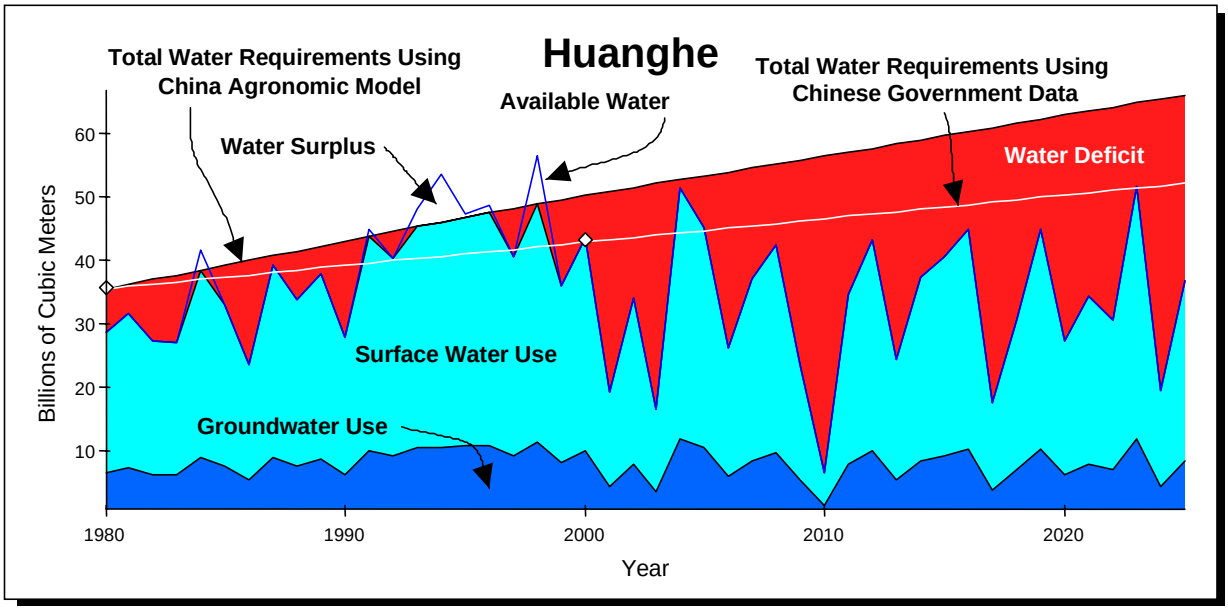

Figure E-5. Comparison of the results of a single run of stochastic modeling of available water with projected total water requirements in the Huanghe drainage region. The total water requirements were generated using 1) agricultural water requirements computed by the China agronomic model and 2) a linear projection of agricultural water requirements based on data from the China Ministry of Water Resources.

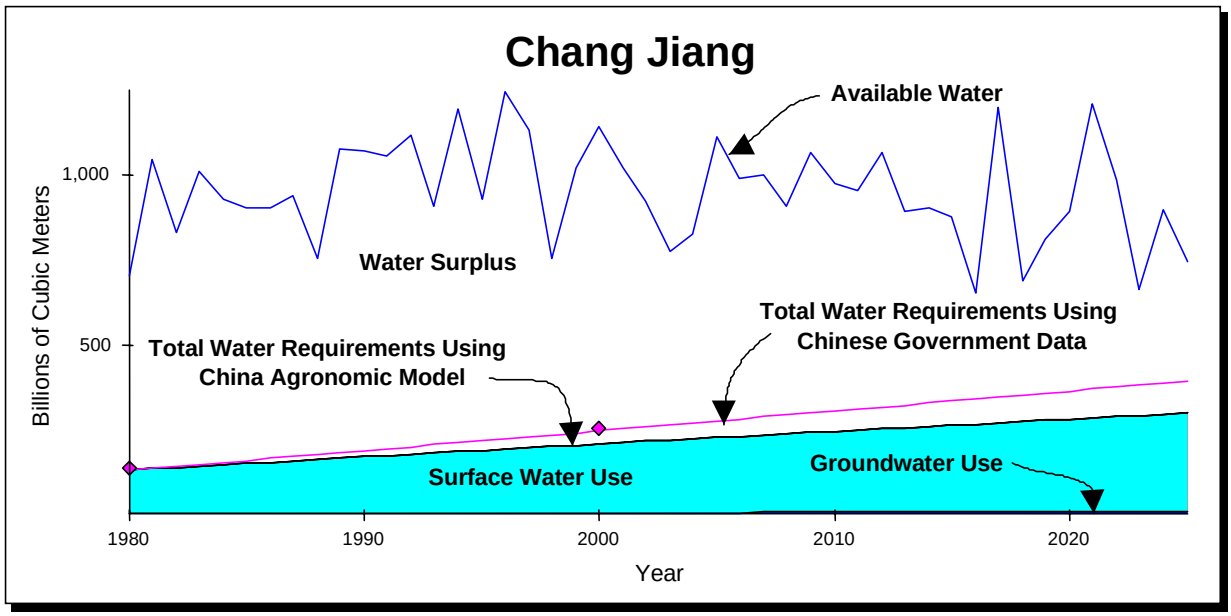

Figure E-6. Comparison of the results of a single run of stochastic modeling of available water with projected total water requirements in the Chang Jiang drainage region. The total water requirements were generated using 1) agricultural water requirements computed by the China agronomic model and 2) a linear projection of agricultural water requirements based on data from the China Ministry of Water Resources.

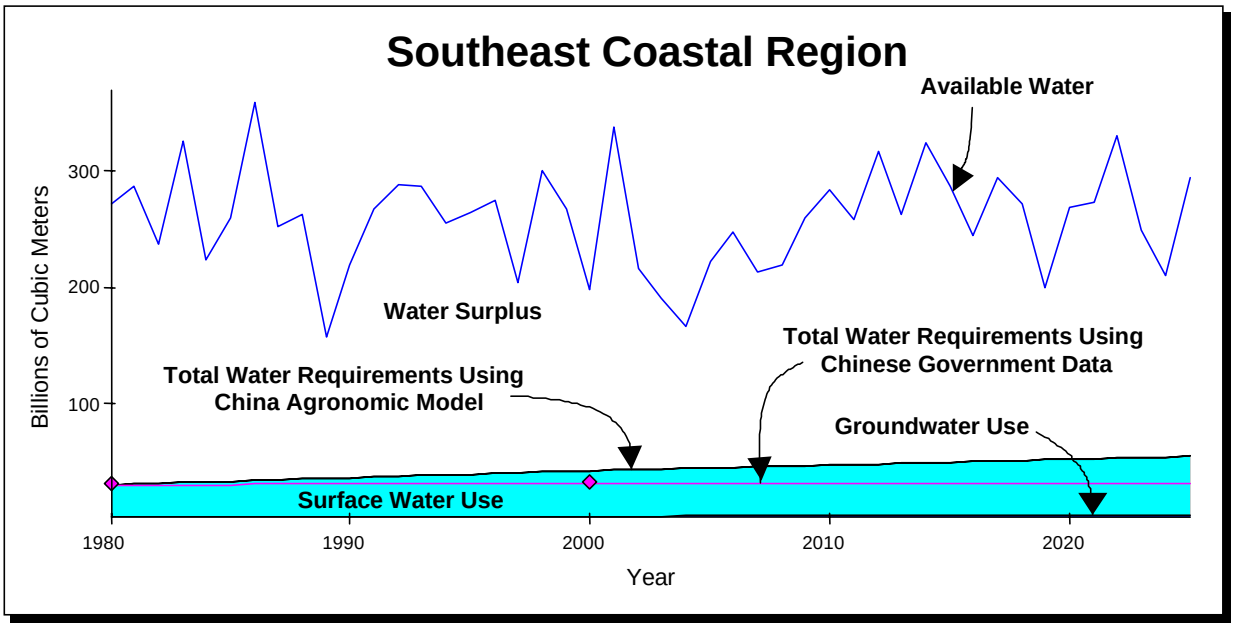

Figure E-7. Comparison of the results of a single run of stochastic modeling of available water with projected total water requirements in the Southeast Coastal drainage region. The total water requirements were generated using 1) agricultural water requirements computed by the China agronomic model and 2) a linear projection of agricultural water requirements based on data from the China Ministry of Water Resources.

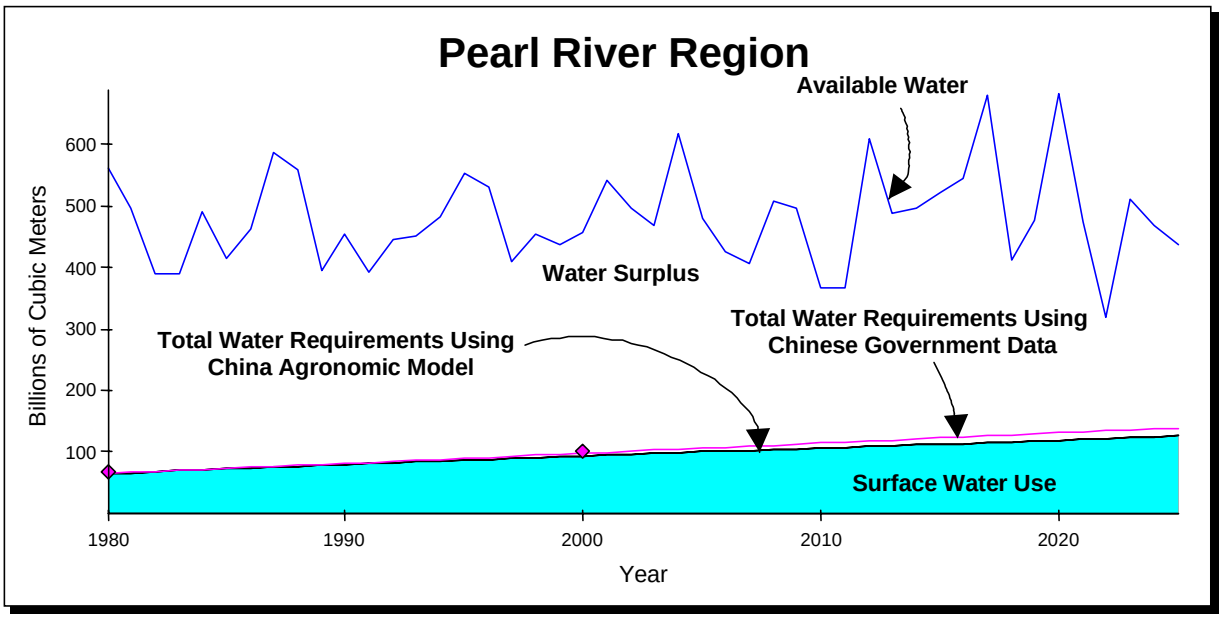

Figure E-8. Comparison of the results of a single run of stochastic modeling of available water with projected total water requirements in the Pearl River drainage region. The total water requirements were generated using 1) agricultural water requirements computed by the China agronomic model and 2) a linear projection of agricultural water requirements based on data from the China Ministry of Water Resources.

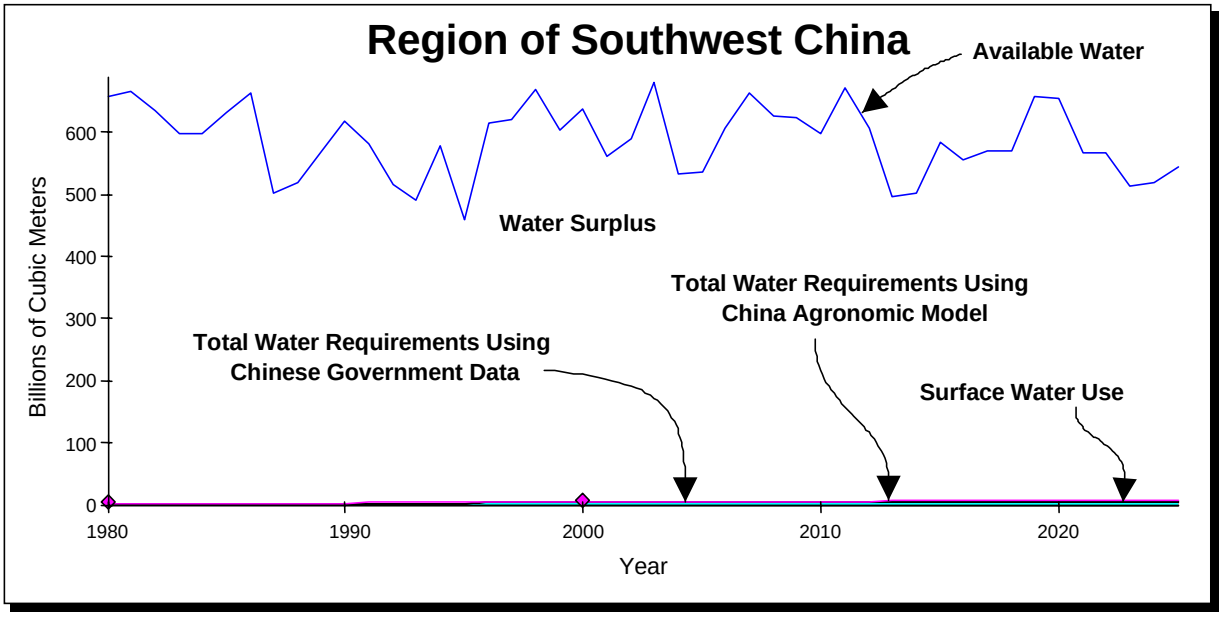

Figure E-9. Comparison of the results of a single run of stochastic modeling of available water with projected total water requirements in the Southwest China drainage region. The total water requirements were generated using 1) agricultural water requirements computed by the China agronomic model and 2) a linear projection of agricultural water requirements based on data from the China Ministry of Water Resources.

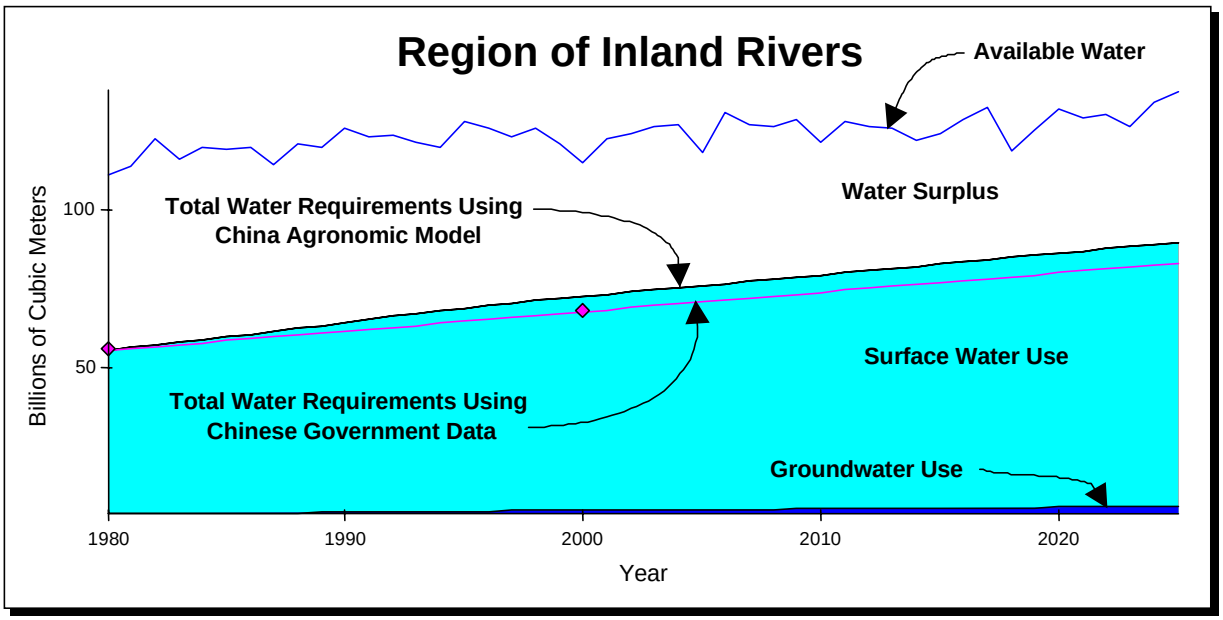

Figure E-10. Comparison of the results of a single run of stochastic modeling of available water with projected total water requirements in the Inland Rivers drainage region. The total water requirements were generated using 1) agricultural water requirements computed by the China agronomic model and 2) a linear projection of agricultural water requirements based on data from the China Ministry of Water Resources.

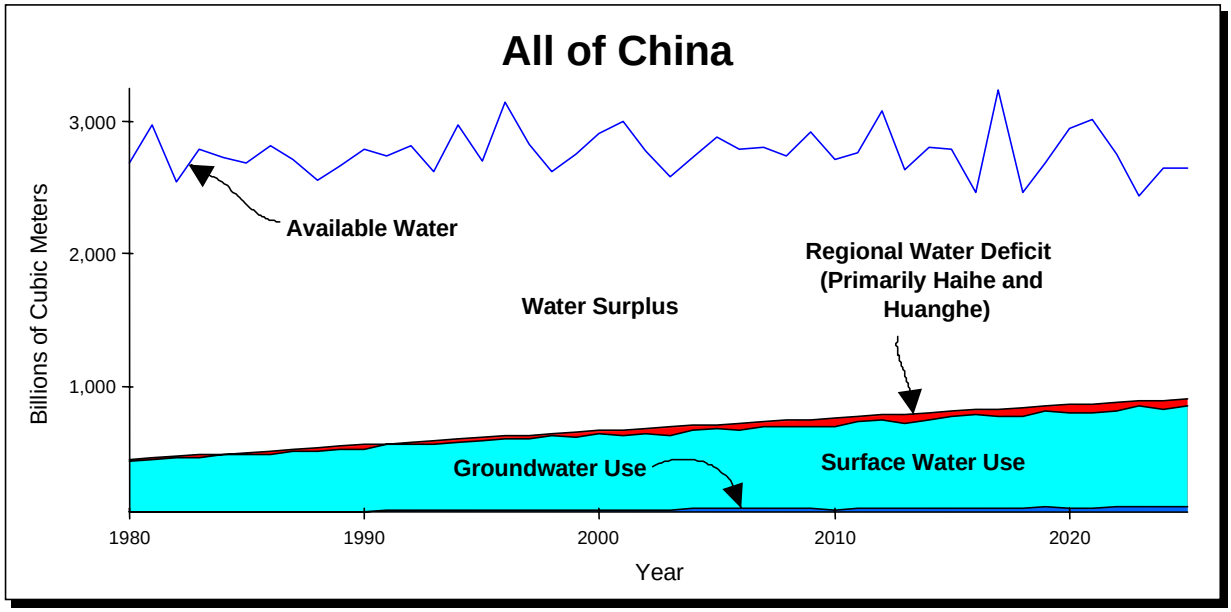

Figure E-11. Comparison of the results of a single run of stochastic modeling of available water with projected total water requirements for all of China based on regional data. The total water requirements were generated using agricultural water requirements computed by the China agronomic model.

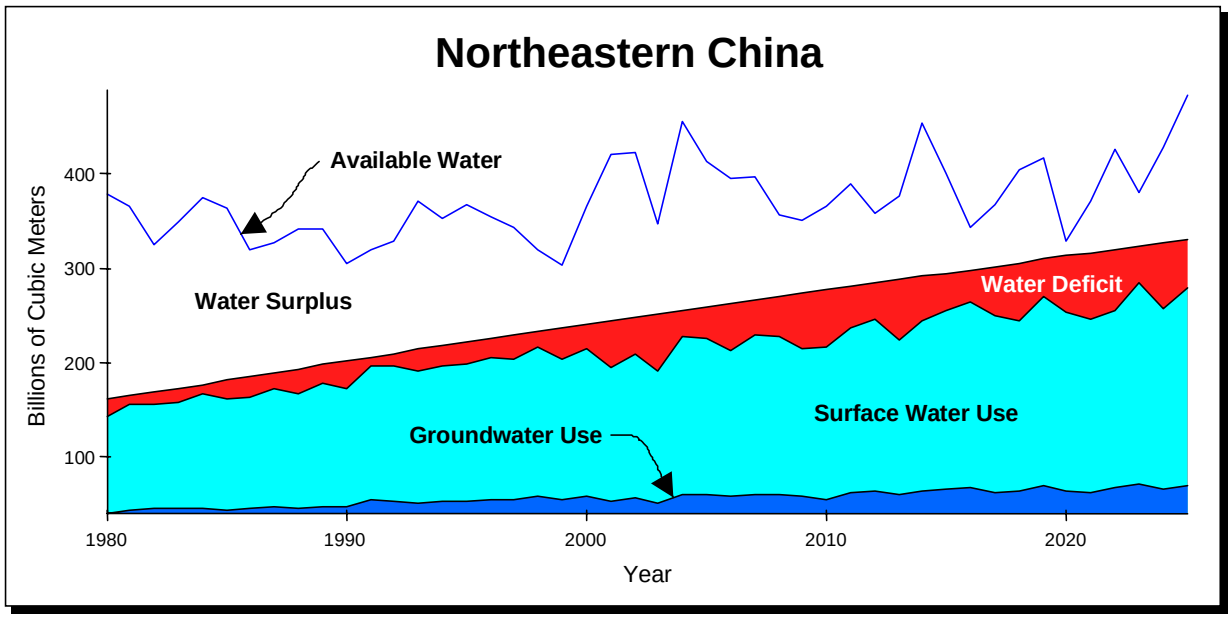

Figure E-12. Comparison of the results of a single run of stochastic modeling of available water with projected total water requirements based on regional data for northeastern China. The total water requirements were generated using agricultural water requirements computed by the China agronomic model.

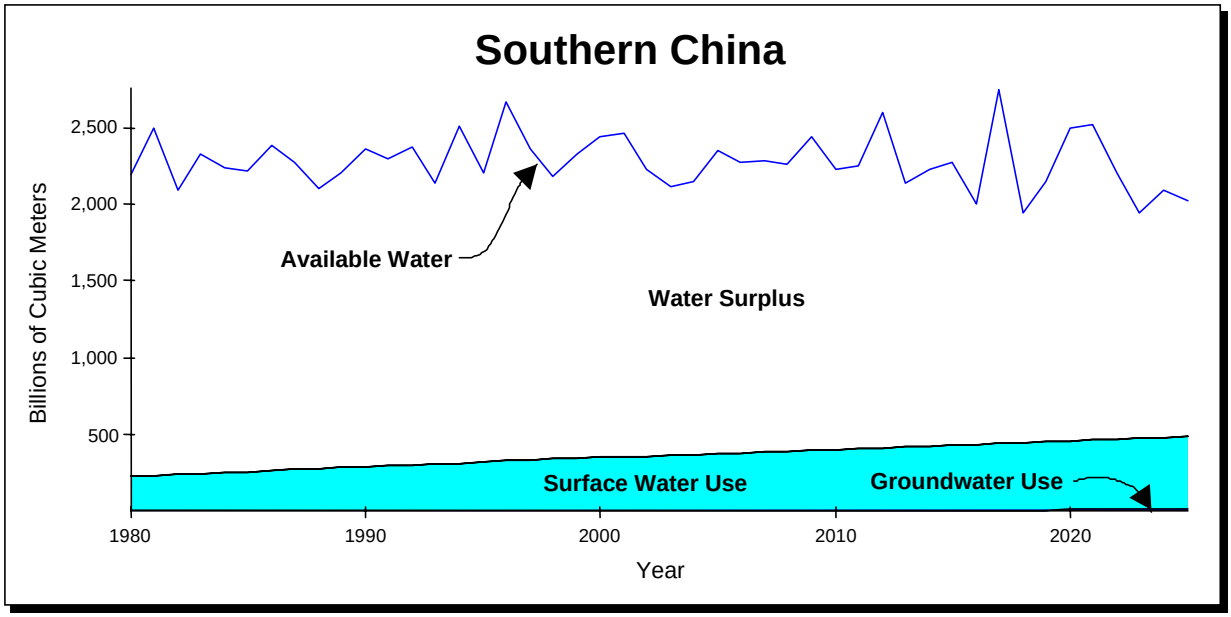

Figure E-13. Comparison of the results of a single run of stochastic modeling of available water with projected total water requirements based on regional data for southern China. The total water requirements were generated using agricultural water requirements computed by the China agronomic model.

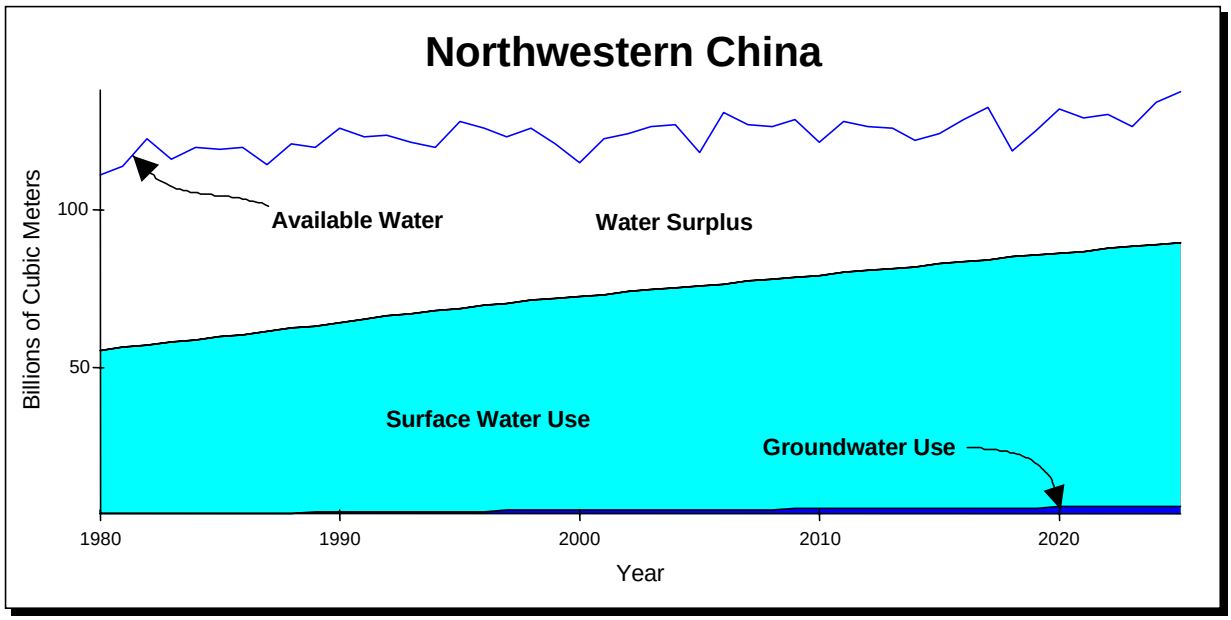

Figure E-14. Comparison of the results of a single run of stochastic modeling of available water with projected total water requirements based on regional data for northwestern China. The total water requirements were generated using agricultural water requirements computed by the China agronomic model.

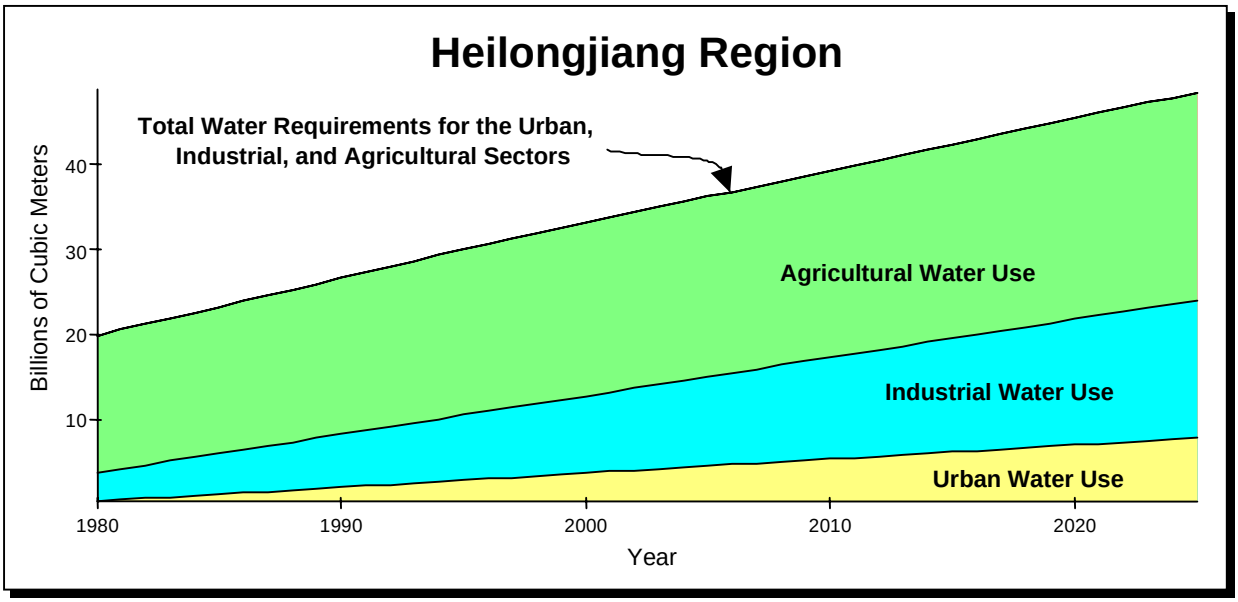

Figure E-15. Comparison of the results of a single run of stochastic modeling of total available water and water use in the urban, industrial, and agricultural sectors with linear projection of total water requirements in the Heilongjiang drainage region.

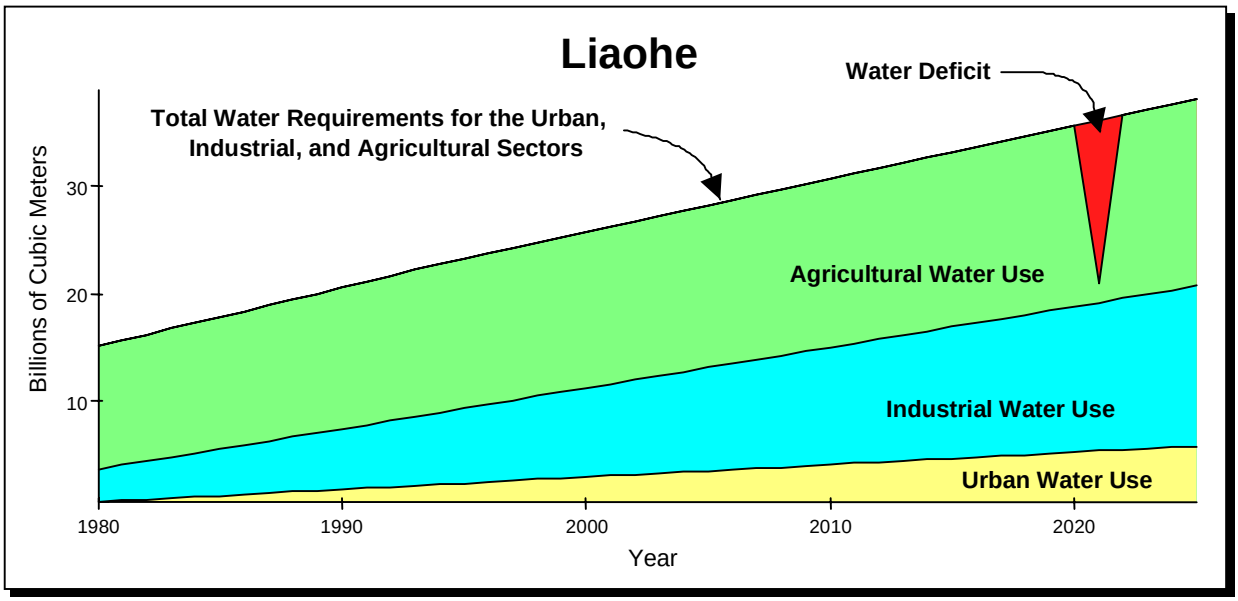

Figure E-16. Comparison of the results of a single run of stochastic modeling of total available water and water use in the urban, industrial, and agricultural sectors with linear projection of total water requirements in the Liaohe drainage region.

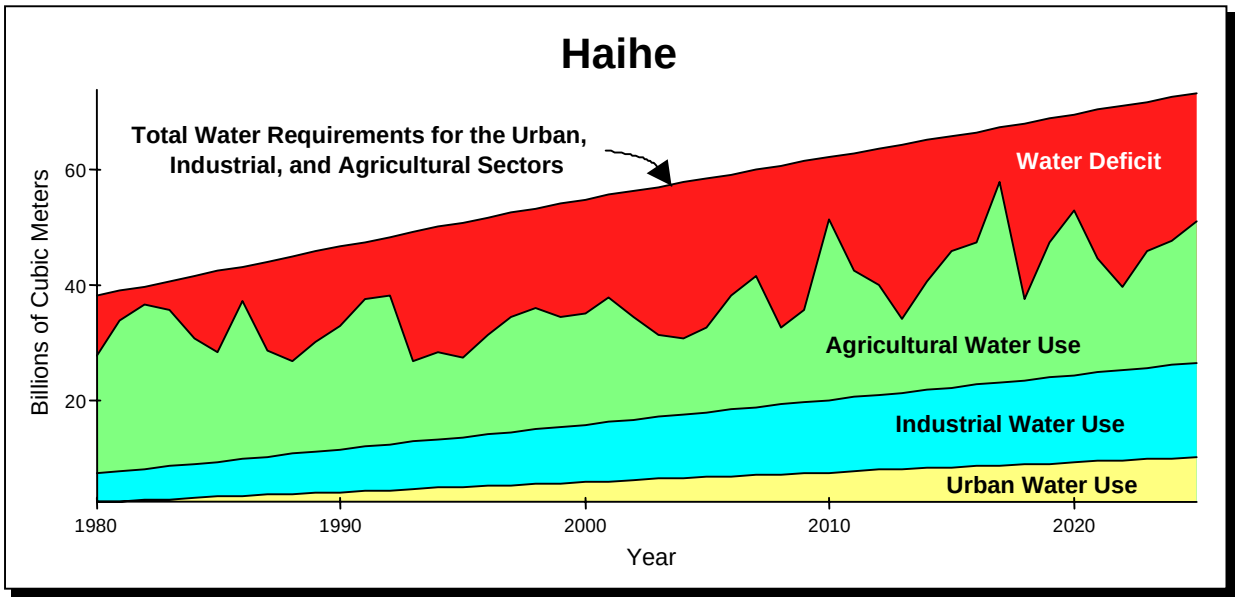

Figure E-17. Comparison of the results of a single run of stochastic modeling of total available water and water use in the urban, industrial, and agricultural sectors with linear projection of total water requirements in the Haihe drainage region.

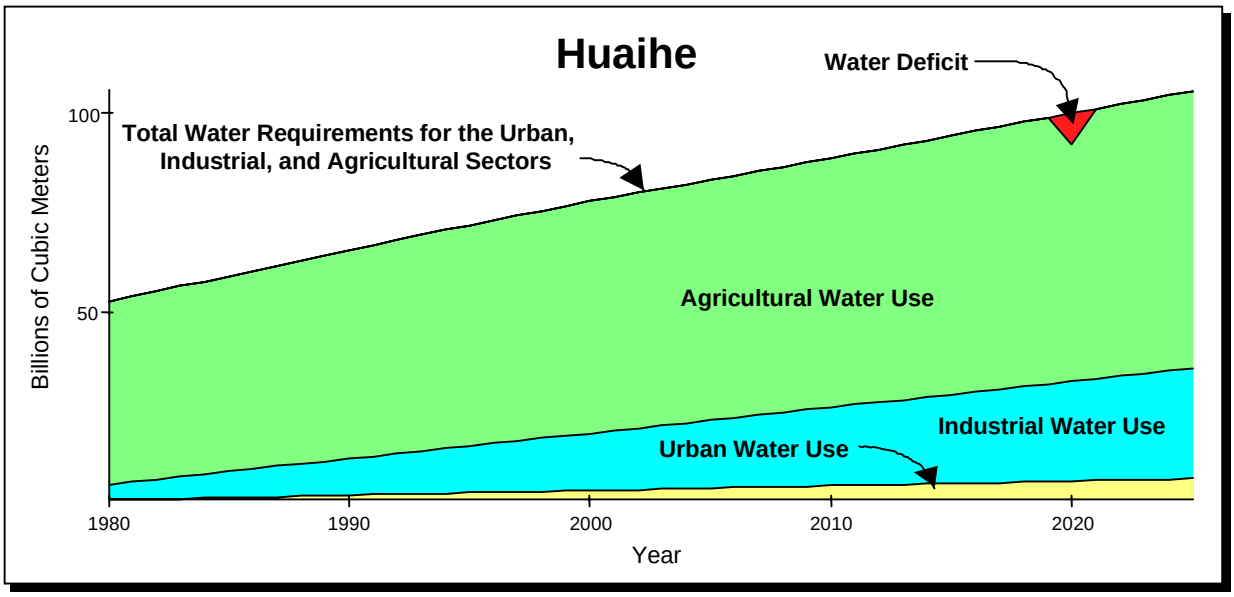

Figure E-18. Comparison of the results of a single run of stochastic modeling of total available water and water use in the urban, industrial, and agricultural sectors with linear projection of total water requirements in the Huaihe drainage region.

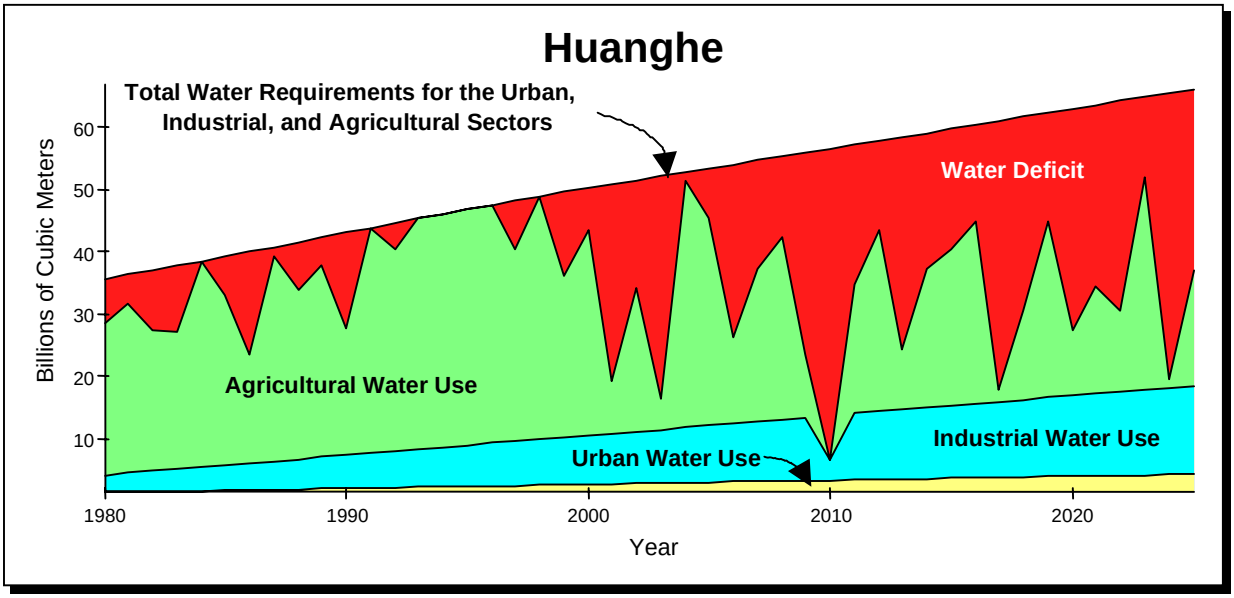

Figure E-19. Comparison of the results of a single run of stochastic modeling of total available water and water use in the urban, industrial, and agricultural sectors with linear projection of total water requirements in the Huanghe drainage region.

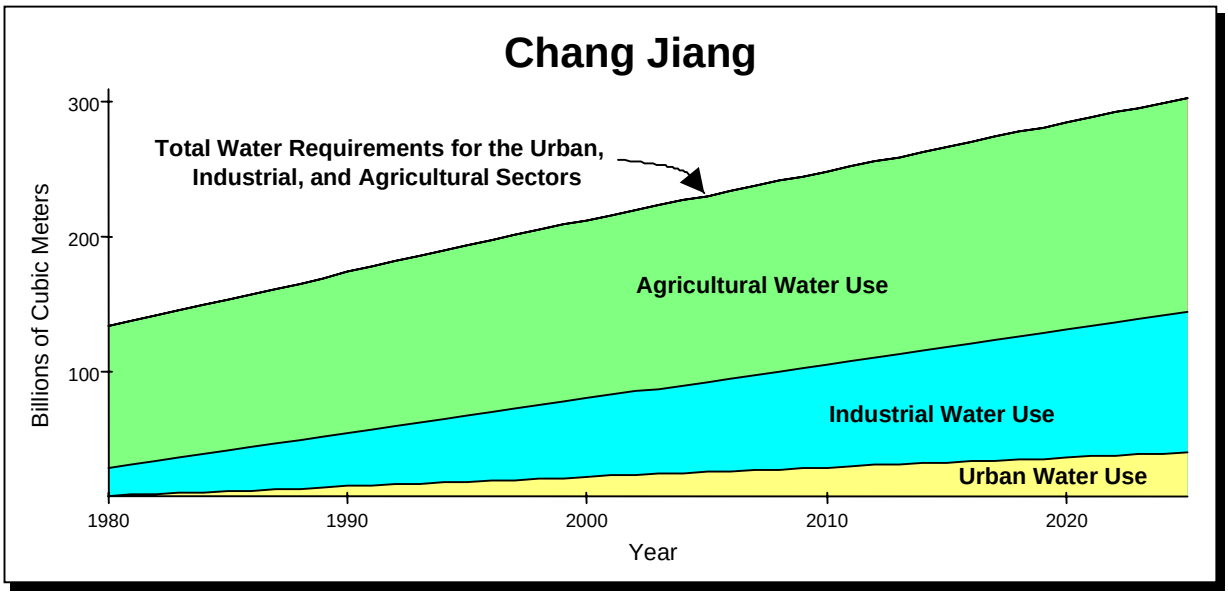

Figure E-20. Comparison of the results of a single run of stochastic modeling of total available water and water use in the urban, industrial, and agricultural sectors with linear projection of total water requirements in the Chang Jiang drainage region.

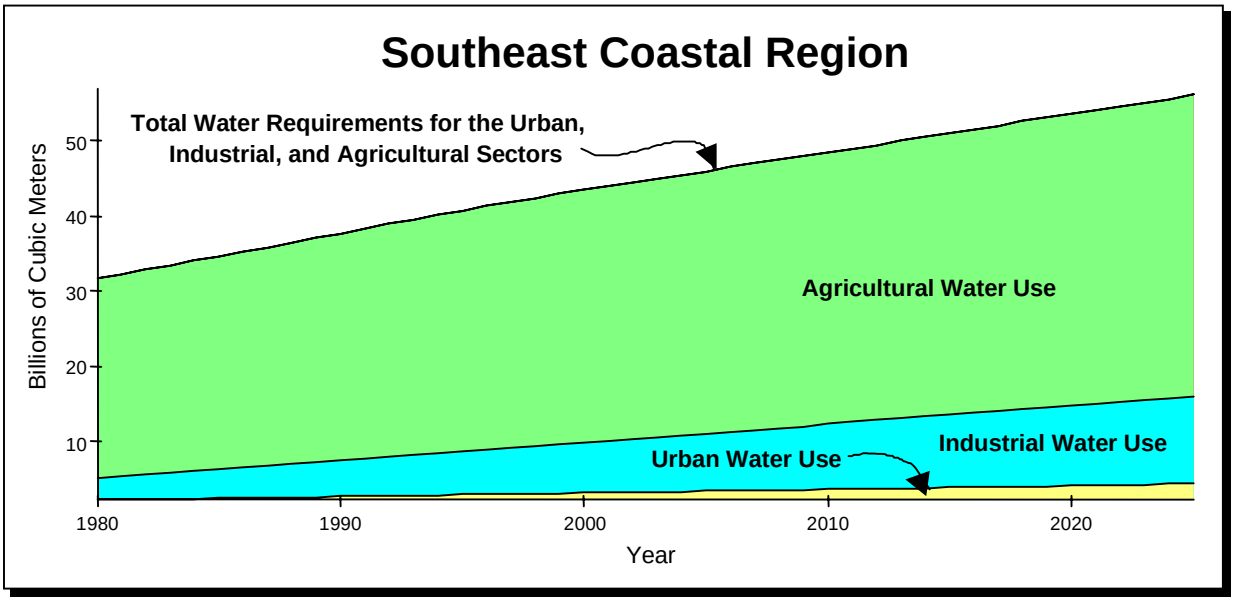

Figure E-21. Comparison of the results of a single run of stochastic modeling of total available water and water use in the urban, industrial, and agricultural sectors with linear projection of total water requirements in the Southeast Coastal drainage region.

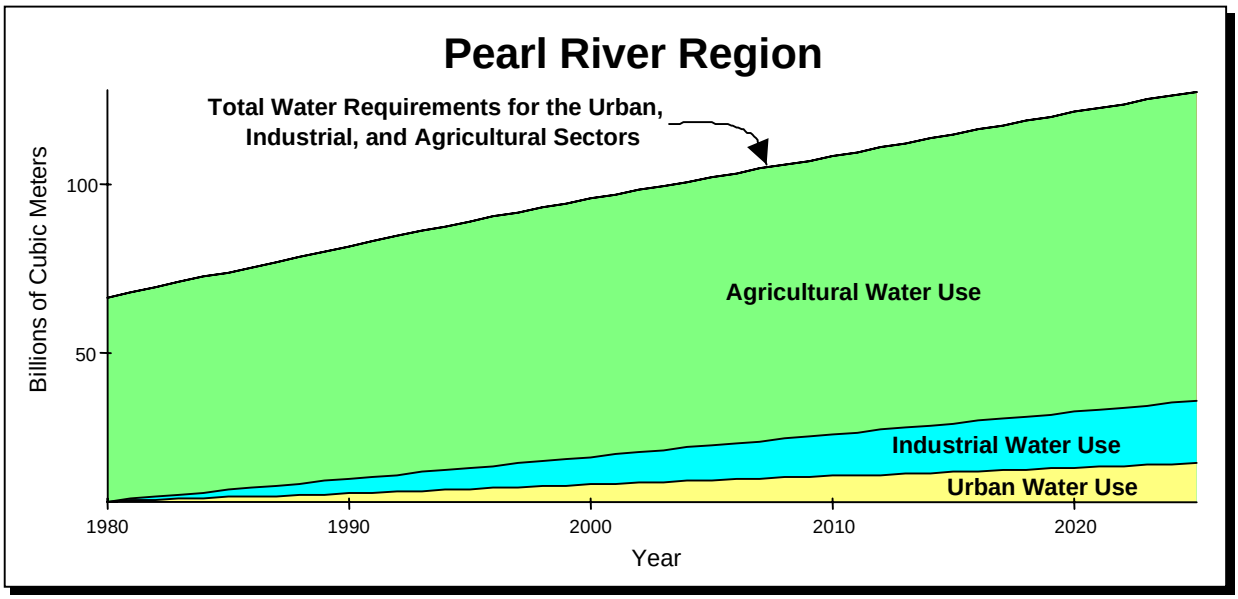

Figure E-22. Comparison of the results of a single run of stochastic modeling of total available water and water use in the urban, industrial, and agricultural sectors with linear projection of total water requirements in the Pearl River drainage region.

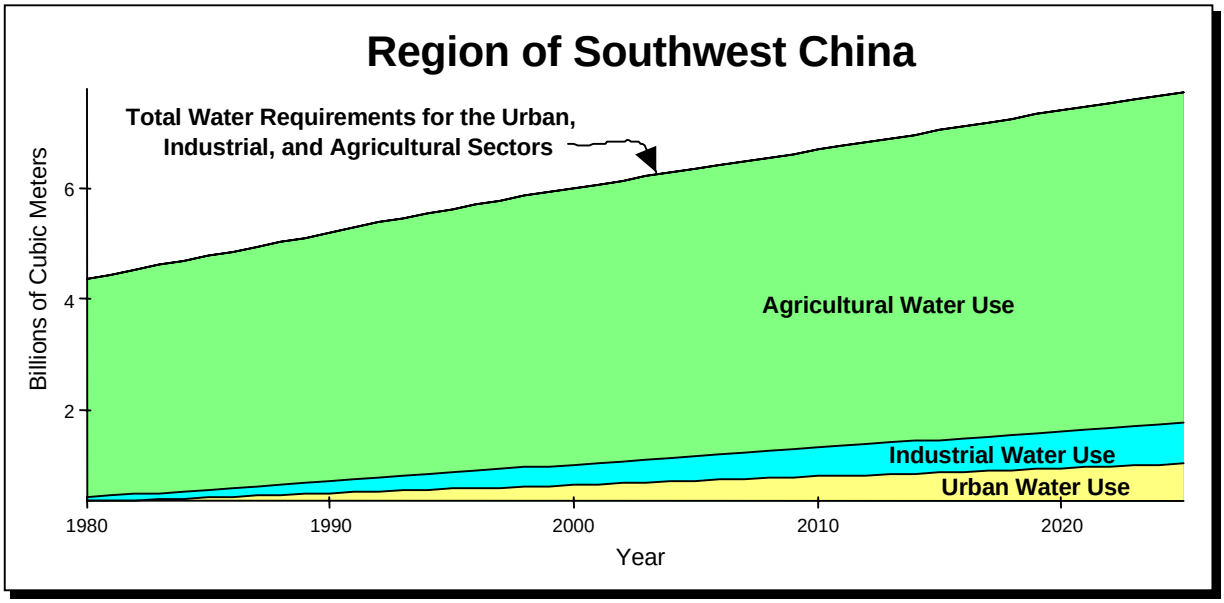

Figure E-23. Comparison of the results of a single run of stochastic modeling of total available water and water use in the urban, industrial, and agricultural sectors with linear projection of total water requirements in the Southwest China drainage region.

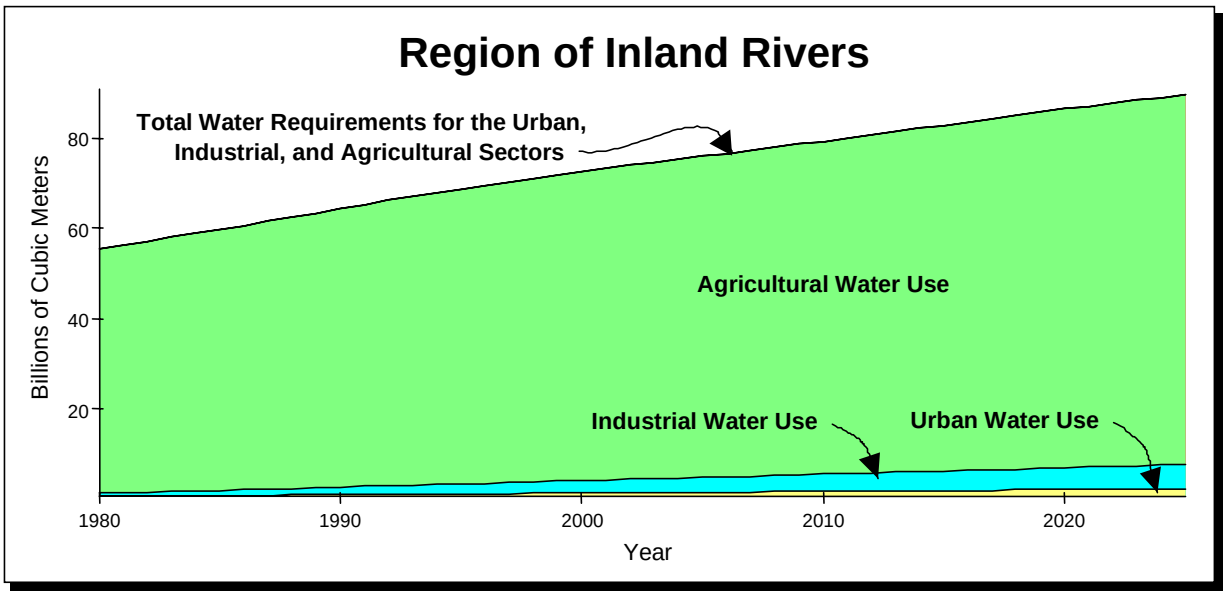

Figure E-24. Comparison of the results of a single run of stochastic modeling of total available water and water use in the urban, industrial, and agricultural sectors with linear projection of total water requirements in the Inland Rivers drainage region.

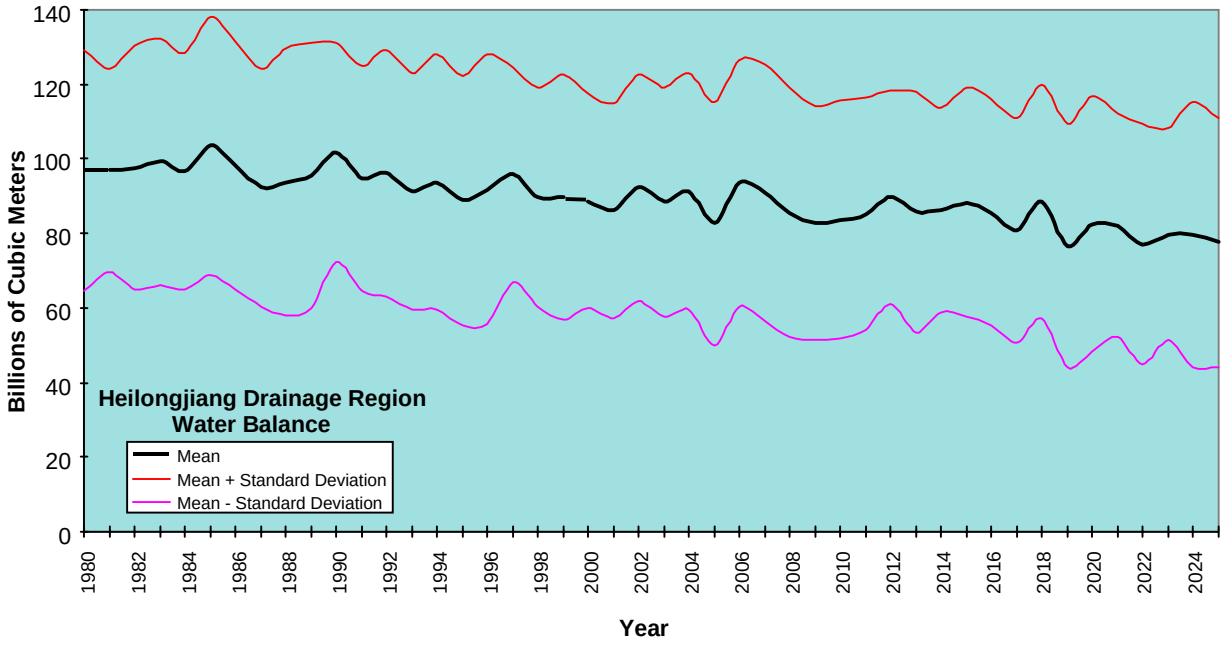

Figure E-25. Predicted water surplus for the Heilongjiang drainage region through the year 2025 generated in 100 replications of the simulation model.

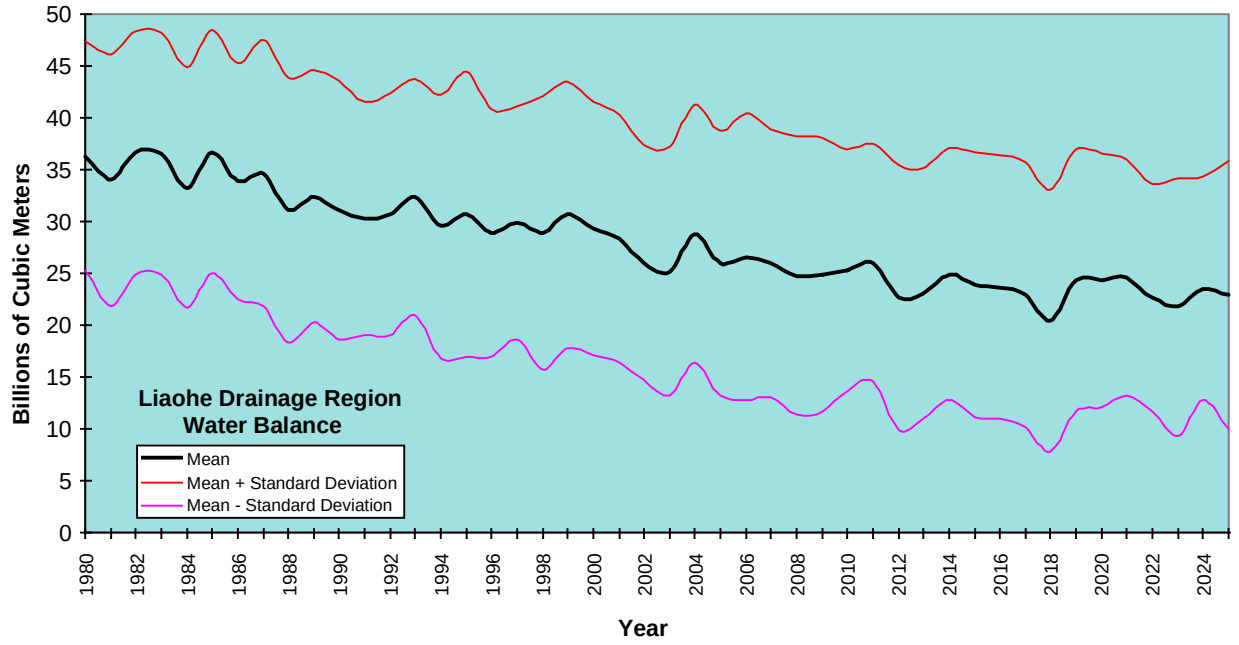

Figure E-26. Predicted water surplus for the Liaohe drainage region through the year 2025 generated in 100 replications of the simulation model.

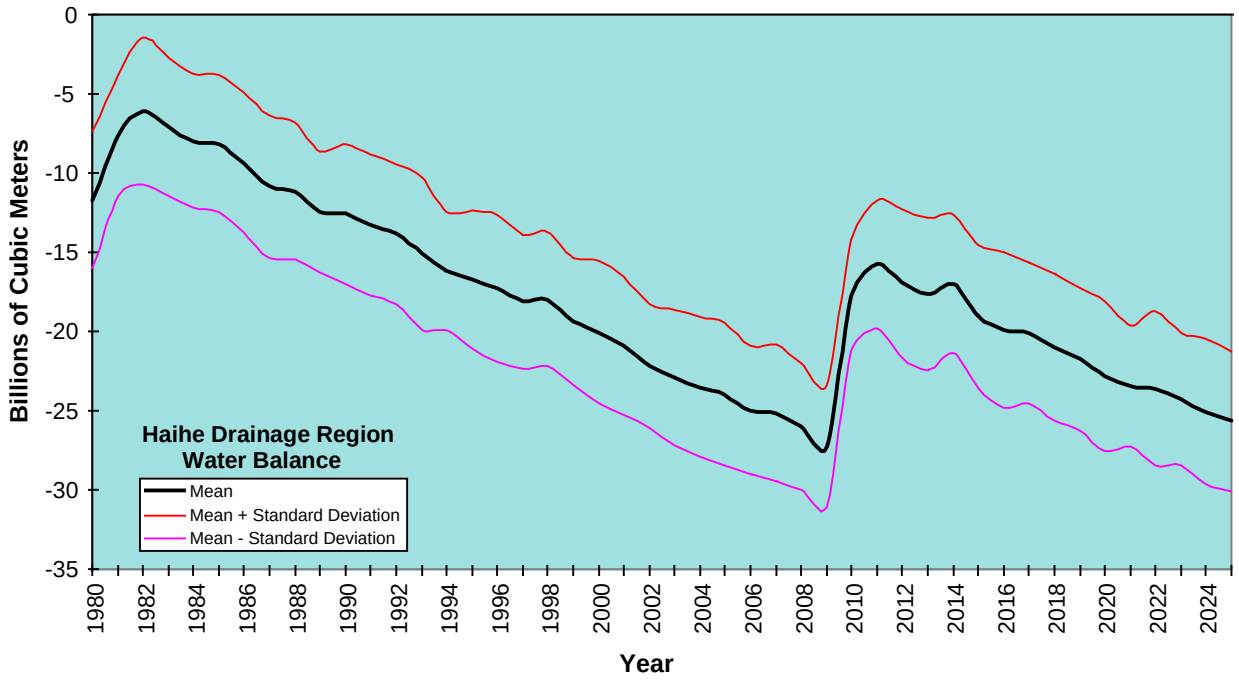

Figure E-27. Predicted water deficit for the Haihe drainage region through the year 2025 generated in 100 replications of the simulation model.

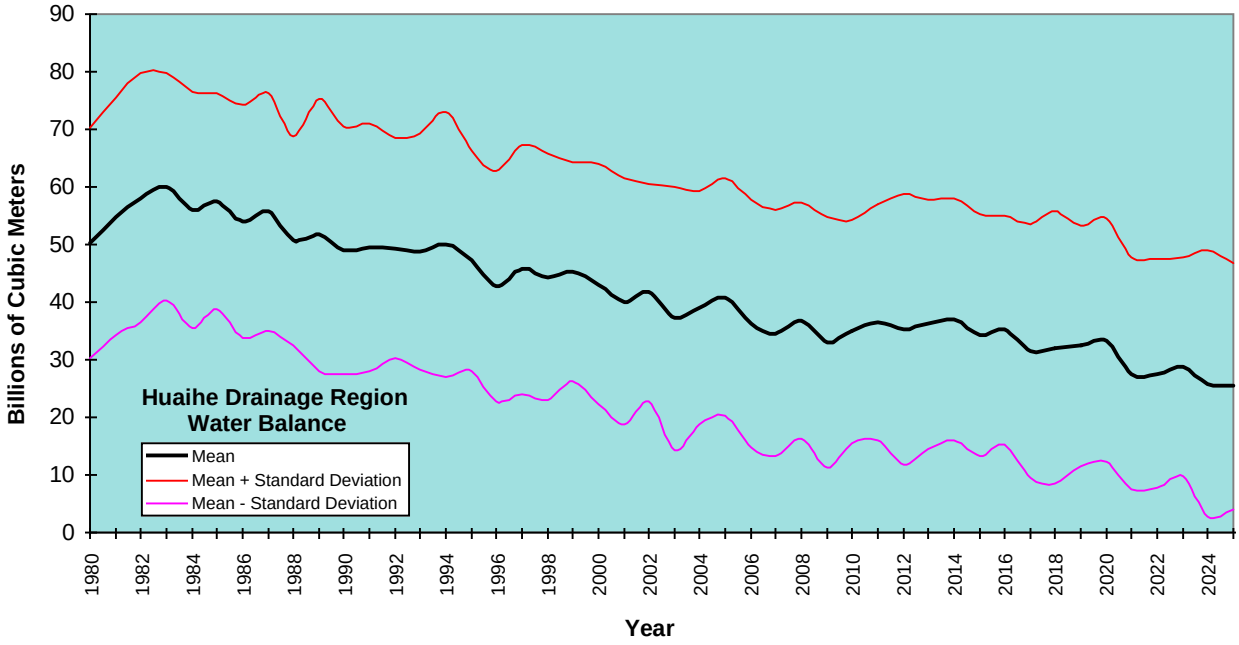

Figure E-28. Predicted water surplus for the Huaihe drainage region through the year 2025 generated in 100 replications of the simulation model.

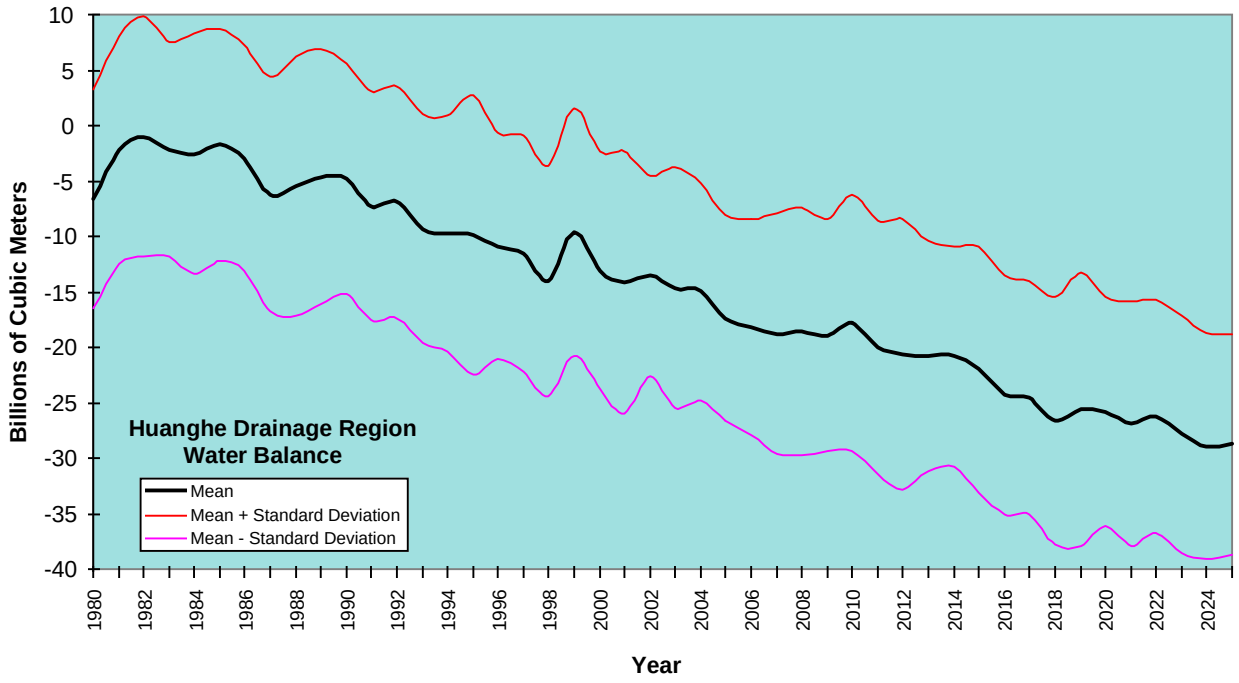

Figure E-29. Predicted water balance for the Huanghe drainage region through the year 2025 generated in 100 replications of the simulation model.

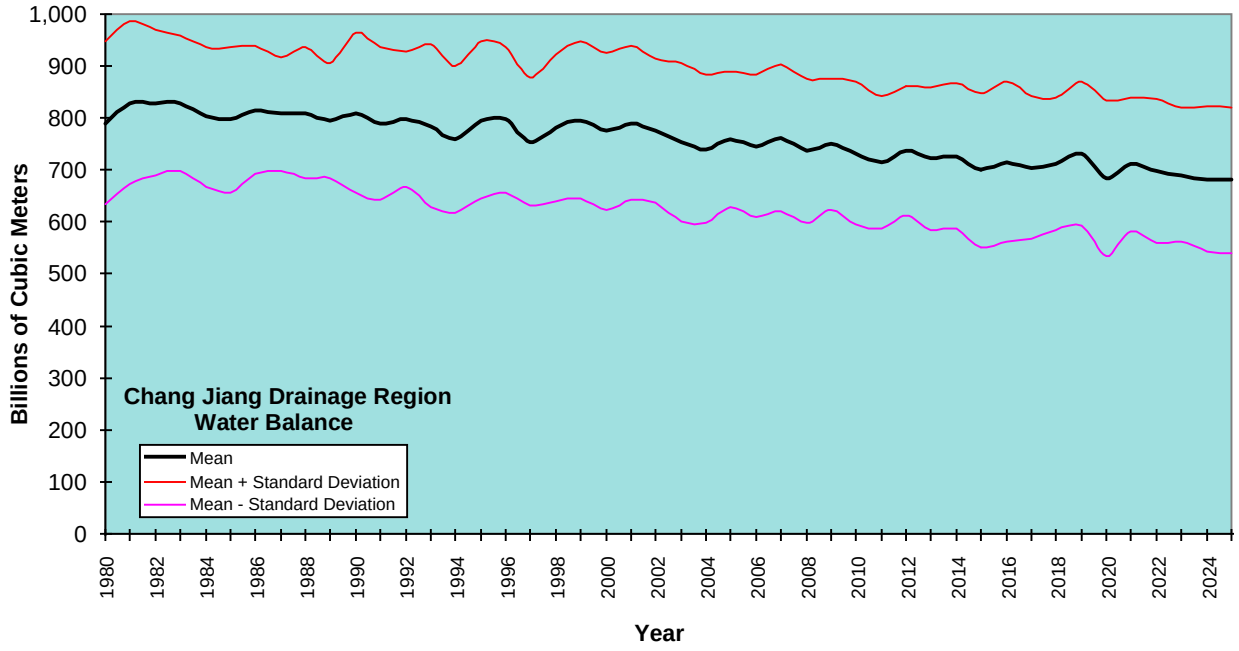

Figure E-30. Predicted water surplus for the Chang Jiang drainage region through the year 2025 generated in 100 replications of the simulation model.

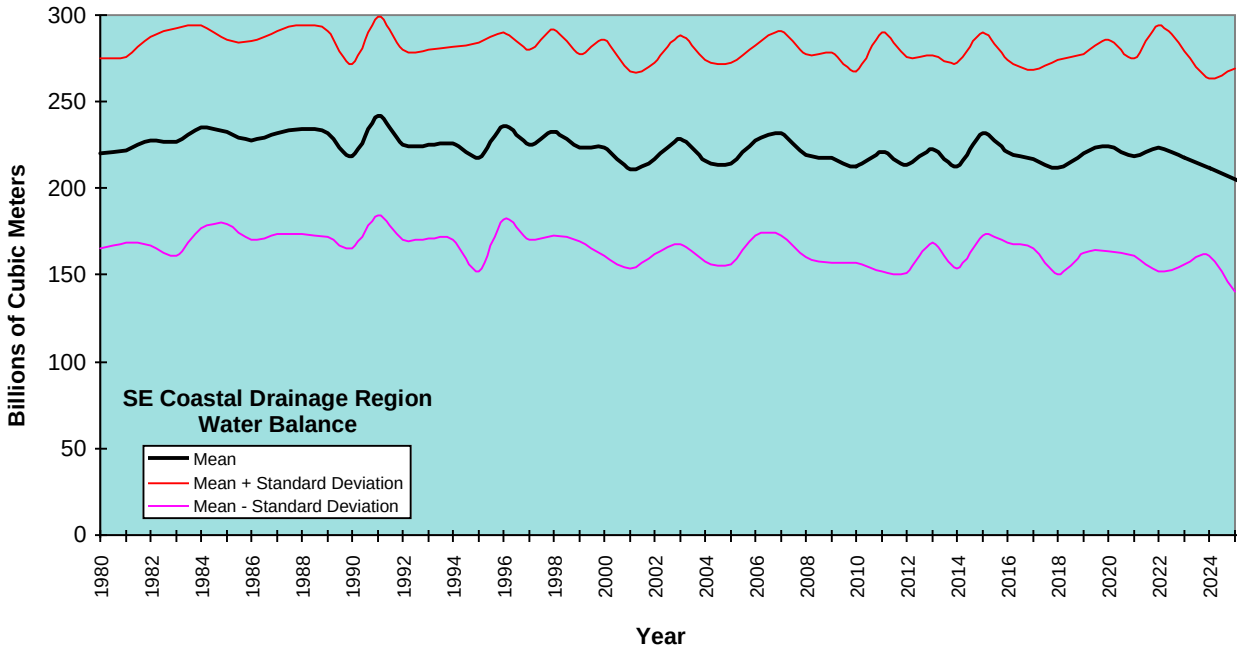

Figure E-31. Predicted water surplus for the Southeast Coastal drainage region through the year 2025 generated in 100 replications of the simulation model.

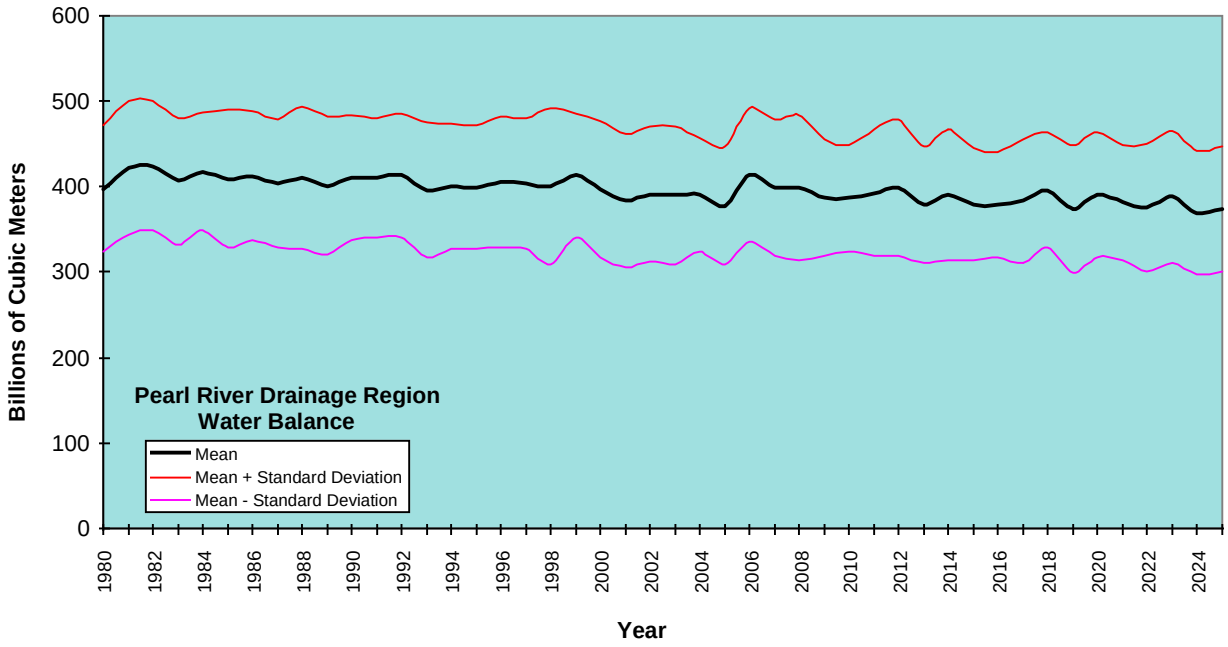

Figure E-32. Predicted water surplus for the Pearl River drainage region through the year 2025 generated in 100 replications of the simulation model.

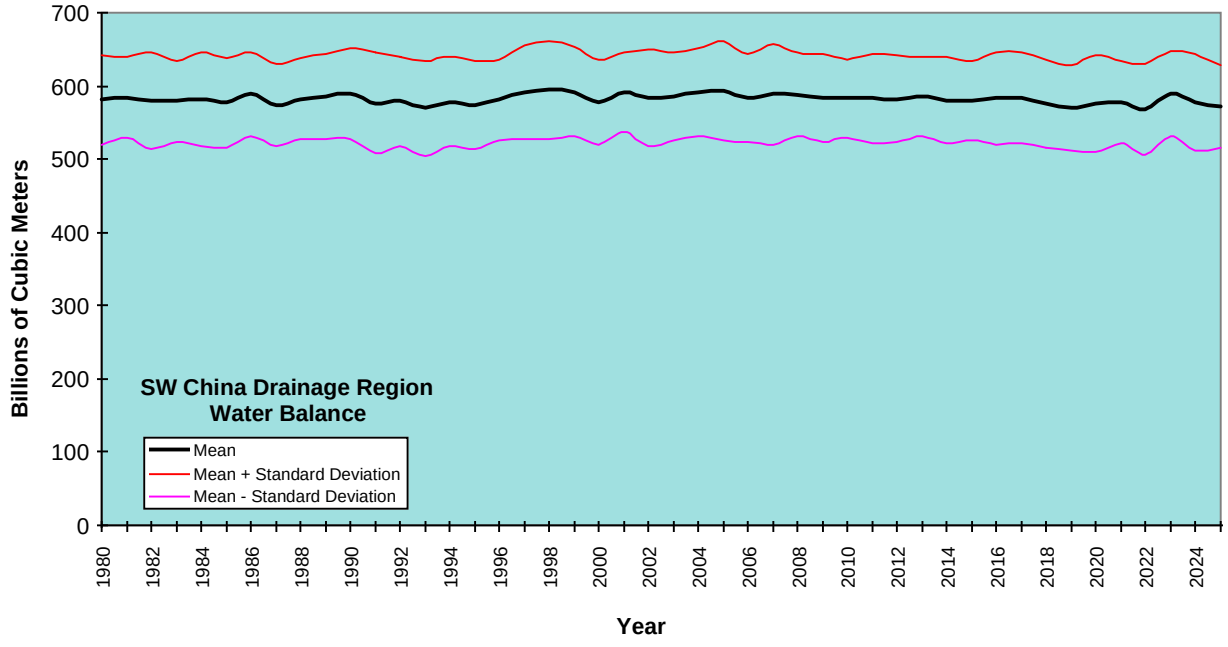

Figure E-33. Predicted water surplus for the Southwest China drainage region through the year 2025 generated in 100 replications of the simulation model.

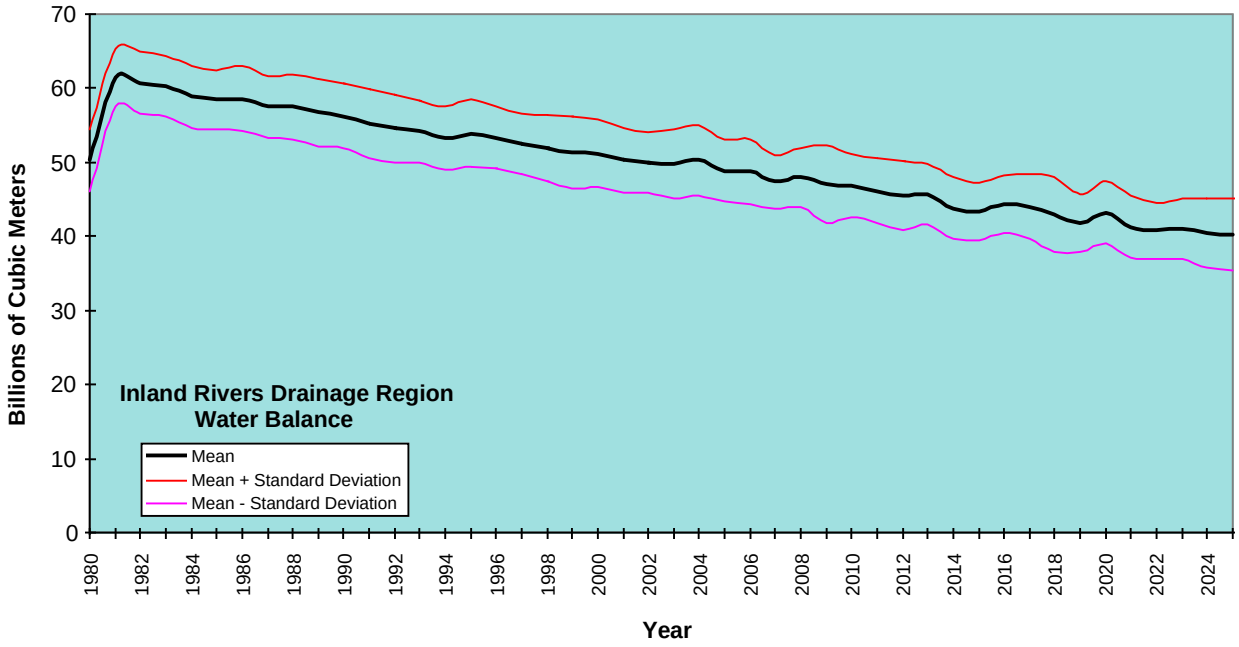

Figure E-34. Predicted water surplus for the Inland Rivers drainage region through the year 2025 generated in 100 replications of the simulation model.

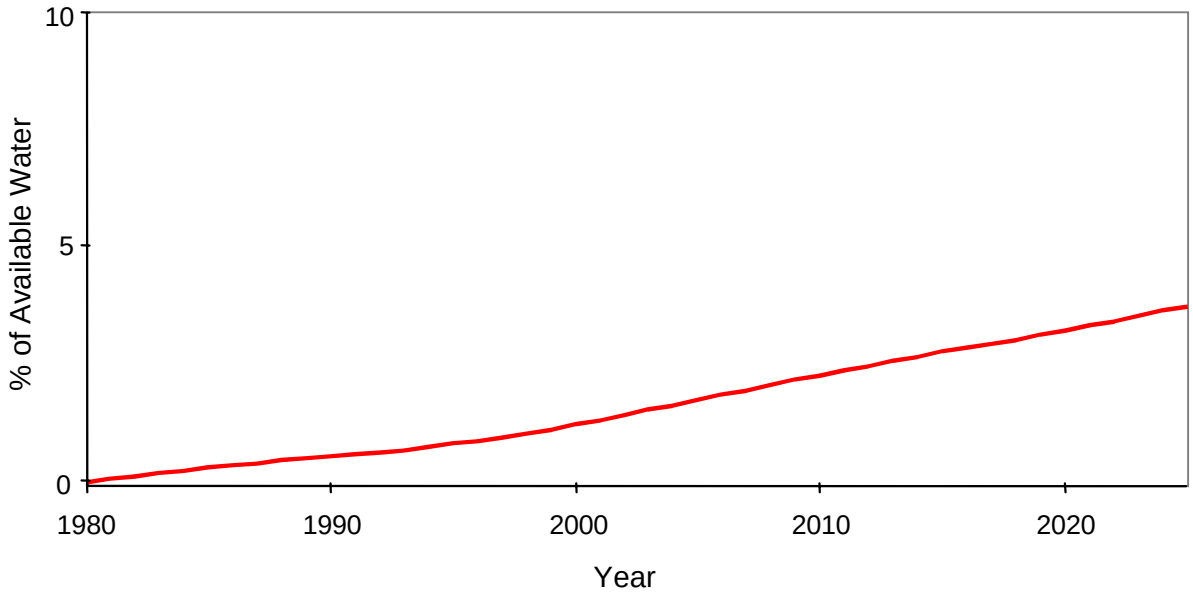

Figure E-35. The sum of the differences between total water requirements generated using agricultural water requirements computed by the agronomic model and total water requirements generated using data from the China Ministry of Water Resources shown for the 10 regions as a percentage of the available water for all of China.

China Agronomic Model – Additional Results

Figures E-36 through E-45 present the results generated in the China agronomic model for the 10 Chinese water drainage regions, the Heilongjiang, the Haihe, the Huaihe, the Huanghe, the Chang Jiang, the Liaohe, the Pearl River, Southeast Coastal, Southwest China, and the Region of Inland Rivers. Each figure presents the grain demand of each region and the land and water needed to produce the grain to meet that demand. For comparison, the figures also present the estimated total arable land and the total water available for agriculture within each region. The land and water requirements were generated using the deterministic option for grain yields and water consumption. The amount of arable land (a constant) was estimated using a geographic information system (GIS) analysis that identified all land with a slope less than 1%. The available water was computed in a single deterministic run of the China water model (average annual precipitation and average annual runoff were used in each time step).

Figures E-46 and E-47 present additional results for the Haihe and Huanghe regions in which the stochastic option for grain yields and water consumption was used to generate land needs and agricultural water requirements.

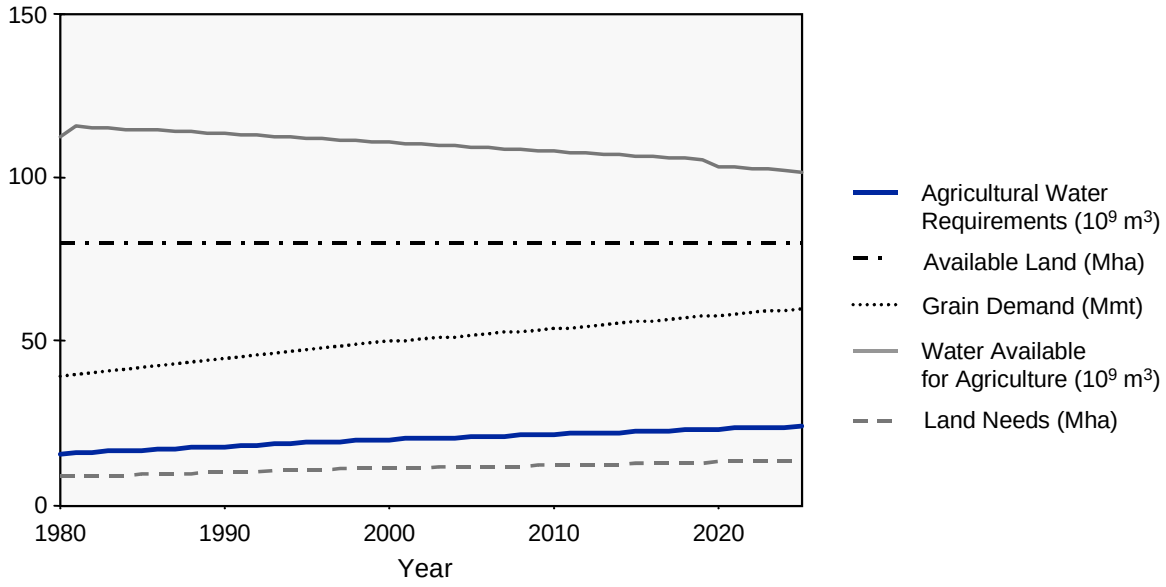

Figure E-36. Grain demand and land and water needs and availability for the Heilongjiang region, 1980–2025.

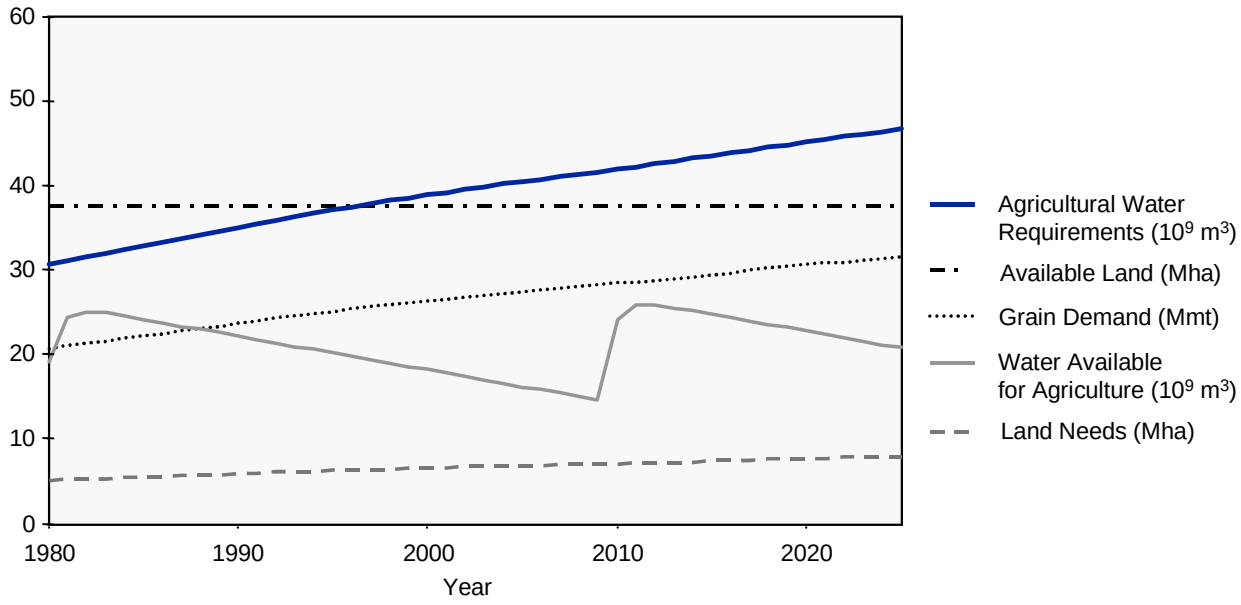

Figure E-37. Grain demand and land and water needs and availability for the Haihe region, 1980–2025.

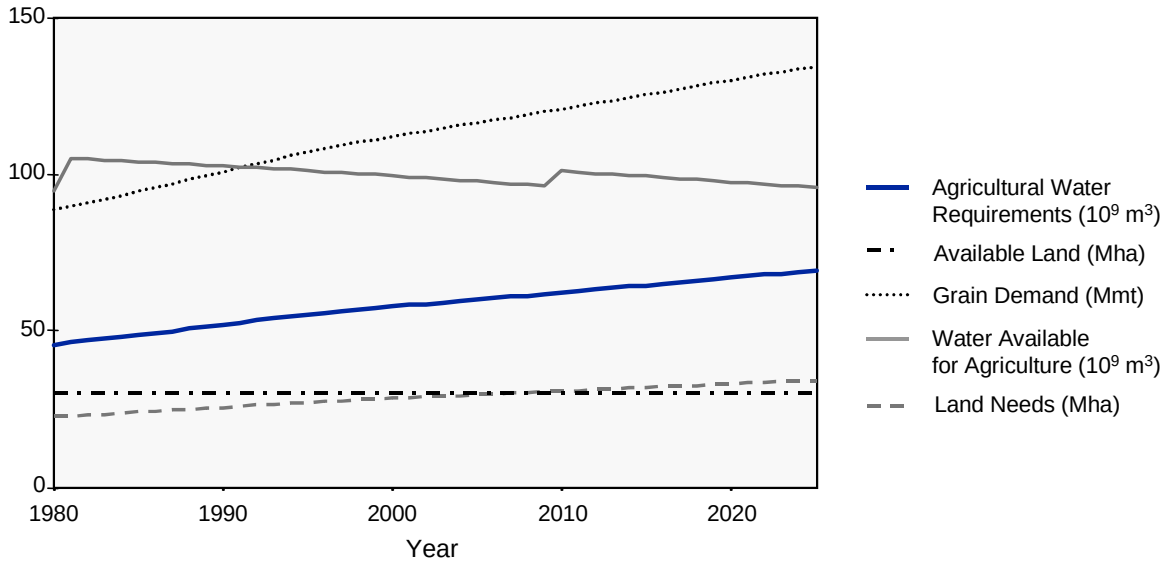

Figure E-38. Grain demand and land and water needs and availability for the Huaihe region, 1980–2025.

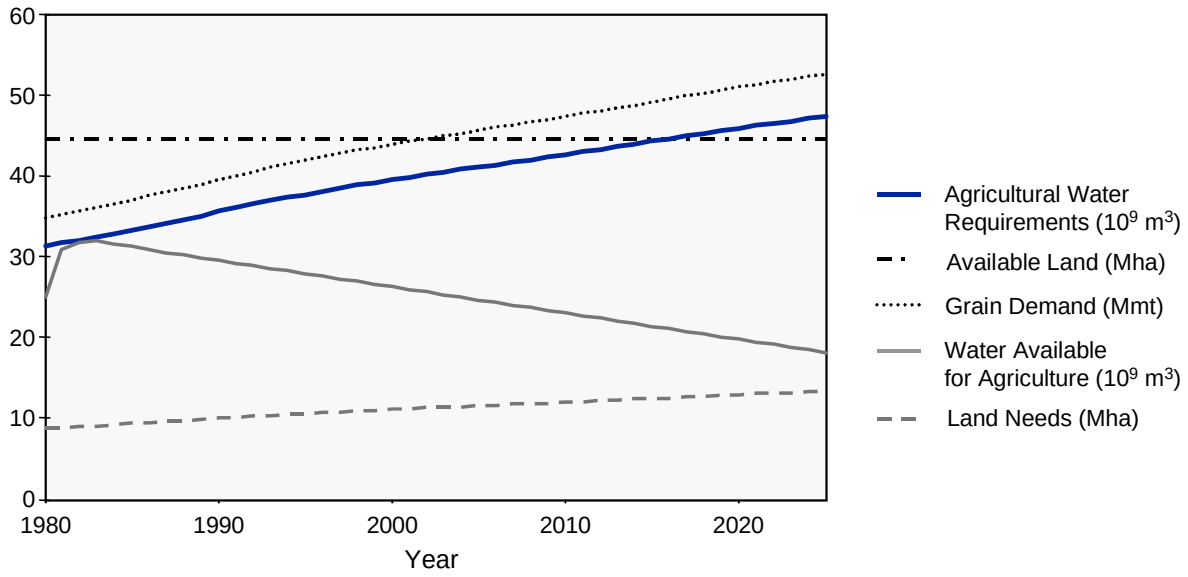

Figure E-39. Grain demand and land and water needs and availability for the Huanghe region, 1980–2025.

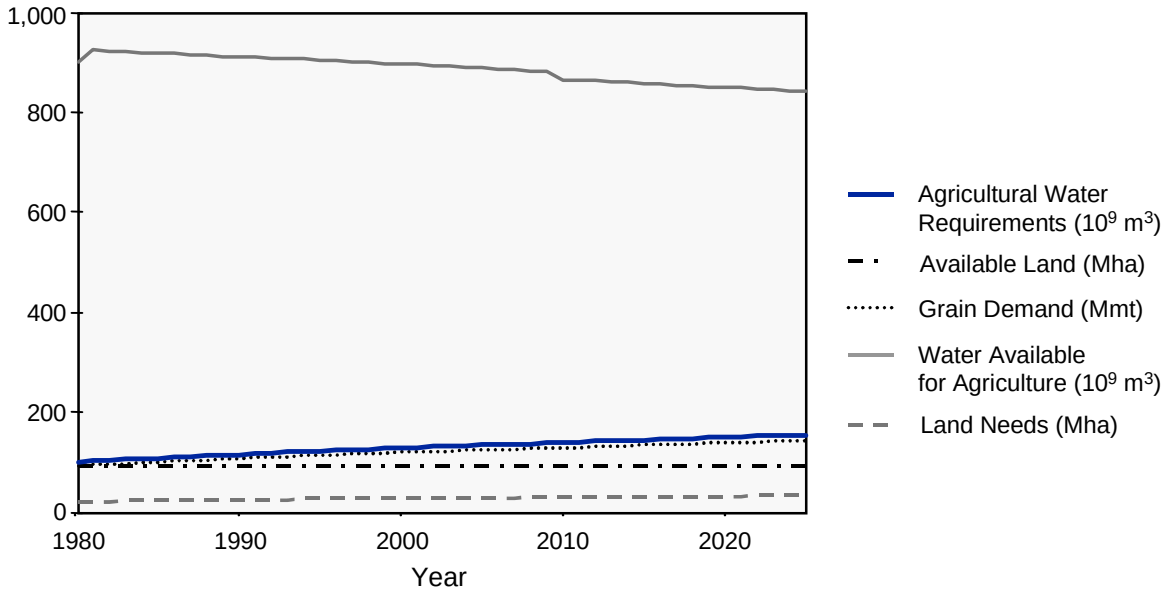

Figure E-40. Grain demand and land and water needs and availability for the Chang Jiang region, 1980–2025.

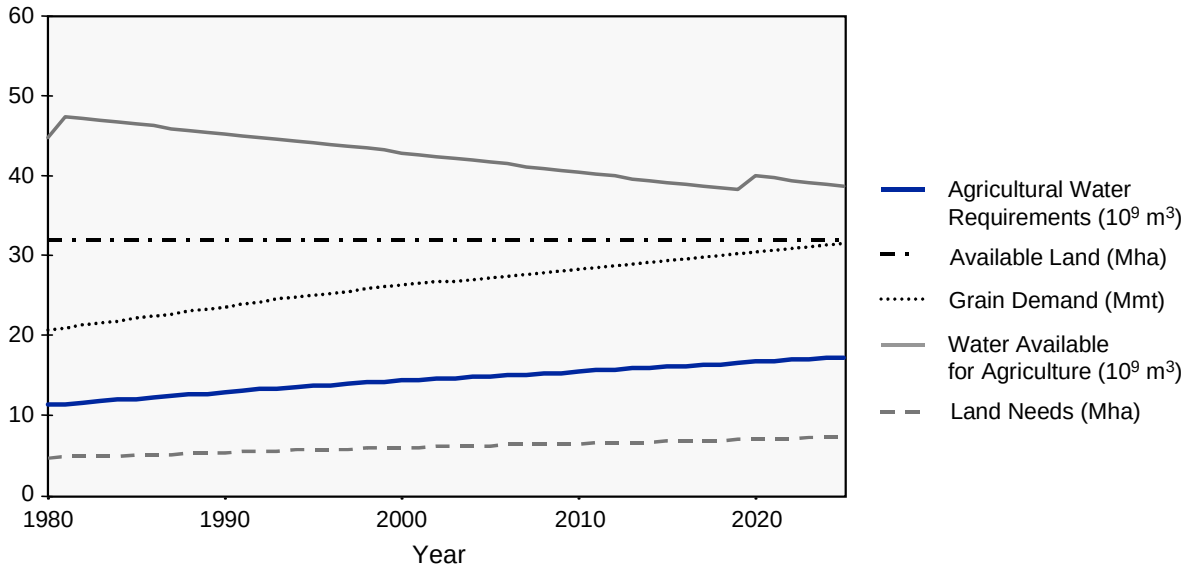

Figure E-41. Grain demand and land and water needs and availability for the Liaohe region, 1980–2025.

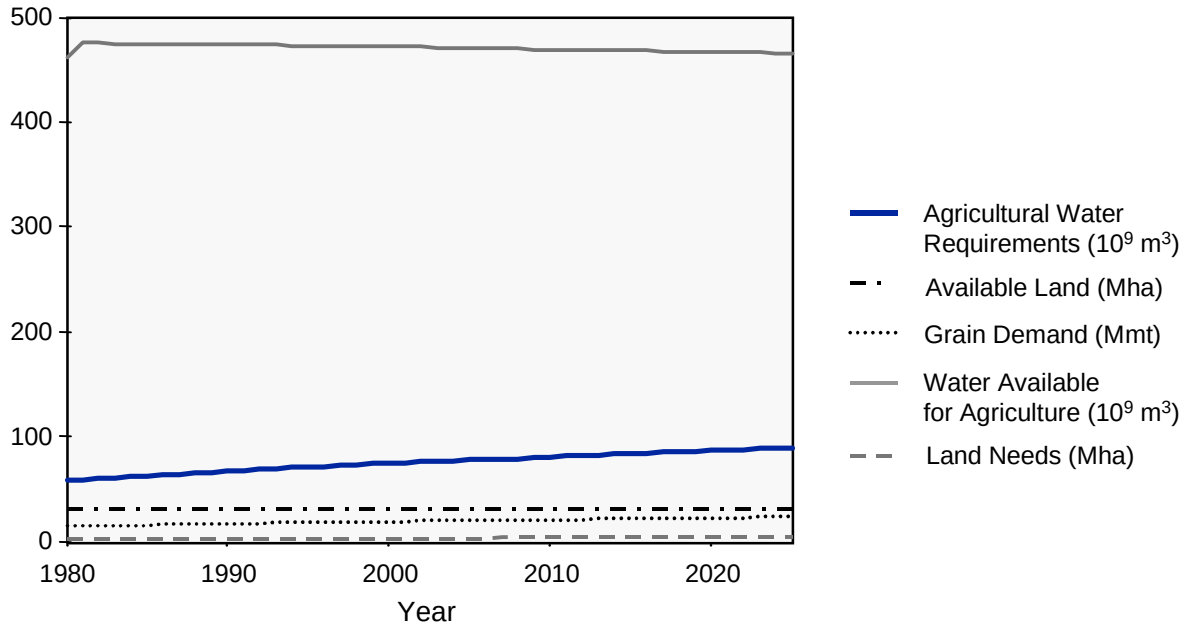

Figure E-42. Grain demand and land and water needs and availability for the Pearl River region, 1980–2025.

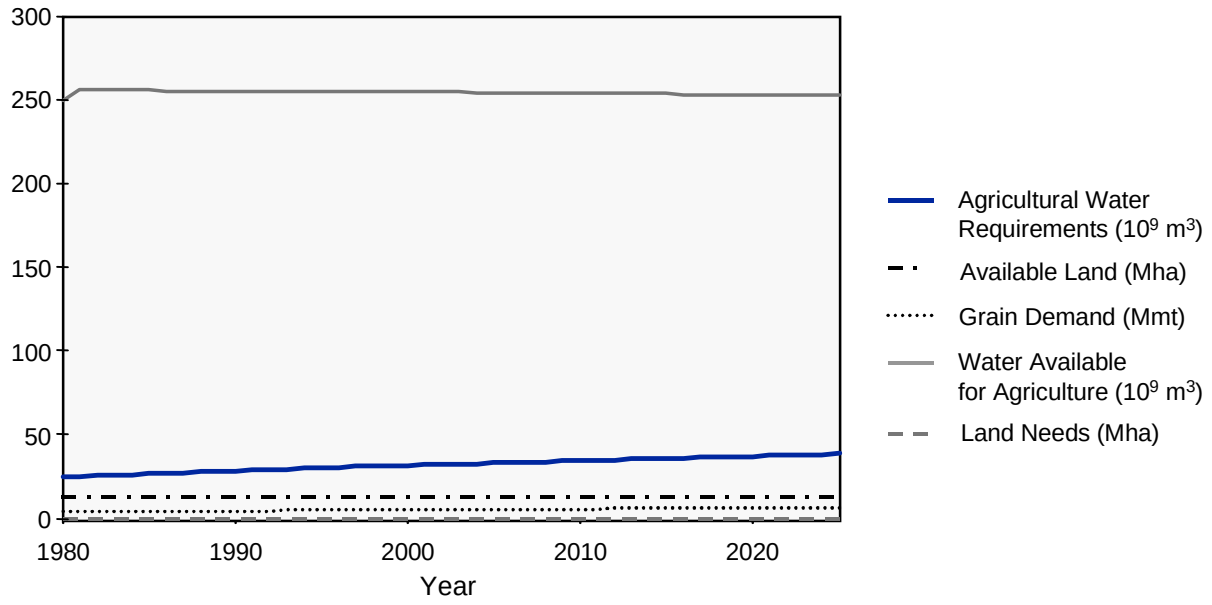

Figure E-43. Grain demand and land and water needs and availability for the Southeast Coastal region, 1980–2025.

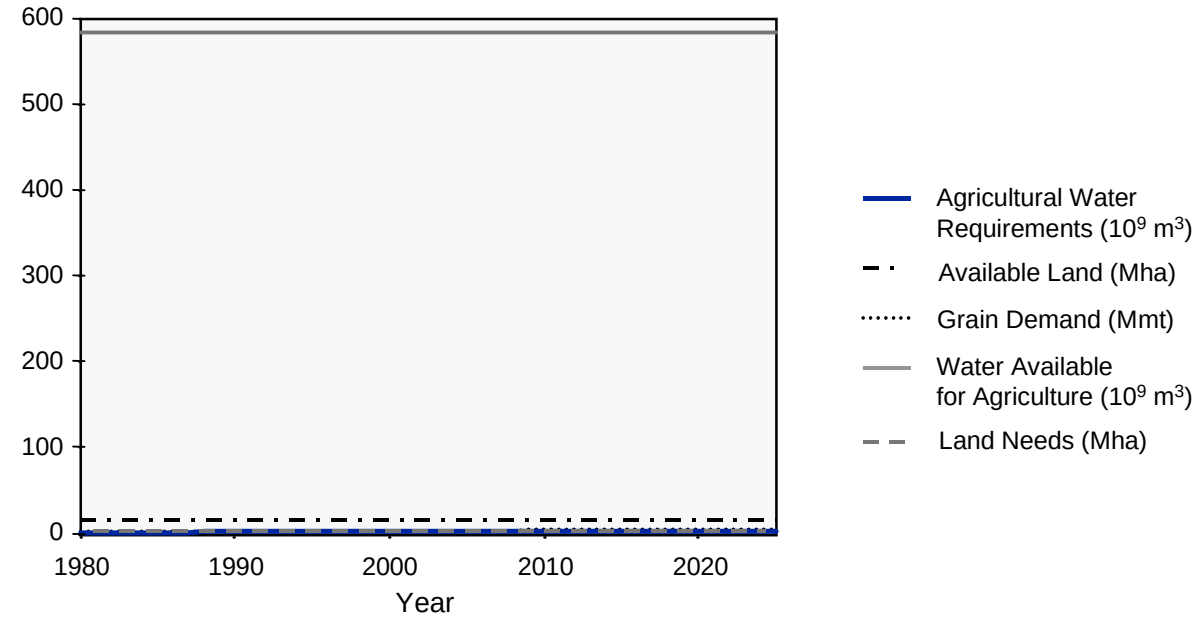

Figure E-44. Grain demand and land and water needs and availability for the Southwest China region, 1980–2025.

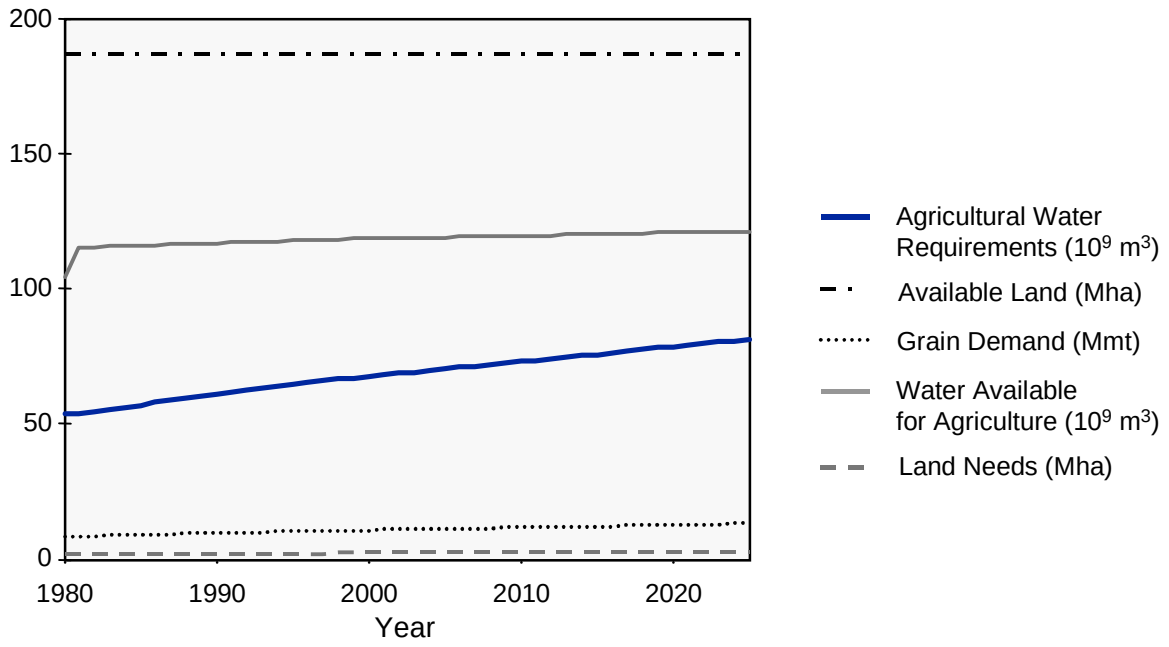

Figure E-45. Grain demand and land and water needs and availability for the Region of Inland Rivers, 1980–2025.

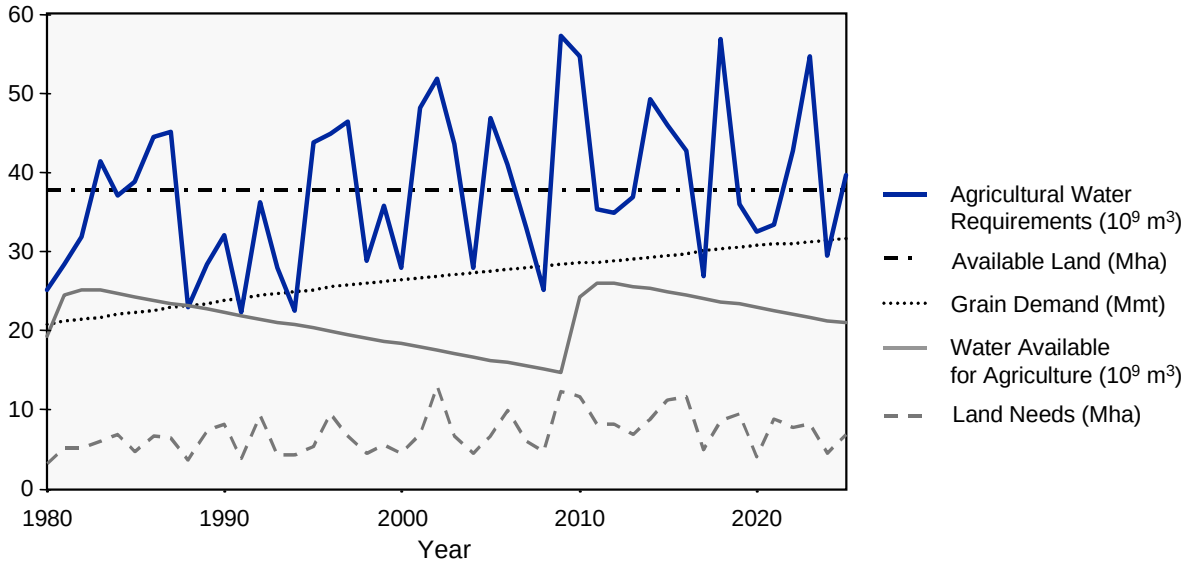

Figure E-46. Grain demand and land and water needs and availability for the Haihe region, 1980–2025. Land needs and agricultural water requirements were generated using the stochastic option for grain yields and water consumption.

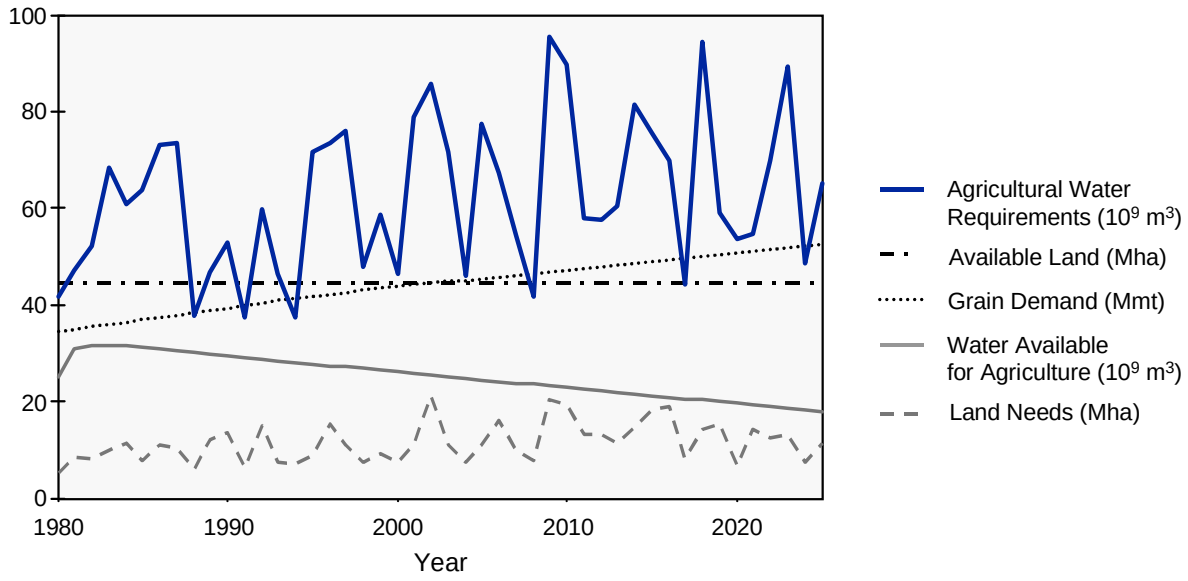

Figure E-47. Grain demand and land and water needs and availability for the Huanghe region, 1980–2025. Land needs and agricultural water requirements were generated using the stochastic option for grain yields and water consumption.

References

Water Resources and Hydropower Design Institute of the Ministry of Water Resources and Electric Power, *Water Resources Utilization in China*, Beijing: Water and Power Press, February 1989.

DISTRIBUTION

1 Environmental Defense Fund
Attn: Ms. Marcia Aronoff
Deputy Director of Programs
257 Park Avenue South
New York, NY 10010

1 Department of State
Bureau of East Asian and Pacific Affairs
Attn: Ms. Constance Arvis
Science Affairs Officer
Room 317
Washington, DC 20520

1 Department of Commerce/NOAA
Attn: Honorable James Baker
Under Secretary for Oceans and Atmosphere
Main Commerce Building
14th and Constitution
Washington, DC 20230

1 PowerSim Corp.
Attn: Michael Bean
Suite 399
12030 Sunrise Valley Drive
Reston, VA 22091

1 OSTP
Attn: Deanna Behring, Assistant Director for International Affairs
Office of Science and Technology Policy
Executive Office of the President
Room 494 Old Executive Office building
Washington, DC 20500

1 House Committee on International Relations
Attn: Mr. Paul Berkowitz
Professional Staff Member
2170 Rayburn HOB
Washington, DC 20515-6128

1 Georgetown University/Department of History
Attn: Professor Nancy Bernkopf Tucker
School of Foreign Service
Washington, DC 20057-1058

1 U.S. – China Business Council
Attn: Mr. Rich Brecher
Vice President and Director for Business
Advisory Services
1818 N Street, NW, Suite. 200
Washington, DC 20036

1 WorldWatch Institute
Attn: Lester R. Brown
1776 Massachusetts Ave., NW
Washington, DC 20036

1 Defense Intelligency Agency
Attn: Ronald F. Burger,
Director for Policy Support
Office of the DIO for Acquisition, Counterproliferation & Arms Control
The Pentagon, Room 2A540
7400 Defense Pentagon
Washington, DC 20301-7400

1 Battelle Advanced International Studies Unit
Attn: Dr. William U. Chandler
901 D Street, NW, Suite #900
Washington, DC 20024

1 Pennsylvania State University
Attn: Kalyan Chatergee
Distinguished Professor of Management Science and Economics
309 Beam BAB
University Park, PA 16802

1 Department of State
Attn: Honorable Eileen Claussen
Assistant Secretary of OES
2201 C Street, NW, Room 7831
Washington, DC 20520

1 UMBC Department of History
Attn: Professor Warren Cohen
11500 South Glen Road
Potomac, MD 20854

1 U.S. Department of Agriculture/Economic Research Service
Attn: W. Hunter Colby
1301 New York Avenue, NW
Washington, DC 20005-4788

1 Olsson Associates
Attn: James Condon
1111 Lincoln Mall
PO Box 84608
Lincoln, NB 68501-4608

1 U.S. Department of Agriculture/Economic Research Service
Attn: Frederick W. Crook
1301 New York Avenue, NW
Washington, DC 20005-4788

1 The Woodrow Wilson Center
Attn: Dr. Geoffrey D. Dabelko
Director, Environmental Change & Security Project
1000 Jefferson Drive, SW
Washington, DC 20560

1 General Motors
Attn: Mr. Louis Donato
Chinese Program Manager
3044 West Grand Blvd.
Detroit, MI 48202

1 Council on Foreign Relations
Attn: Dr. Elizabeth Economy
Fellow for China
58 East 68th Street
New York, NY 10021

1 Rensselair Polytechnic Institute
Attn: Professor Jon D. Erickson
Department of Economics – RPI
Sage Building – Room 504
Troy, NY 12180-3590

1 Mary Evans
4628 Butterworth Place, NW
Washington, DC 20016

1 Natural Resources Defense Council
Attn: Barbara A. Finamore
Senior Attorney
1350 New York Avenue, NW – Suite 300
Washington, DC 20005

1 DCI Environmental Center
Attn: Terry Flannery
Room 2S37
1041 Electric Avenue
Vienna, VA 22180

1 The Woodrow Wilson Center
Attn: Aaron Frank
Executive Secretary, Working Group on Environment in U.S. – China Relations
1000 Jefferson Drive, SW
Washington, DC 20560

1 U.S. Department of Commerce
Attn: Mr. Eric Fredell
Environmental Trade Specialist
International Trade Administration Environmental Technologies Exports
HCHB Room 1003
Washington, DC 20230

1 National Intelligence Council
Attn: Dr. Lawrence K. Gershwin
National Intelligence Officer for Science & Technology
Room 2E42
Washington, DC 20505

1 US–ASEAN Council for Business and Technology
Attn: Ms. Karen Goddin
Executive Director
1400 L Street, NW – Suite 375
Washington, DC 20005

1 University of California at Davis
Attn: Dr. Jack Goldstone
Professor of Sociology
2251 Social Sciences & Humanities Building
Davis, CA 95616

1 Center for Strategic and International Studies
Attn: Dr. Gerrit Gong
Director of Asian Studies
1800 K Street, NW – Suite 400
Washington, DC 20006

1 Honorable Sherri W. Goodman
Deputy Undersecretary of Defense
3400 Defense, The Pentagon
Attn: ODUSD (ES)
Washington, DC 20301-3400

1 CNA/AEC
Attn: Peter R. Gourlay
Director of International Business Development
CNA Plaza, 36 South
Chicago, IL 60685

1 United States Council for International Business
Attn: Mr. Adam Greene
Director of Environmental Affairs
1212 Avenue of the Americas
New York, NY 10036

1 SAIC
Attn: Dr. Clifford W. Greve, Director
Imaging & Remote Sensing Information Systems
8301 Greensboro Drive
PO Box 50132, MS E-7-3
McLean, VA

1 The World Conservation Union
Attn: Mr. Scott a. Hajost
Executive Director
1400 16th St., NW
Washington, DC 20036

1 WorldWatch Institute
Attn: Brian Halweil
1776 Massachusetts Ave., NW
Washington, DC 20036

1 The George Washington University
Attn: Dr. Harry Harding, Dean
Elliot School of International Affairs
2013 G. Street, NW – Stuart Hall 101
Washington, DC 20052

1 ICF Kaiser International, Inc.
Attn: Mr. David Hartman
Executive Vice President & Director for International Business Development
9300 Lee Highway
Fairfax, VA 22031-3278

1 U.S. Department Of Energy
Attn: Abraham E. Haspel
DAS for Energy, Environment and Economic Policy Analysis
PO-6, 7C-034
Forrestal Building
Washington, DC 20585

1 Environmental Protection Agency
Attn: Mr. Alan D. Hecht
Principal Deputy Assistant Administrator
Office of International Activities
401 M Street, SW
Washington, DC 20460

1 University of Maryland
Attn: Dr. Erland Heginbotham, Chief
China Agriculture Project
Institute for Global Chinese Affairs
Holzaffel Hall, Room 1122
College Park, MD 20742-3210

1 Amoco Corporation
Attn: Mr. Richard Herold
Director, International Relations
1615 M Street, NW
Washington, DC 20036

1 New Mexico State University
Department of Civil, Agricultural, and Geological Engineering
Attn: Professor John W. Hernandez
Box 3CE
Las Cruces, NM 88003

2 Tech Reps
Attn: Nancy Hetrick
5000 Marble Ave., NE
Albuquerque, NM 87110

1 US State Department
Attn: Frederic B. Hill, Director
Special Programs, Foreign Service Institute
4000 Arlington Blvd, F4801
Arlington, VA 22204

1 Los Alamos National Laboratory
Attn: Mr. Dennis L. Hjeresen
EM-PD, MS J591
Los Alamos, NM 87545

1 Carnegie Endowment
Attn: Dr. Yasheng Huang
Senior Associate
2400 N Street, NW
Washington, DC 20037

1 American Consulting Engineers Council
Attn: Angelo Iasiello, Director
1015 15th Street, NW, Suite 802
Washington, DC 20005-2605

1 Larry Icerman
2999 Calle Cerrada
Santa Fe, NM 87505

1 World Bank
Attn: Mr. Todd Johnson
Consultant East Asia Division
1818 H Street, NW – Room MC8170
Washington, DC 20433

1 DCI Environmental Center
Attn: Norman Kahn
Room 2S37
1041 Electric Avenue
Vienna, VA 22180

1 Department of State
Attn: Ms. Elena Kim
Bureau of Oceans and International
OES/EX/PSD – Room 7821
Washington, DC 20520

1 National Committee on United States–China Relations
Attn: Ms. Elizabeth Knup, Director
71 West 23rd Street – 19th Floor
New York, NY 10010-4102

1 Rensselair Polytechnic Institute
Attn: Peter Kobos
RPI – Department of Economics
Sage Building, Room 3504
Troy, NY 12180-3590

1 Woodrow Wilson Center
Attn: Dr. Paul H. Kreisberg
3013 Ordway Street, NW
Washington, DC 20008

1 Brookings Institute
Attn: Dr. Nick Lardy, Senior Fellow
Foreign Policy Studies
1775 Massachusetts Ave.
Washington, DC 20036

1 US House of Representatives
Attn: Enere H; Levi, Esq
Legislative Counsel
Office of Congressman Eni Faleomavaega
2322 RHOB
Washington, DC 20515

1 Department of State
Attn: Mr. Hank Levine
Deputy Director and Chief for Economic Affairs
2201 C Street – Room 2254
Washington, DC 20520

1 University of Michigan
Attn: Dr. Kenneth Lieberthal
Center for Chinese Studies
Political Science
202 S. Thayer – 1608
Ann Arbor, MI 48104

1 American Enterprise Institute for Public Policy Research
Attn: Ambassador James R. Lilley
Resident Fellow, Director of Asian Studies
1150 Seventeenth Street, NW
Washington, DC 20036

1 U. S. Department of State
Attn: E. Mark Linton
Director, China Division
Bureau of Intelligence and Research
Room 8840 N.S.
Washington, DC 20520-6510

1 Smithsonian Institution
Attn: Dr. Thomas Lovejoy
Counselor to the Secretary for Biodiversity
1000 Jefferson Drive, SW – Castle 320
Washington, DC 20560

1 Harvard University
Attn: Dr. Michael B. McElroy
Director Earth & Planetary Sciences
Hoffman Lab
20 Oxford Street
Cambridge, MA 02138

1 The MITRE Corp.
Attn: Dr. Thomas E. McEntee, Jr.
Group Leader, Energy, Resources & Environmental Systems Division
7525 Colshire Drive
McLean, VA 22102

1 Department of Commerce
Attn: Mr. Will Martin
Deputy Assistant Secretary for International Affairs, NOAA
14th and Constitution Avenue
Washington, DC 20230

1 Council on Foreign Relations
Attn: Dr. Jessica T. Mathews, Senior Fellow
2400 N Street, NW
Washington, DC 20037

1 Embassy of the Republic of Korea
Attn: You-Hyun Moon, Science Counsellor
2450 Massachusetts Avenue, NW
Washington, DC 20008

1 US Department of State
Attn: Sarah Mullen
Director Intelligence Technology Analysis Division
Arms Control & Disarmament Agency
320 21st Street, NW, Room 4930
Washington, DC 20451

1 Jaideep Mukherjee
1919 West Main, Apt. 2
Houston, TX 77098-3443

1 Lingnan Foundation
Attn: Mr. Douglas P. Murray, President
809 United Nations Plaza
New York, NY 10017

1 Harvard University
Attn: Dr. Chris P. Nielsen
Coordinator, University Committee on Environment,
Research Project on Energy & Environment in China
201 A Geological Museum
240 Oxford Street
Cambridge, MA 02138

1 James E. Nickum
Shirokanedai 5-11-8-402
Minato-ku, Tokyo 108-0071 JAPAN

1 Office of the Vice President of the United States
Attn: Mr. John Norris
Military Advisor to the Vice President
Old Executive Office Building – Room 298
Washington, DC 20506

1 Stanford University
Attn: Dr. Michael C. Oksenberg
Senior Fellow
Institute for International Studies
Encia Hall
Stanford, CA 94305-6055

1 U.S. Department Of Energy
Attn: Michael G. Ortmeier
Office of Intelligence
IN-1, GA-301
Forrestal Building
Washington, DC 20585

1 Ted Petersen
4628 Butterworth Place, NW
Washington, DC 20016

1 Spiegel & McDiarmid
Attn: Mr. David Pomper, Associate
1350 New York Avenue, NW – Suite 1100
Washington, DC 20005-4798

1 Global WaterPolicy Project
Attn: Dr. Sandra Postel
107 Larkspur
Amherst, MA 01002

1 DOE/Office of Science and Technology Policy and Cooperation
Attn: Mr. Robert Price, Director
1000 Independence Ave., SW – Room 1G-218
Washington, DC 20585-1113

1 Georgetown University
Attn: Dr. James Reardon-Anderson
Director of Asian Studies
School of Foreign Service
Washington, DC 20057

1 Department of State
Attn: Mr. John Sammis, Special Advisor
Planning Staff
Room 7411
Washington, DC 20520

1 World Wildlife Fund
Attn: Ms. Frances J. Seymour, Director
Development Assistance Policy
1250 Twenty-Fourth Street, NW
Washington, DC 20037-1175

1 Carnegie Endowment for International Peace
Attn: P. J. Simmons
1779 Massachusetts Avenue, NW
Washington, DC 20036

1 University of Manitoba
Attn: Dr. Vaclav Smil
Geography Division
Winnipeg, Manitoba, Canada R3T2N2

1 Mr. Sameul A. Stern
Attorney-at-Law
2445 M Street, NW
Washington, DC 20037

1 Jay Stewart
16015 Emory Lane
Rockville, MD 20853

1 Congressional Research Service
Attn: Dr. Robert Sutter
Senior Specialist in International Politics
4301 Ann Fitz Hugh Drive
Annandale, VA 22003

1 The World Bank
Attn: Lee Travers
1818 H Street, N.W.
Washington, DC 20433

1 The Woodrow Wilson Center
Attn: Michael Vaden
Environmental Change & Security Project
1000 Jefferson Drive, SW
Washington, DC 20560

1 Harvard University
Attn: Dr. Ezra Vogel
Professor of Social Sciences
1737 Cambridge Street, Room 308
Cambridge, MA 02138

1 The Rockerfeller Brothers Fund
Attn: Dr. Jane Wales
Project Director of Project on World Security
11 Dupont Circle – Suite 610
Washington, DC 20036

1 Dr. Douglas S. Way
205 Ashcroft Court
Ashton, MD 20861

1 National Intelligence Council
Attn: Linda Wiessler-Hughes
National Intelligence Officer for Science & Technology
Room 2E42
Washington, DC 20505

1 US House of Representatives, RHOB
Attn: Congressman Curt Weldon
Washington, DC 20515

1 Consortium for International Earth Science Information Network
Attn: Robert C. Worrest
Director, Government & International Programs
1747 Pennsylvania Ave., NW
Suite 200
Washington, DC 20006

1 MEDA
Attn: Dr. Linda Zall
Executive Director
ORD/LF-7
Reston, VA 20505

1 W. Alton Jones Foundation
Attn: Dr. Ji-Qiang Zhang
232 East High St.
Charlottesville, VA 22902

1 NSA
Information Technology Office
9800 Savage Rd
Ft. Meade, MD 20755-6000

1 Eric Webb
• Richard P. Thomas, MS-1147

1	MS-0749	Arnold Baker, 6217
1	MS-1097	Chui Fan Chen Cheng, 7522
1	MS-1345	Stephen H. Conrad, 6416
1	MS-1345	Paul A. Davis, 6416
1	MS-0719	Thomas E. Drennen, 6217
1	MS-0160	Virgil Dugan, 4100
1	MS-060	Dennis Engi, 4303
1	MS-1363	Belinda Garcia, 6231
1	MS-0185	David Goldheim, 4300
1	MS-1041	John R. Guth, 7522
1	MS-0451	David L. Harris, 7238
1	MS-0149	Dan L. Hartley, 4000
1	MS-1217	Kathie Hiebert-Dodd, 5913
1	MS-0451	David M. Jeppesen, 6238
30	MS-0160	Laurie McMahon, 4303
1	MS-0149	Chuck Meyers, 4001

1	MS-0736	Nestor Ortiz, 6400
1	MS-1373	Arian L. Pregenzer, 5341
1	MS-0746	Laura Swiler Painton, 6411
1	MS-0455	Marjorie L. Tatro, 6231
3	MS-1147	Richard P. Thomas, 6416
1	MS-0451	Ronald E. Trellue, 6238
1	MS-0741	Sam Varnado, 6200
1	MS-0724	Joan Woodard, 6000
1	MS-9018	Central Technical Files, 8940-2
2	MS-0899	Technical Library, 4916
1	MS-0619	Review and Approval Desk, 15102 For DOE/OSTI